HYDROLOGIC INVESTIGATION OF THE UPPER JEFFERSON RIVER VALLEY, MONTANA:

WHITEHALL GROUNDWATER MODELING REPORT

Ali F. Gebril and Andrew L. Bobst

Montana Bureau of Mines and Geology

Ground Water Investigation Program

MBMG
Montana Bureau of Mines and Geology

Cover photo by Ali Gebril, 2019

HYDROLOGIC INVESTIGATION OF THE UPPER JEFFERSON RIVER VALLEY, MONTANA:

WHITEHALL GROUNDWATER MODELING REPORT

September 2020

Ali F. Gebril and Andrew L. Bobst

Montana Bureau of Mines and Geology

Ground Water Investigation Program

Montana Bureau of Mines and Geology Report of Investigation 27

TABLE OF CONTENTS

FIGURES

TABLES

ABSTRACT

This modeling study focuses on the Whitehall area of the Upper Jefferson River Valley. In the Whitehall area, the Jefferson River is a major recharge source to groundwater, and groundwater discharges back to the Jefferson River and other surface-water features, such as the Jefferson and Slaughterhouse Sloughs. Groundwater discharge to the river is particularly important during the late summer when the river's flow is low, and surface-water temperatures are elevated.

Major irrigation canals within the area are the Parrot and the Jefferson. Leakage from these canals provides significant groundwater recharge to the alluvial aquifer. Excess water applied to irrigated fields also provides substantial groundwater recharge. The groundwater recharge provided by irrigation activities eventually flows back to the Jefferson River, the Jefferson and Slaughterhouse Sloughs, and to a network of drains and minor channels. There are concerns that increased groundwater pumping by residential wells may affect the existing equilibrium and decrease the volume of groundwater discharged to surface water.

We developed a numerical groundwater model of the Whitehall area to assess the likely effects from new subdivisions. The basis of this model was a conceptual model of the area developed from analysis of groundwater and surface-water monitoring data, aquifer tests, well logs, and GIS analysis of soil, climate, vegetation, land-use, and water-rights data. A steady-state version of the model performed well under long-term average conditions. Based on changes in the model's calibration statistics RMS and RSS, this model was most sensitive to changes in hydraulic conductivity, river stages, and to a lesser degree to non-irrigation recharge. A transient version of this model simulated groundwater/surface-water interactions over the 2–yr monitoring period (2013–2015) using time-dependent stresses (seasonal irrigation activities and changes in precipitation).

The transient model was extended by 10 yr (2013 to 2025) to run predictive scenarios simulating changing land use. Seven hypothetical scenarios tested placing subdivisions with 5- to 20-acre lots in three locations within the model area. Results focused on the effects to August streamflow since this is when surface-water flows are the lowest. Estimated reductions in groundwater discharge to surface water ranged from 0.001 cfs to 0.2 cfs (0.24% of overall baseflow). The greatest effect occurred when simulating a subdivision in a previously irrigated area. Groundwater drawdown was limited to areas near the pumping centers due to the prevalence of hydrologic boundaries (streams/sloughs).

INTRODUCTION

The Jefferson River, a tributary to the Missouri River, begins at the confluence of the Beaverhead, Big Hole, and Ruby Rivers near Twin Bridges, Montana. The river is about 83 mi long, and irrigated agriculture and recreation are its main uses. Residents of the valley rely on the alluvial aquifer for potable water.

The Upper Jefferson River Valley, which includes the town of Whitehall (fig. 1), is a region critical to providing groundwater baseflow to the Upper Jefferson River. During the late summer, low stream flows and elevated stream temperatures are most pronounced. These conditions trigger irrigation water shortages and trout population declines (MT-FWP, 2012), especially during drought years. Understanding the effects of increased groundwater use related to residential growth in the Whitehall area will inform decisions about future development in the valley.

Purpose and Scope

The Montana Bureau of Mines and Geology (MBMG) developed a numerical groundwater model to understand and quantify the interactions between surface water and groundwater in the Whitehall area. This included evaluating the potential impacts of increased groundwater development on those interactions, especially during critical low-flow periods—late summer months or drought years. Planners and decision makers can use the groundwater model to evaluate various development scenarios, or changes in irrigation management practices, and examine effects of these changes on water resources. This report documents model construction, calibration, and its application to several land-use scenarios. It complements the Upper Jefferson Interpretive Report, which focuses on the geological setting and hydrogeology of the Upper Jefferson project area (Bobst and Gebril, in prep.).

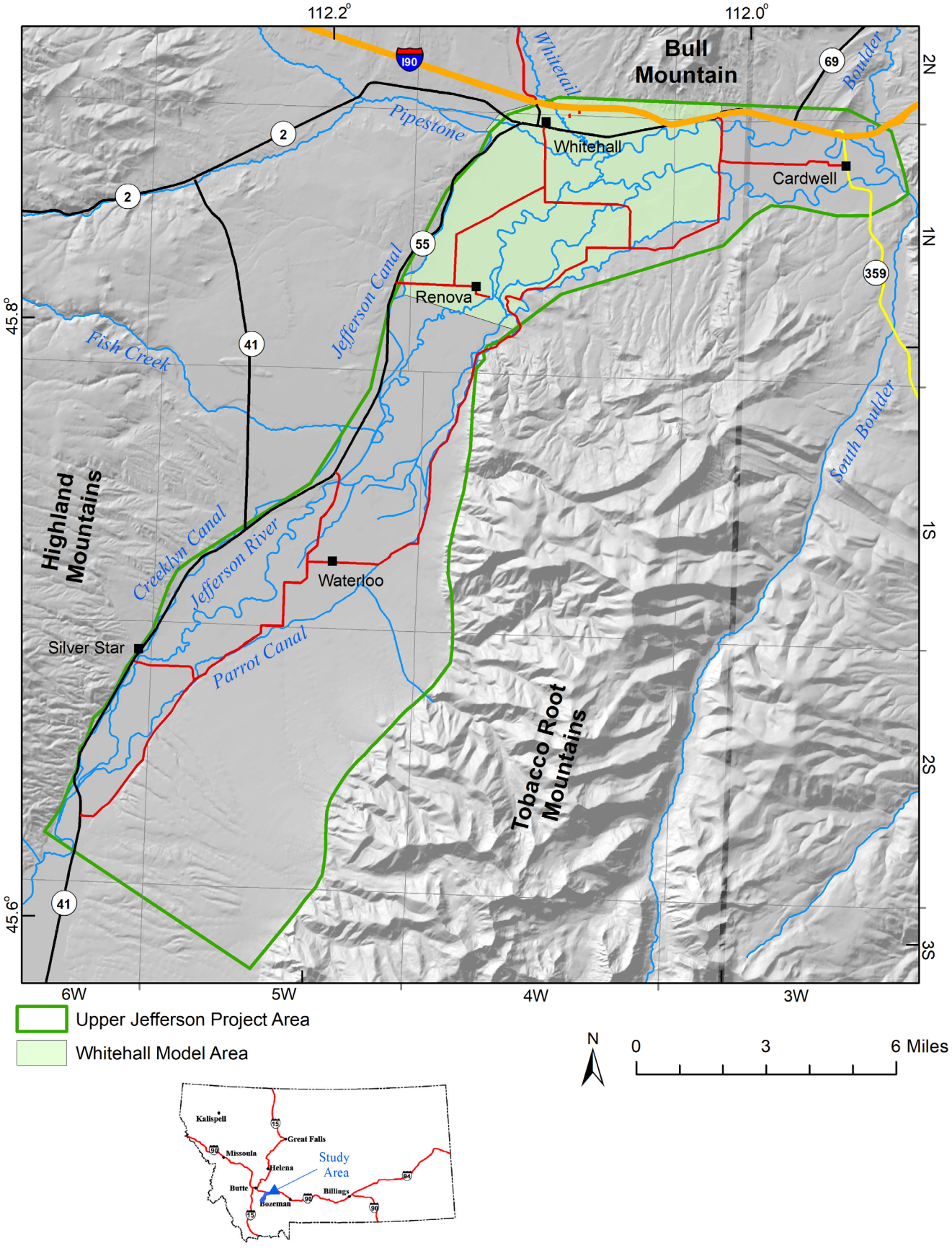

Figure 1. Upper Jefferson River Project Area. Whitehall model area is a part of the Upper Jefferson River groundwater investigation.

Location

The Whitehall model area spans the Jefferson River alluvial valley from approximately 0.5 mi upstream of the diversion from the Jefferson River to Slaughterhouse Slough (0.7 mi south of Renova) and extends to Mayflower Road/Tebay Lane (approximately 4 mi downstream from Whitehall (fig. 2). The model area is about 3 mi wide by 7 mi long, and covers a total area of 24 mi^2.

Previous Studies

Several geologic and hydrogeologic studies have been conducted near the Whitehall model area. Brancheau (2015) conducted a groundwater/surface-water interaction study near Waterloo, about 13 mi south of Whitehall, in the Jefferson Valley (fig. 1). This study evaluated the relationships among surface water, groundwater, and irrigation practices. Brancheau developed a detailed groundwater budget and estimated the net groundwater discharge to the Jefferson River. The MBMG performed a groundwater investigation in the nearby Boulder Valley (Bobst and others, 2016; Butler and Bobst, 2017). Hydrogeologic information concerning the Boulder and Upper Jefferson Valleys was summarized by Kendy and Tresch (1996), including climate, population, land and water use, geology, surface water, and aquifer hydraulic characteristics. Vuke and others (2004) developed maps of the surficial geology of the Jefferson Valley (fig. 3) that show the surficial extent of geologic units, the locations of known or inferred faults, and geologic cross sections.

Description of Study Area

Physiography

The Upper Jefferson Valley is an intermontane basin. The Whitehall area is bounded by the Highland Mountains to the west and northwest, Bull Mountain to the northeast, and the Tobacco Root Mountains to the south (fig. 1). Important water features include the Jefferson River, Slaughterhouse Slough, Jefferson Slough, Pipestone Creek, and Whitetail Creek (fig. 2). Numerous canals and drains and several ponds are within the study area.

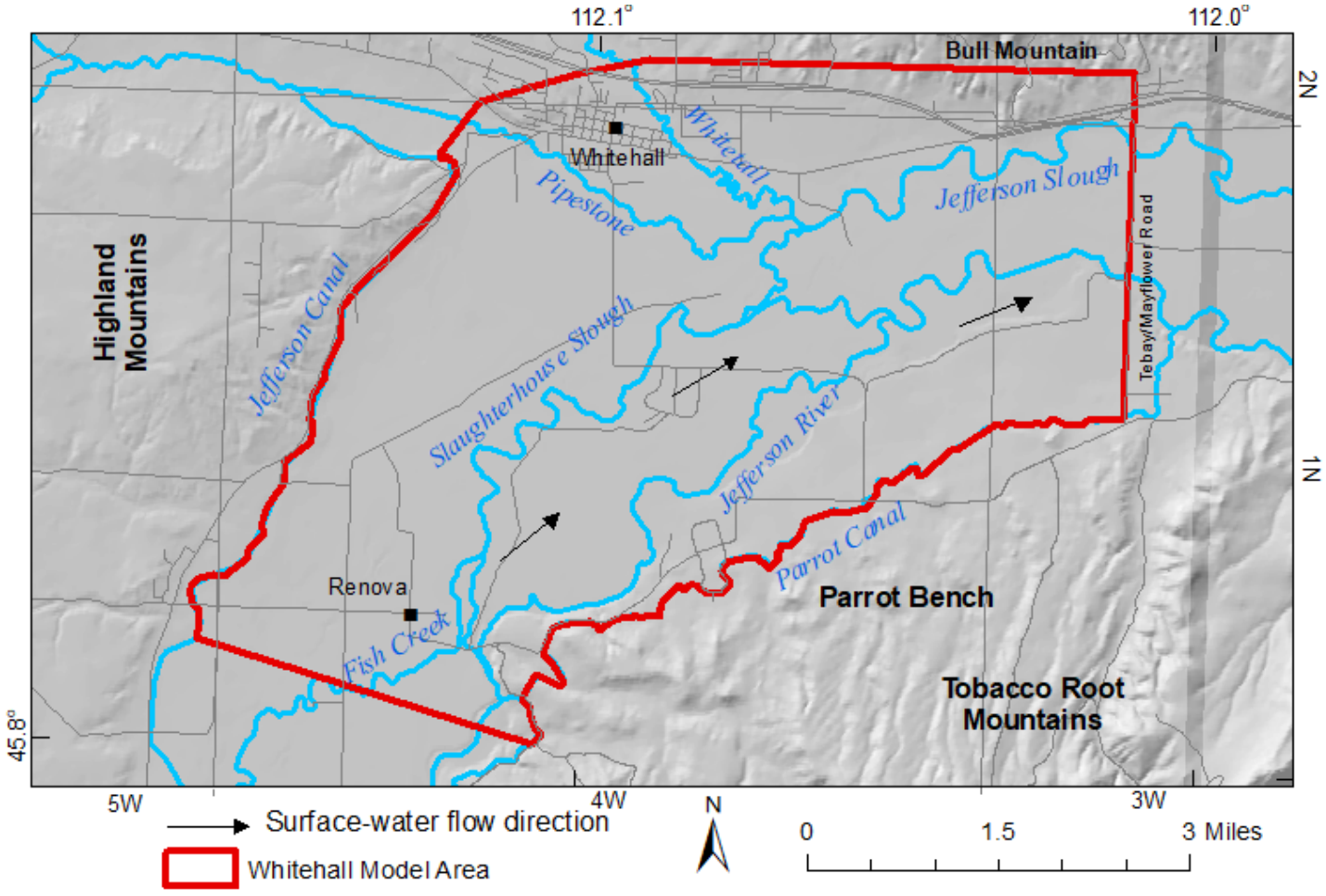

Figure 2. The Whitehall Model Area extends along the Jefferson Valley from just upstream (south) of Renova in the southwest to Tebay/Mayflower Road in the northeast. The edges of the model include the Parrot Canal on the south, Jefferson Canal on the west, and bedrock associated with Bull Mountain on the north.

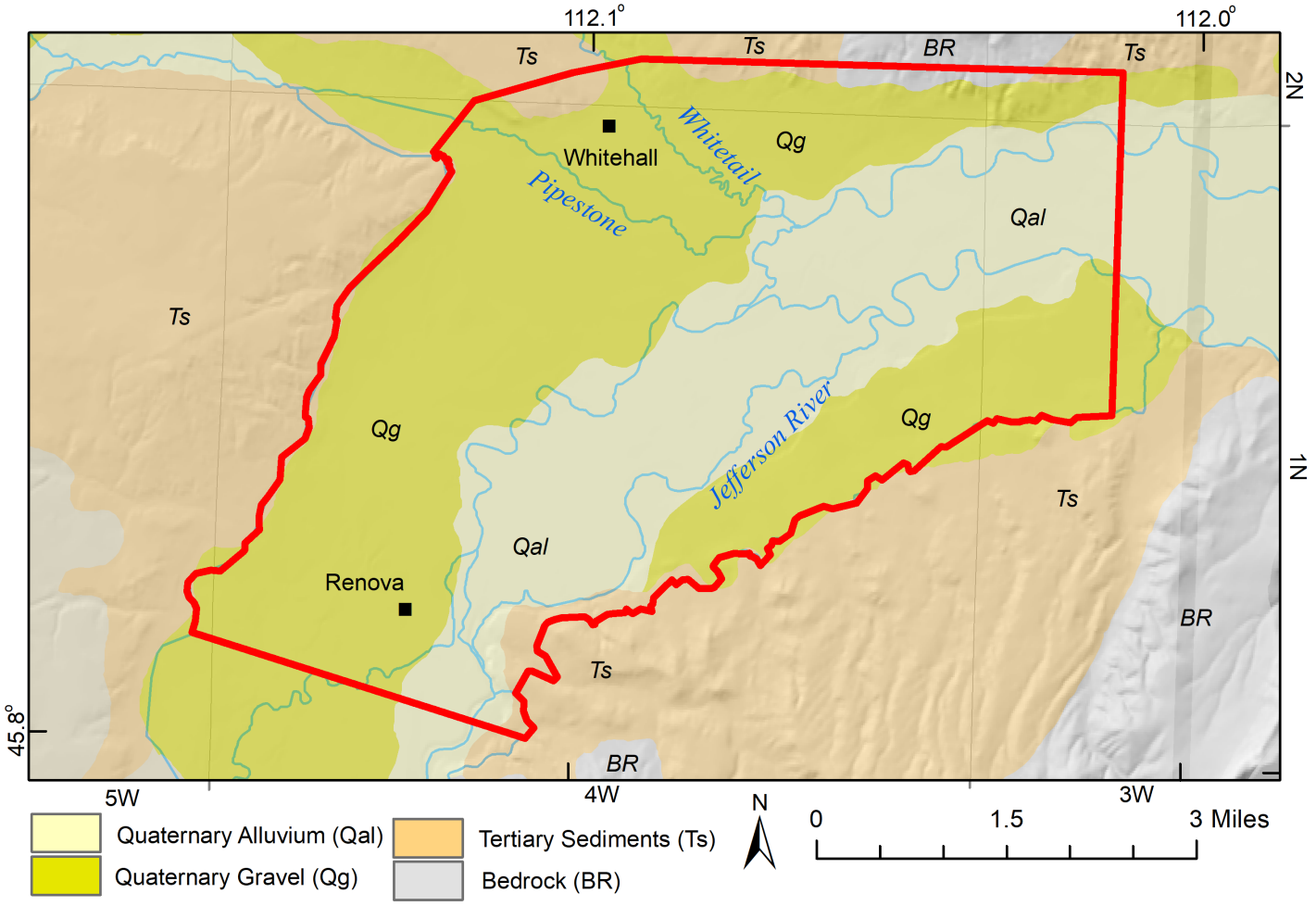

Figure 3. Surficial geology of the Whitehall model area. Units were simplified into four geologic units (modified from Vuke and others, 2004).

The Jefferson River near Twin Bridges (about 20 mi south of Whitehall) had an average annual flow of 1,107 cubic feet per second (cfs) between 1941 and 2014 [United States Geological Survey (USGS) gauging station 06026500]. The average annual peak flow was 9,467 cfs, and the lowest mean monthly flow (August) was 760 cfs.

Land surface elevations within the model area range from 4,290 ft (amsl) near the eastern boundary along the Jefferson River and Jefferson Slough, to 5,500 ft (amsl) near the northern boundary in the foothills of Bull Mountain (fig. 2).

Climate

The Jefferson Valley has cold winters and mild summers. Climate records for Twin Bridges from 1981 to 2010 (NOAA, 2011) show that December is the coldest month, with a mean monthly temperature of -5.2°C (23°F). July is the warmest month with a mean monthly temperature of 65°F (18.4°C).

Thirty-year normal precipitation data (1981–2010) obtained from Oregon State's Parameter-Elevation Regressions on Independent Slopes Model (PRISM, 2014) show that average annual precipitation near Whitehall city is about 10 in. Precipitation increases with elevation; the Highland Mountains receive up to 32 in/yr while the Tobacco Root Mountains receive up to 42 in/yr. Weather data from Twin Bridges (NWS Cooperative Network Station 248430-2; 1950–2016) indicate that average annual precipitation is 10.1 in, June is the wettest month (2.0 in), and February is the driest (0.2 in). During the period of this study (2013–2015), precipitation was below average at 9.0, 9.4, and 8.1 in. in 2013, 2014, and 2015, respectively.

Vegetation

Vegetation in the Whitehall model area varies based on topography, water availability, and underlying substrate. Within the alluvial floodplain and along some tributaries of the Jefferson River, the dominant riparian vegetation consists of willows, cottonwoods,

and wetland grasses. These phreatophytes grow where shallow groundwater may be accessed by their roots. Grass and sagebrush cover un-irrigated areas of the valley bottom and adjacent benches. Irrigated agricultural areas are mainly alfalfa and grass hay.

Land Use

About 60% of the land in the Whitehall model area is irrigated. Of the irrigated land, approximately 44% of the area is flood irrigated, and 56% is pivot or sprinkler irrigated (MDOR, 2012). Irrigation ditches convey surface water diverted from the Jefferson River to most of the irrigated fields. Cattle grazing dominates the remaining 40% of the model area; this is un-irrigated land.

Water Infrastructure

Within the Whitehall model area, the water infrastructure includes irrigation canals, irrigated fields, irrigation wells, municipal water supply wells, domestic and stock wells, and septic systems. The Jefferson River provides water for irrigation canals and most irrigated fields. Twenty-two wells within the alluvial aquifer provide water for irrigation.

Two major irrigation canals run through the Whitehall area. These canals derive their water from the Jefferson River outside of the model area. The Parrot Canal runs along the south side of the valley, while the Jefferson Canal runs along the west side. Unused water from the Parrot Canal returns to the Jefferson River approximately 0.5 mi downstream (east) of the model area, and unused water from the Jefferson Canal flows into Pipestone Creek approximately 1.3 mi upstream (west) of the model area (fig. 2). Canals recharge groundwater where they lose water to the underlying alluvial aquifer through leakage; in addition, irrigated fields provide irrigation recharge when water is applied in excess of crop demand. Recharge from irrigation activities is particularly important because it supplies the alluvial aquifer during critical low-flow periods (WET, 2006).

There are 302 domestic wells in the area (GWIC, 2019). Wells pump water and septic systems return a portion of that water to aquifers. For this study, domestic well pumping rates were based on their net consumptive use rates; that is, their pumping rate less the amount of water returning to the groundwater system via septic systems.

CONCEPTUAL MODEL

This conceptual model describes the characteristics and dynamics of the physical processes within the groundwater and surface-water flow system and is based on available hydrogeologic information for the study area. The conceptual model includes the system's geologic framework, aquifer properties, groundwater flow directions, locations and rates of recharge and discharge, and the locations and hydraulic characteristics of natural boundaries (ASTM, 2014).

Geologic Framework

The Jefferson River Valley is filled with sediment eroded from surrounding mountains and from the Jefferson River drainage area to the south. Tertiary sediments, including the relatively fine-grained Renova Formation, and the coarse-grained Sixmile Creek Formation, occur at the base of the mountains. Quaternary pediment gravels overlie the Tertiary sediments in some areas outside the floodplain. Quaternary alluvium underlies the modern floodplain, and Tertiary sediments underlie the alluvium (fig. 3). The deepest well in the model area was 300 ft deep (GWIC 227257) and did not penetrate the bottom of the Tertiary.

Within the model domain, bedrock is exposed at the northern edge of the valley (fig. 3). The bedrock includes Cretaceous volcanic and sedimentary rocks, Paleozoic sedimentary rocks, and Precambrian rocks. The depth to bedrock changes dramatically over short distances due to vertical offsets where faults cross the valley. These valley-crossing faults are generally northwest trending (Vuke and others, 2004).

Hydrogeologic Setting

Literature review, geologic maps, well logs, and results from aquifer tests conducted in the Upper Jefferson River project area (Bobst and Gebril, 2020) provided information to establish the hydrogeologic setting of the study area. Eighty-seven drillers' logs were reviewed from MBMG and Ground Water Information Center data (GWIC; note that well identification in this report is by GWIC number; i.e. well 43587) . These wells are included on the Ground Water Investigation Project (GWIP) project page: http://mbmg.mtech.edu/gwip/projectupdate.asp?projectid=BWIPUJ&. Detailed information on the methods and hydrogeologic interpretation are included in Bobst and Gebril (in prep.).

Water-bearing geologic formations in the Upper Jefferson area were grouped into four hydrogeologic units (HGUs) according to their abilities to transmit and store water. These are: (1) alluvium (Quaternary alluvium); (2) bench sediments (Tertiary Sixmile Creek Formation and Quaternary fan deposits); (3) Renova Formation; and (4) bedrock.

Alluvium

The alluvium is a mixture of gravel, sand, and silt and clay deposited by modern rivers and streams and is typically less than 40 ft thick (Nobel and others, 1982; Vuke and others, 2004). From the literature values, aquifer tests, and results from the Waterloo modeling study (Bobst and Gebril, in prep.), the estimated initial hydraulic conductivities for this unit ranged from 70 to 500 ft/d.

Bench Sediments

This HGU includes the Tertiary Sixmile Creek Formation and younger Quaternary fan deposits. These units, mainly composed of gravel, sand, silt, clay, and ash beds, are coarser than the underlying Renova Formation sediments (Kuenzi and Fields, 1971; Vuke and others, 2004). These sediments outcrop on the benches. No aquifer tests were conducted within these sediments, because they were unsaturated where drilled. Since site-specific hydraulic conductivity estimates were not available for the bench sediments, an initial value of 30 ft/d for the model was based on literature values for sand and gravel (Freeze and Cherry, 1979).

Renova Formation

Older fine-grained sediments of the Renova Formation underlie the Sixmile Creek Formation and alluvium in the floodplain. Some of this Tertiary sediment also outcrops on the benches. Hydraulic conductivity was estimated from two aquifer tests conducted in the model area (Bobst and Gebril, 2020). As shown in figure 4B, the first test (Lazy TP, Floodplain site) was located 2 mi southeast of Whitehall; the second (Lazy TP, Bench site) was located approximately 3.5 mi southeast of Whitehall (close to the Parrot Canal). Estimated hydraulic conductivity from the first test was 27 ft/d and storativity ranged from 8×10^{-4} to 2×10^{-3}. The second test indicated a hydraulic conductivity of 382 ft/d, and storativity of 5×10^{-5}. Leaky confined solutions replicated the observations of both tests.

Bedrock

The various types of bedrock were combined as a single HGU. A relatively low hydraulic conductivity of 1 ft/d was set initially for the bedrock (Freeze and Cherry, 1979).

Groundwater Flow System

Groundwater levels measured in the model area during April 2015 were used to develop a potentiometric surface map (fig. 5). The potentiometric contours generally follow topography. Groundwater flows from the topographic highs—where there is relatively high groundwater recharge—toward the center of the floodplain. In the floodplain some of the groundwater discharges into the Jefferson River, Slaughterhouse Slough, and the Jefferson Slough, where they are gaining. Groundwater also flows through the alluvial aquifer parallel to the river. Groundwater in the alluvial aquifer flows from the southwest (southern boundary) to the northeast (eastern boundary).

Storage of water in the alluvial aquifer is important to maintain baseflow to the Jefferson River and to the Sloughs during low-flow periods (e.g., late summer). Water diverted from the Jefferson River to irrigation canals recharges the underlying aquifer via canal leakage and irrigation recharge. This irrigation-related recharge causes groundwater elevations in the alluvium to rise. During low-streamflow periods, aquifer discharge, that is, baseflow, makes up much of the flow in the Jefferson River and the Sloughs. The aquifer also discharges to minor canals and drains, which feed the river and sloughs. The timing of the water's release from storage will depend on the gradient between the aquifer and boundaries, transmissivity of the aquifer, and the distance along groundwater flow lines between recharge and discharge.

Hydrologic Features

Surface-water features are important hydrologic boundaries in the model area. Naturally occurring surface-water features include the Jefferson River, Slaughterhouse Slough, Jefferson Slough, Pipestone Creek, and Whitetail Creek. The Jefferson River and the Sloughs flow from the southwest to the northeast, while the creeks enter from the northwest where they meet Jefferson Slough. The Parrot and Jefferson irrigation canals are hydrologic boundaries along the south and west sides of the valley, respectively (fig. 2), and

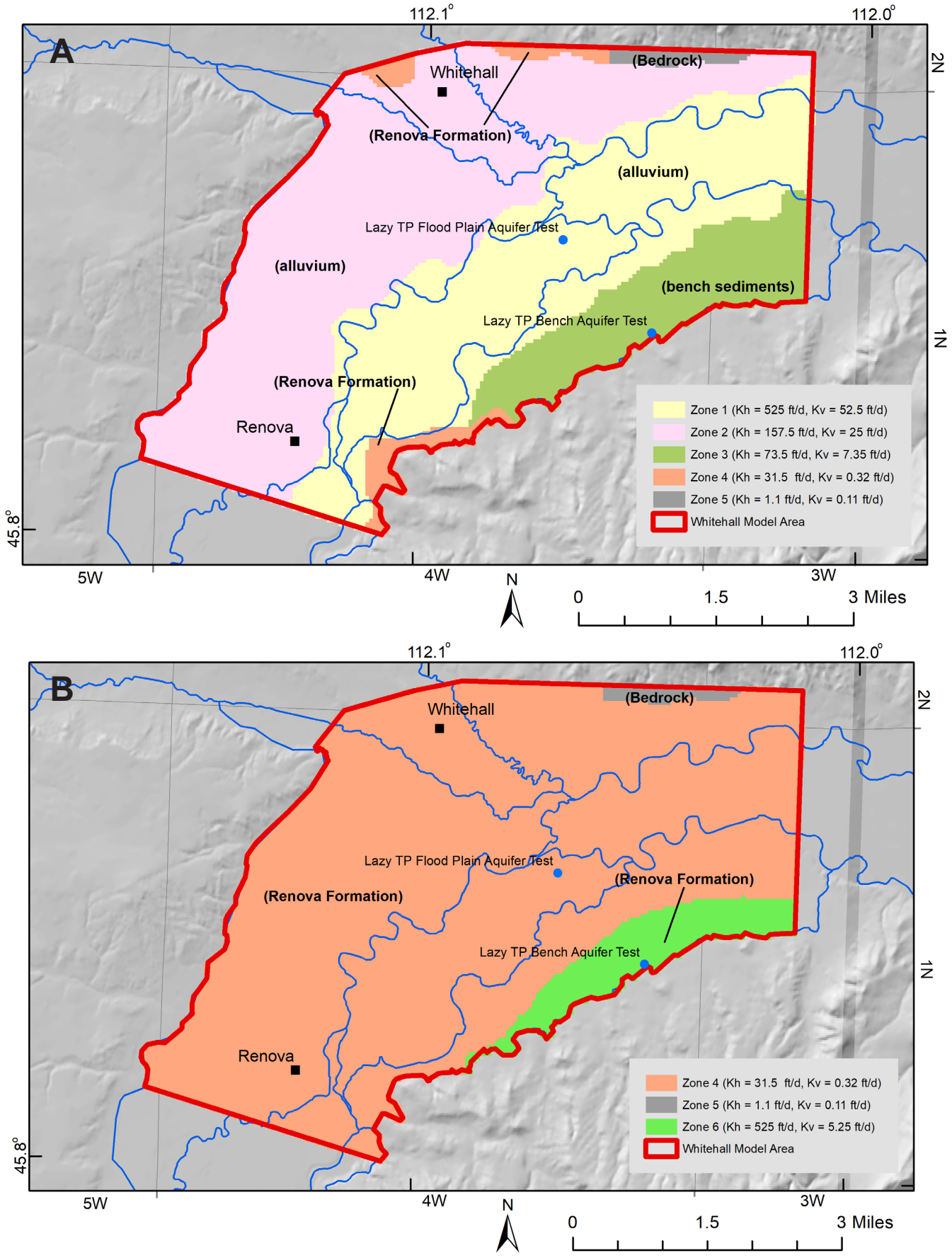

Figure 4. (A) The initial model hydraulic conductivity in layer 1 was based on field data and literature values. Permeable Quaternary alluvium dominates the hydraulic conductivity distribution in model layer 1. Hydrogeologic units are shown in parentheses. (B) The range of the initial hydraulic conductivity in layer 2 was lower than layer one, reflecting the less permeable bedrock and Renova Formation. Hydrogeologic units are shown in parentheses.

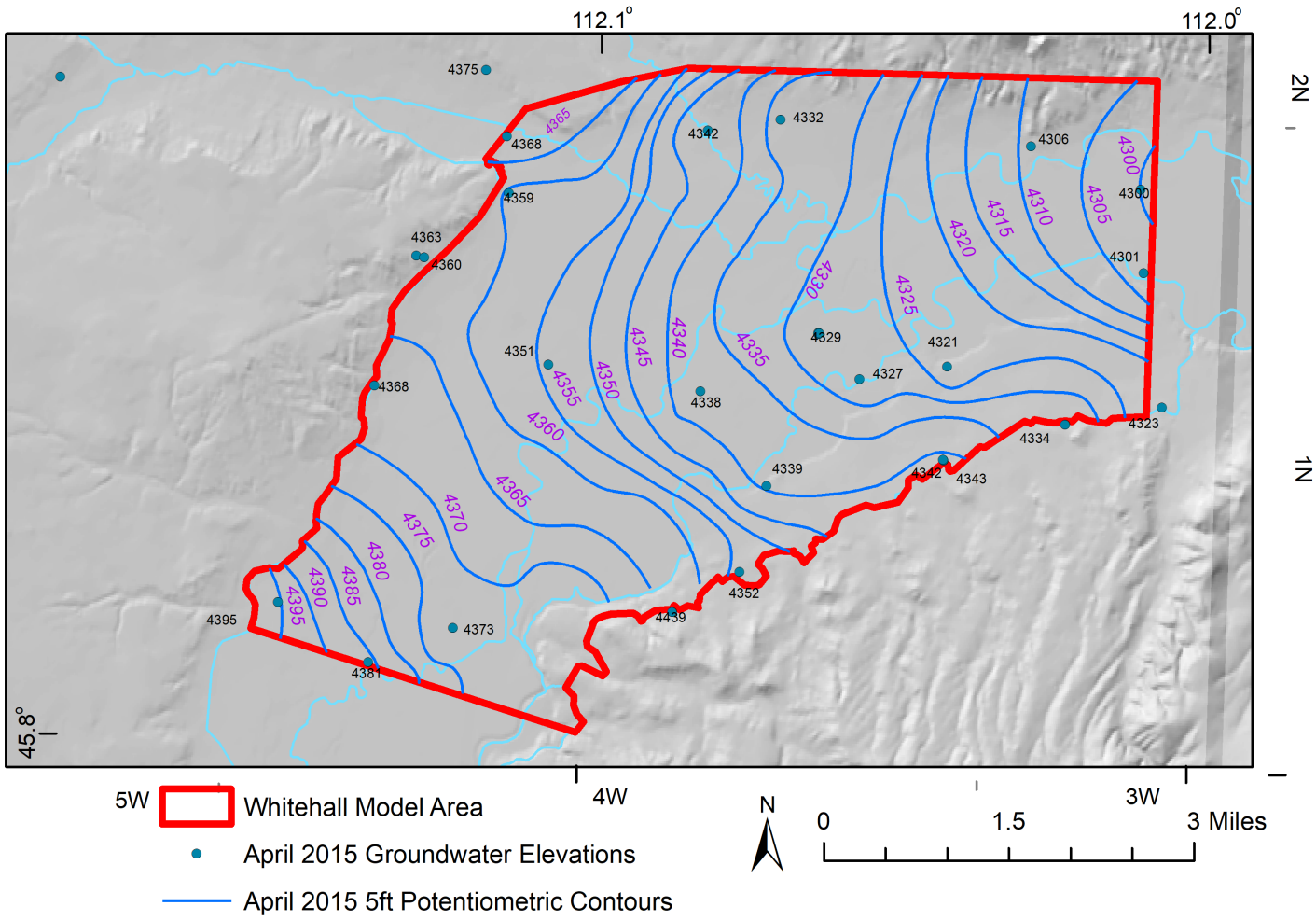

Figure 5. The potentiometric map constructed from April 2015 groundwater elevations. Groundwater flow mainly towards the east–northeast.

they contribute groundwater recharge via canal leakage.

Additional water sources and sinks are also located within the model area. Water is added to the aquifer through irrigation recharge. Water leaves the aquifer from the following sinks: pumping wells, riparian phreatophytes and wetland grasses (through evapotranspiration), and groundwater-fed ponds (through evaporation). A network of drains and minor canals primarily act as sinks for groundwater, although they could be a source of recharge during rare high precipitation or snowmelt events, if groundwater levels were low.

Groundwater Budget

For more understanding of the groundwater flow system in the Whitehall area, a preliminary groundwater budget was developed based on knowledge of the area and field data (e.g., canal leakage, groundwater elevations), and on estimated values from literature and other studies such as well withdrawals, irrigation recharge, evapotranspiration, etc. Later, the estimated values were adjusted during calibration. Conceptually, the groundwater budget for the Whitehall area (fig. 6A) is summarized as:

$$GW_{al-in} + GW_{lat-in} + CL + IR + SW_{in} =$$

$$GW_{out} + SW_{out} + PE + WL + ET_r ,$$

where $GW_{al\text{-}in}$ is alluvial groundwater influx; $GW_{lat\text{-}in}$ is lateral groundwater influx; CL is canal leakage; IR is irrigation recharge; SW_{in} is inflow from surface water; GW_{out} is groundwater outflux; SW_{out} is outflow to surface water; PE is pond evaporation; WL is well withdrawals; and ET_r is riparian evapotranspiration.

Details on water budget calculations are included in appendix A. While the components of this budget are conceptually separate, some of them were simulated in the numerical model with a single boundary condition. For instance, along the Parrot Canal there is lateral groundwater inflow under the canal, upgradi-

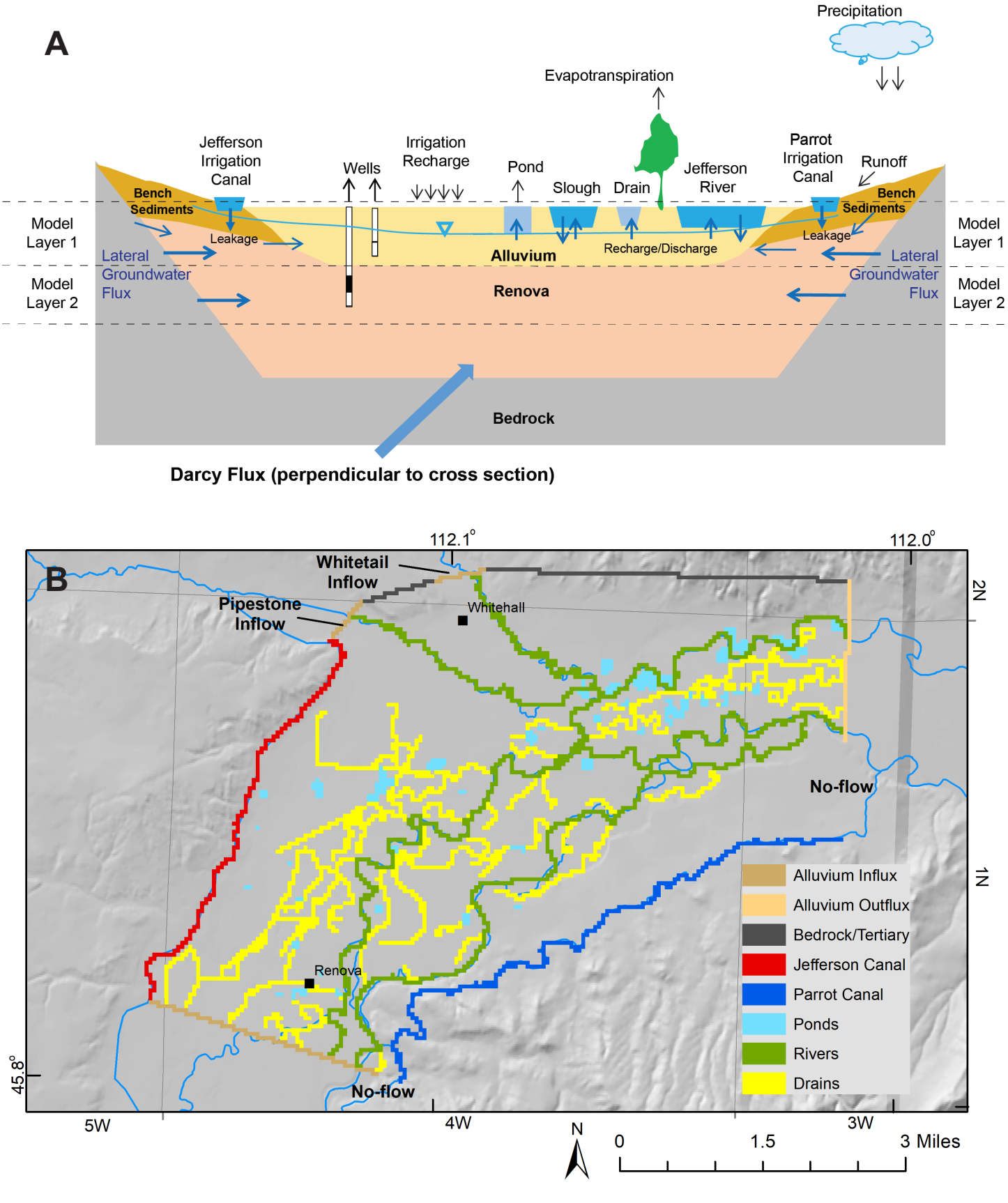

Figure 6. (A) The conceptual model illustrates the sources of recharge to and discharge from the study area. (B) Types of flow boundaries in model upper layer (layer 1). 6C on next page.

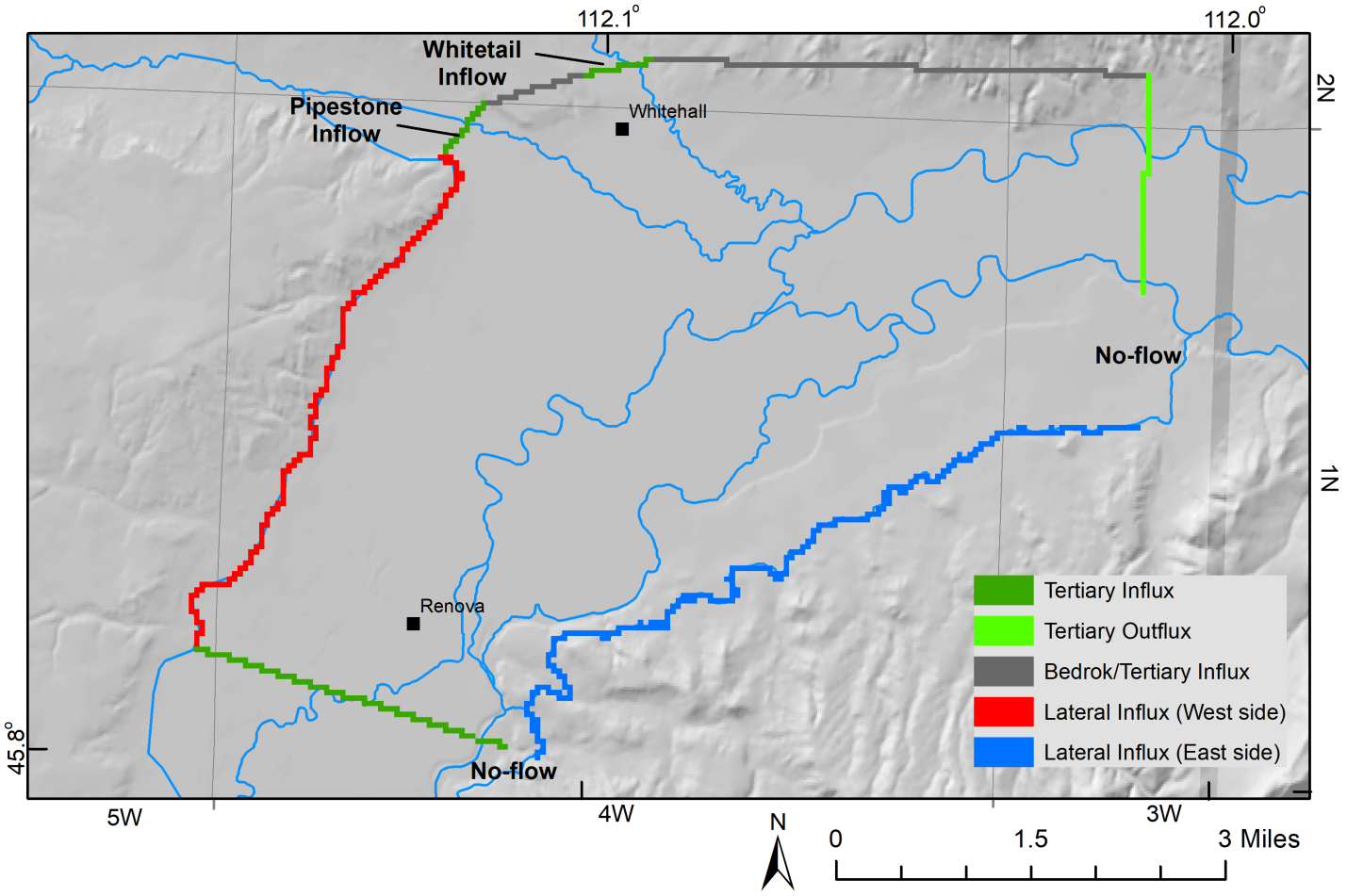

Figure 6C. Types of boundaries in model lower layer (layer 2).

ent irrigation recharge, and canal leakage. These were simulated using a single specified flux boundary.

The relationship between precipitation and recharge becomes linear when mean annual precipitation exceeds 30 in; however, when precipitation values are less than 30 in, most of the infiltrating water is used to replenish soil moisture that has been depleted by evapotranspiration (Dugan and Peckenpaugh, 1985). This is particularly true for semiarid climates, such as the Whitehall area (Nobel and others, 1982; Sweet and others, 2015). The un-irrigated land in the study area is primarily grass and sagebrush, which have an evapotranspiration rate of about 12 in/yr (Johns, 1989), and the mean annual precipitation in this area is from 10 to 12 in. Since evapotranspiration limits precipitation recharge, we considered direct recharge from precipitation negligible for the preliminary groundwater budget.

Alluvial and Lateral Groundwater Influx ($GW_{al\text{-}in}$ and $GW_{lat\text{-}in}$)

Groundwater flux enters into the model area through Quaternary alluvial deposits (fig. 6A). These alluvial deposits are in the Jefferson River floodplain, and underlie Pipestone and Whitetail Creeks. Groundwater flux into the study area (GWal-in) was estimated using Darcy's Law:

$$Q = -KA\,(dh/dl),$$

where Q is total flux, volume/time (ft^3/day); K is hydraulic conductivity (ft/day); A is saturated cross-sectional area of the aquifer (ft^2); and dh/dl is groundwater gradient (unitless or ft/ft).

The average hydraulic gradients calculated from April 2015 groundwater elevation data (fig. 5) were used to estimate groundwater inflows and outflows at model boundaries. Groundwater influx through these alluvial deposits was estimated to be 1,188 acre-ft/yr (appendix A).

Lateral groundwater influx enters through the bedrock along the northern model boundary, and through Renova Formation along the eastern and western

model boundaries. This lateral groundwater inflow was also estimated based on Darcy's Law, and totaled 215 acre-ft/yr (appendix A).

Canal Leakage (CL)

Canal leakage occurs on the bench above the floodplain. The canals provide recharge because they are at a higher elevation than the water table. The leakage is assumed to occur uniformly along the Jefferson (5 mi) and Parrot (7.4 mi) Canals. Based on monitoring data throughout the Upper Jefferson Valley, the leakage rates for both canals were set to 1.31 cfs/mi (appendix A; Bobst and Gebril, in prep.). The canals lose water during the irrigation season (about April to October). The total inflow from canal leakage was estimated to be about 5,898 acre-ft/yr (appendix A).

Irrigation Recharge (IR)

Irrigated fields receive water through irrigation and precipitation. The water satisfies crop demand and evaporation, and any excess either runs off or infiltrates through the root zone to recharge the underlying aquifer. The water that reaches the aquifer is irrigation recharge (IR).

Irrigation recharge rates were assigned based on the type of irrigation: flood, sprinkler, or pivot. The rates assigned to each type were based on a similar study in the nearby Boulder Valley (Butler and Bobst, 2017) that were derived from the NRCS's Irrigation Water Requirements program (NRCS, 2003). The Irrigation Water Requirements program (IWR) uses the following equation:

$$IR = [(NIR/IME + P_{eff}) - ET] \times DP_{ex},$$

where IR is irrigation recharge; NIR is net irrigation requirement; IME is irrigation method application efficiency; P_{eff} is effective precipitation; ET is evapotranspiration; and DP_{ex} is the portion of applied water in excess of ET that results in deep percolation. P_{eff} is "the part of rainfall that can be used to meet the evapotranspiration of growing crops" (NRCS, 1993). DP_{ex} was set to 0.5, which is the default value for the IWR program. NIR, P_{eff}, and ET were estimated from the IWR program. The calculated average irrigation recharge was 4,089 acre-ft/yr. Applying the same methodology, irrigation recharge from irrigated fields located upgradient from the model boundaries was estimated to be 374 acre-ft/yr. The total IR is 4,463 acre-ft/yr (appendix A).

Groundwater Outflux (GW_{out})

Based on the geological setting and groundwater elevations, groundwater outflow occurs at the northeastern boundary primarily through alluvium in the Jefferson River floodplain. The estimated groundwater outflow based on Darcy's Law was about 502 acre-ft/yr (appendix A).

Ponds Evaporation (PE)

Based on pond surface elevations estimated from LiDAR (WSI, 2013), and measured groundwater elevations, ponds within the model area appear to be directly fed by shallow groundwater. Thus, the ponds remove groundwater by evaporation. Fifty-eight ponds in the Whitehall model area range in size from 0.2 to 9.2 acres. An evaporation rate for each pond was estimated based on relationships between weather patterns and evaporation (Jensen, 2010). Evaporation rates and pond surface areas were used to calculate the dynamic evaporation from each pond. The total evaporation rate from all ponds was 306 acre-ft/yr (appendix A).

Riparian ET (ET_r)

Evapotranspiration by riparian plants removes water from aquifers in the floodplain during the growing season (April to October). Based on the LANDFIRE vegetation types database (USGS, 2016), the model area contains woody riparian plants (Cottonwood and Willow; 1,013 acres), riparian grasses (1,416 acres), and mesic forest (180 acres). The annual average ET rates were set at 3 in/yr for riparian grasses and mesic forest, and at 22 in/yr for the woody riparian plants (appendix A; Johns, 1989; Lautz, 2008). Evapotranspiration totaled 1,152 acre-ft/yr.

Well Withdrawals (WL)

Groundwater pumped from wells removes water from the aquifer; however, some of the pumped water returns to the groundwater system through irrigation return flow and septic effluent. The remainder of the withdrawal is considered consumptive use. Well types and numbers in the Whitehall model area include 8 public water supply wells, 312 domestic wells, 25 livestock wells, and 23 irrigation wells. We assigned pumping rates for wells based on their use (appendix A). The calculated consumptive use from all wells was 1,288 acre-ft/yr (appendix A).

Outflow to Surface Water (SW_{out})

The net groundwater discharge to surface water was estimated from the difference between inflows and outflows in the water budget. Calculated inflows exceeded outflows by 8,485 acre-ft/yr, and this provided a preliminary estimate of net groundwater discharge to surface waters.

MODEL DESIGN AND CONSTRUCTION

Mathematical Framework

In groundwater, under saturated conditions, a combination of continuity (mass conservation) and Darcy's Law leads to the following mathematical description of groundwater flow:

$$\frac{\partial}{\partial x}\left(K_x \frac{\partial h}{\partial x}\right)+\frac{\partial}{\partial y}\left(K_y \frac{\partial h}{\partial y}\right)+\frac{\partial}{\partial z}\left(K_z \frac{\partial h}{\partial z}\right)=S\frac{\partial h}{\partial t}-W^*. \quad (1)$$

In this equation (Anderson and others, 2015), the dependent variable is change in hydraulic head (δh) over time (δt), which is defined in the traditional Cartesian coordinate system (x, y, z). The horizontal and vertical hydraulic conductivities (K_x, K_y, and K_z) and storage coefficient (S) are specified. Boundary conditions (W*) and initial head conditions must also be specified to use equation 1 to solve for head values at particular times. The boundary conditions may be specified head (Dirichlet), specified flux (Neumann), or head-dependent flux (Cauchy).

Numerical Model Approximation and Computer Code

The United States Geological Survey (USGS) groundwater flow modeling software MODFLOW-2000 (Harbaugh and others, 2000) was the primary tool for simulating the groundwater system. The code solves the governing equation over the model domain for each time step. MODFLOW uses the finite-difference (FD) method to approximate the groundwater flow equation as a set of algebraic equations in a discretized three-dimensional grid of rectangular cells. Groundwater Vistas (Version 6.77 Build9) was used as the graphical user interface for MODFLOW (Environmental Simulations Incorporated, 2011).

Spatial Discretization

The model grid has 150 rows and 190 columns (28,500 cells per layer), with a uniform grid spacing of 220 ft x 220 ft (fig. 7). Cells outside the model boundaries (e.g., irrigation canals) were inactivated (fig. 7). The projection was set to the North American Datum 1983, Montana State Plane coordinate system, in units of International Feet, a standard by the State of Montana. No conversion to US Feet was made when International Feet was used.

The model uses two layers to represent the groundwater system. This simplified model construction and achieved reasonable solution stability and run times.

Initial model parameters for layer 1 were based on having bench sediments along the sides of the model and alluvium in the central area. Small portions of layer 1 contained the Renova Formation (fig. 4A). The layer is unconfined, and generally extends from the land surface to the top of the Renova Formation. We interpolated and refined available LiDAR data (WSI, 2013), the USGS 10 m DEM for the area (USGS, 2013), and surveyed select locations (fig. 8), to establish the top of layer 1. The thickness of layer 1 varies from 10 ft to 341 ft, based on well logs in the area.

Initial model parameters for layer 2 were based on it being mostly Renova Formation, with some areas of bedrock and bench sediments (fig. 4B). Layer 2 is set as confined (table 1), with a uniform thickness of 100 ft. This thickness was selected because most wells penetrate less than 100 ft into the Renova sediments, and deeper flow paths will have little influence on the groundwater/surface-water interactions that are the focus of this modeling effort. While a greater thickness of layer 2 would simulate a greater volume of aquifer, it would not affect the flux to and from surface waters.

Initial Heads

April 2015 water levels were the basis for the initial heads in the model. These measured values were used to assign heads over the modeling domain, using Surfer 9, to create the initial head distribution (matrix). This head matrix was modified during the calibration process (see Model Calibration Section).

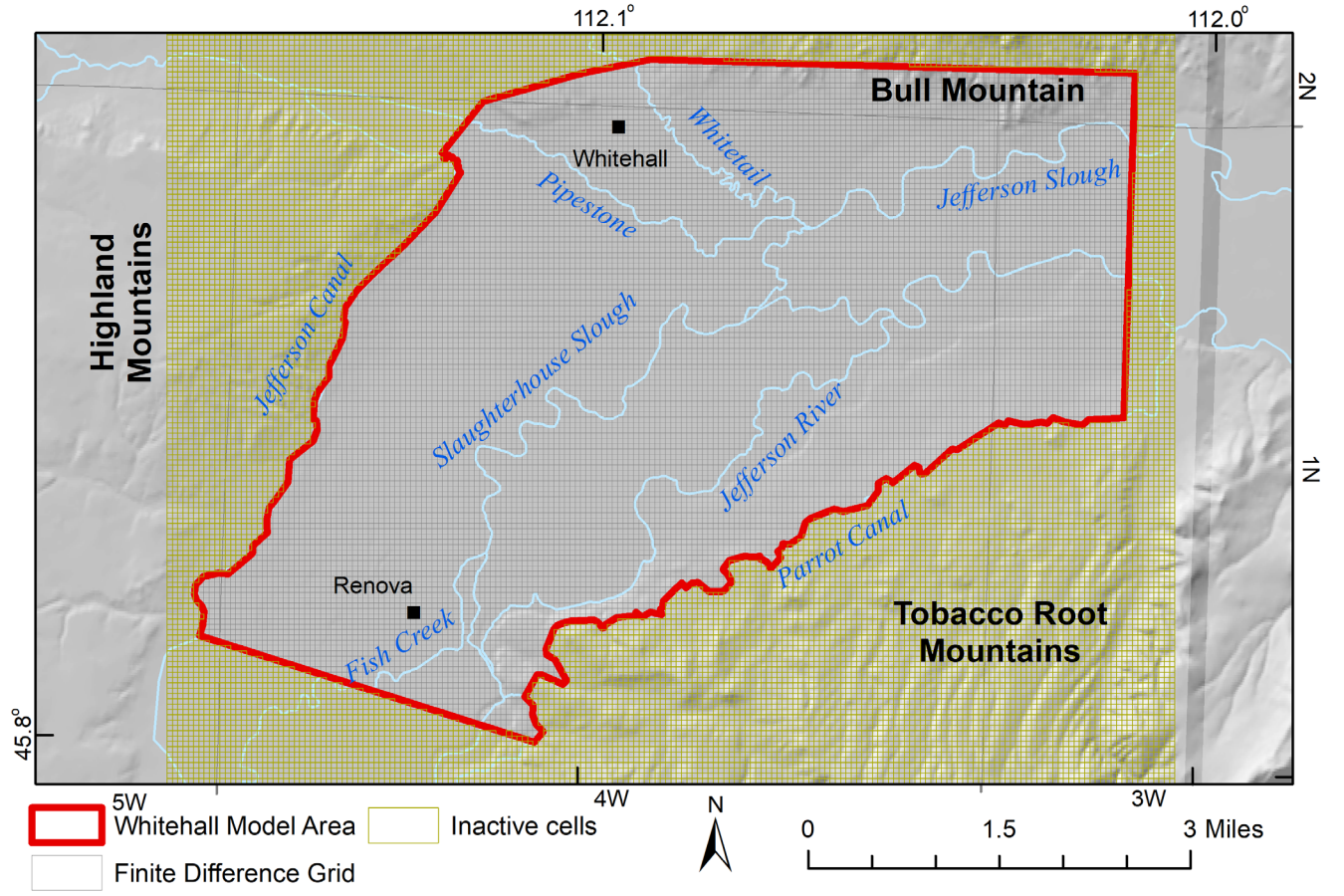

Figure 7. Whitehall flow model grid consists of a uniform 220 ft x 220 ft grid spacing.

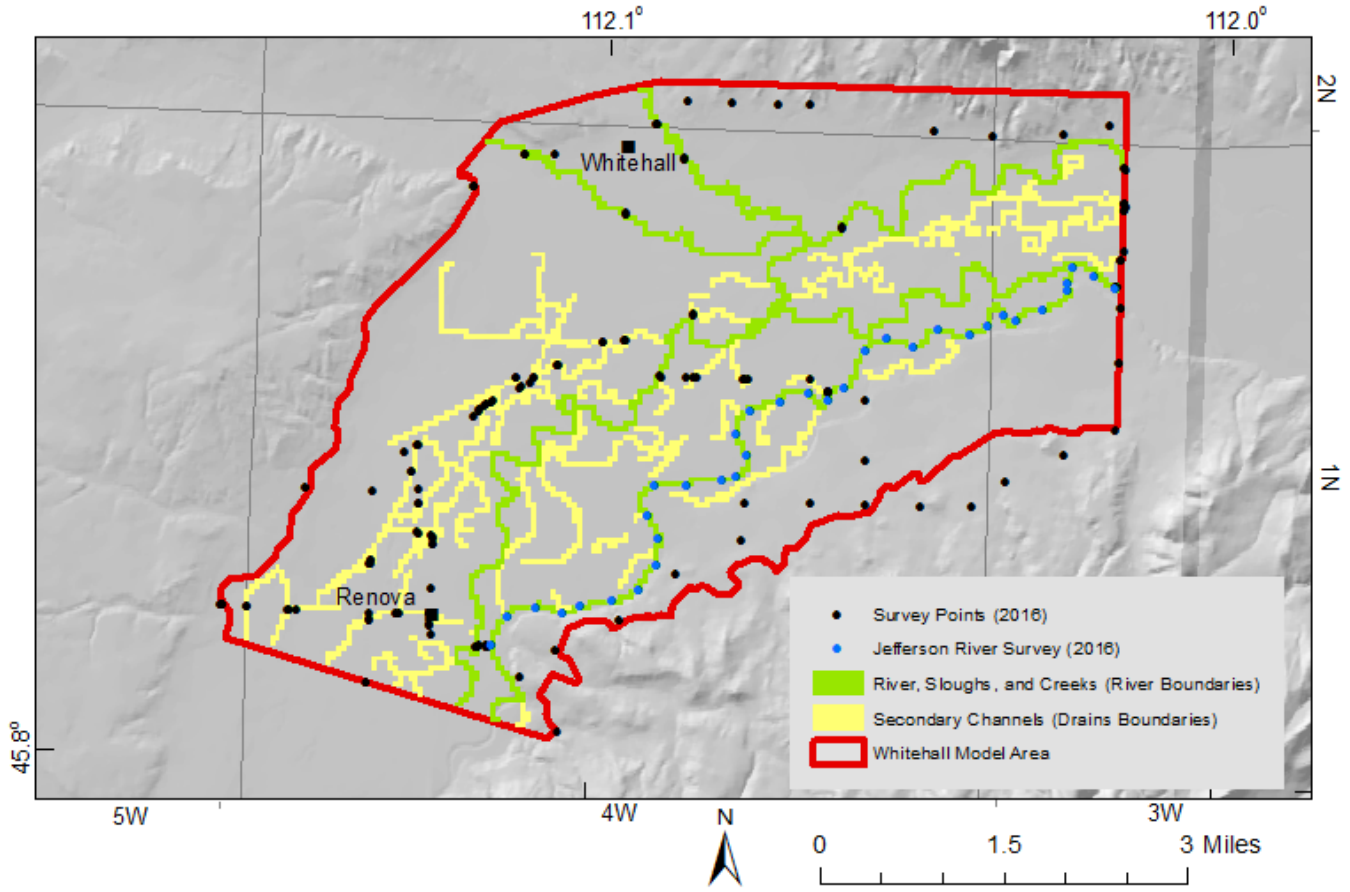

Figure 8. Model boundaries and survey points. Fieldwork included surveying 41 land surface and secondary channel bottom elevations (black) and 35 points on Jefferson River (blue).

Table 1. General stratigraphy, hydrostratigraphy, and model layers.

Geology*		Hydrogeologic Unit	Model Layer 1	Model Layer 2
Quaternary	Alluvium (Qal)	Alluvium	X	
Quaternary	Gravel (Qg)	Bench sediments	X	
Tertiary	Sixmile Creek Formation (Ts)			
Tertiary	Renova Formation (Ts)	Renova Formation		X
Bedrock (BR)		Bedrock	X	X

*For surficial distribution see figure 3.

Temporal Discretization

The transient model imposes monthly stress periods to simulate variations in surface-water flows and seasonal stresses, such as irrigation practices. Each stress period consists of six time steps to accommodate field observations, support numerical stability, and minimize model run time. The duration of each time step depends on the length of the month and ranges from 4.7 to 5.2 days (table 2).

The transient calibration period had 34 stress periods. The first 1-day-long stress period was set as steady-state to generate average boundary conditions and initial heads for the successive stress periods. The other 33 stress periods represent the months from April 1, 2013 to December 31, 2015.

Hydraulic Parameters

With no available information to support horizontal anisotropy, the K_x and K_y terms are represented as a single horizontal hydraulic conductivity term K_h. Vertical hydraulic conductivity term (K_z) is replaced by (K_v). Prior to model calibration, initial values of horizontal hydraulic conductivity (K_h), vertical hydraulic conductivity (K_v), specific yield (S_y), and specific storage (S_s) were assigned to both layers using 5 zones in layer 1 and 5 zones in layer 2. These zones represent areas within the hydrogeologic units: the alluvium, the underlying Renova Formation, the bench sediments, and the bedrock units (figs. 3, 4A, 4B). K_h values ranged from 1 ft/d for the bedrock to 500 ft/d for the alluvium, and K_v was set as 10% of K_h. Parameter values were modified during the calibration process (see Calibration section).

Boundary Conditions

Flow model boundary conditions control the addition or removal of water (mass) from the model. These boundary conditions are mathematical expressions of the aquifer system that constrain the numerical model. They are assigned to the edges of the model domain and to internal sources and sinks (ASTM, 2010). In equation 1, boundary conditions are represented by the W* term. In this model, boundary conditions follow the conceptual model discussed in the Hydrologic Boundaries and Groundwater Budget sections and include both head-dependent flux and specified-flux formulations.

Head-Dependent Flux Boundaries

The Whitehall model uses three MODFLOW packages that implement head-dependent flux boundaries. These represent surface-water features and removal of groundwater by riparian plant evapotranspiration (ET_r). The MODFLOW river package (RIV) simulates the Jefferson River, Slaughterhouse Slough, Jefferson Slough, Pipestone Creek, and Whitetail Creek (figs. 6A, 6B). The MODFLOW drain package (DRN; figs. 6A, 6B) simulates flow in the ditch network, which collects excess water from irrigated areas and from low lands. ET_r is simulated with the MODFLOW EVT package (figs. 6A, 9).

Seasonal changes in heads at these boundaries, including those specified by the user and those simulated in the aquifer, affect the rate at which water flows to or from these head-dependent boundaries. During model runs, MODFLOW calculates the amount of water entering and leaving the model through head-dependent boundary cells. For instance, the simulated fluxes at these boundaries can be used to calculate reductions or

Table 2. Model stress periods.

Stress Period	Month	# Days	# Time Steps	# Days in Time Step	Type
1	March 2013	1	1	1	SS
2	April 2013	30	6	5.00	TR
3	May 2013	31	6	5.17	TR
4	June 2013	30	6	5.00	TR
5	July 2013	31	6	5.17	TR
6	August 2013	31	6	5.17	TR
7	September 2013	30	6	5.00	TR
8	October 2013	31	6	5.17	TR
9	November 2013	30	6	5.00	TR
10	December 2013	31	6	5.17	TR
11	January 2014	31	6	5.17	TR
12	February 2014	28	6	4.67	TR
13	March 2014	31	6	5.17	TR
14	April 2014	30	6	5.00	TR
15	May 2014	31	6	5.17	TR
16	June 2014	30	6	5.00	TR
17	July 2014	31	6	5.17	TR
18	August 2014	31	6	5.17	TR
19	September 2014	30	6	5.00	TR
20	October 2014	31	6	5.17	TR
21	November 2014	30	6	5.00	TR
22	December 2014	31	6	5.17	TR
23	January 2015	31	6	5.17	TR
24	February 2015	28	6	4.67	TR
25	March 2015	31	6	5.17	TR
26	April 2015	30	6	5.00	TR
27	May 2015	31	6	5.17	TR
28	June 2015	30	6	5.00	TR
29	July 2015	31	6	5.17	TR
30	August 2015	31	6	5.17	TR
31	September 2015	30	6	5.00	TR
32	October 2015	31	6	5.17	TR
33	November 2015	30	6	5.00	TR
34	December 2015	31	6	5.17	TR

Note. Type: SS, steady-state; TR, transient. Highlighted: months with available water-level measurements.

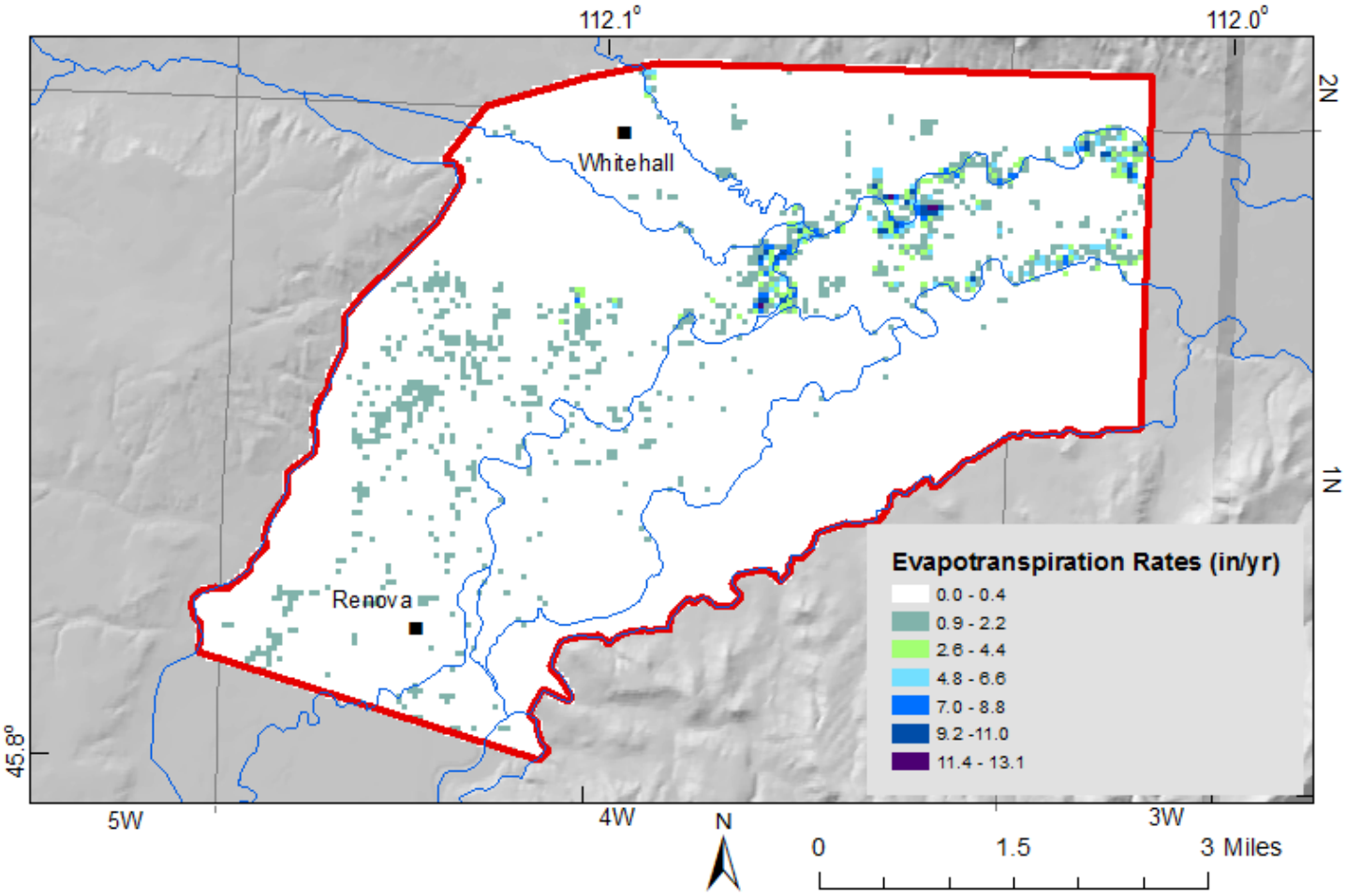

Figure 9. Steady-state model evapotranspiration rate distribution, limited to the model's upper layer (layer 1). Based on the LANDFIRE vegetation types database (USGS, 2016), the model area contains woody riparian plants (Cottonwood and Willow; 1013 acres), riparian grasses (1,416 acres), and mesic forest (180 acres). The annual average ET rates for riparian grasses and mesic forest were set at 3 in/yr, and 22 in/yr for the woody riparian plants.

increases in groundwater flow to river cells if groundwater heads rise or fall due to changes in pumping.

Major Surface-Water Features

The river package was used to simulate interactions between the aquifer and the Jefferson River, Slaughterhouse Slough, Jefferson Slough, Pipestone Creek, and Whitetail Creek. This package simulates flow between these surface waters and groundwater. Unlike MODFLOW's stream packages (STR or SFR), the RIV package does not perform any surface-water routing computations, but it efficiently calculates flux to and from groundwater through an interface that represents the riverbed. The package applies user-specified stage in river cells to simulate monthly variation in surface-water features during model execution.

The RIV package calculates flux across the streambed (riverbed) as:

$$Q = C\,(h_b - h_a),$$

where Q (ft^3/d) is the flux across the riverbed, C (ft^2/d) is the riverbed conductance (a function of riverbed materials thickness, its vertical hydraulic conductivity (K_v), the river width, and the length of the river segment in each cell), h_b is the river stage, and h_a is aquifer head (fig. 10). An initial estimate of K_v was based on 10% of the initial estimate of aquifer horizontal hydraulic conductivity (K_h), and was adjusted during model calibration.

A field survey conducted in September 2016 provided information about the Jefferson River. We surveyed river stage and measured depth to streambed at 35 locations along the river (fig. 8). Streambed elevation was calculated by subtracting measured stream depth from surveyed river stage. Stage and streambed elevations in model cells were interpolated with Groundwater Vistas software. We assumed that the surveyed river stage represents the average stage during September 2016, in part because no major rainfall event occurred during the month; maximum daily

precipitation near Whitehall was 0.42 in (MesoWest Synoptic Data, 2020). Consequently, these data were used to extrapolate the average monthly stages for the remaining months in 2016 based on stage monitoring data (appendix B), and assumed that this pattern is repeated each year.

The RIV package assigns numbers to river reaches, each composed of one or more cells, to enhance processing the model results. Table 3 presents a summary of river reaches used with the RIV package.

Secondary Surface-Water Features

An extensive network of drains and minor channels in the study area facilitate drainage from irrigated fields and low-lying areas to the Jefferson River and other major streams. These features are represented with the MODFLOW Drain package (DRN; figs. 6A, 6B). The drain conductance and the difference between the groundwater head and drain elevations determine the flux to the drain (fig. 10). MODFLOW implements the same formula used in the RIV package with the exception that water cannot flow from the drain to aquifer. Thus, if groundwater elevation (h_a) in the drain cell—or adjacent cells—is equal to or less than the drain elevation (h_b), there is no simulated flux. Twenty-six drain segments (fig. 8) represent drains and minor channel networks in the model.

The September 2016 field work included surveying land-surface and channel-bottom elevations at 41 drains and channels. The survey and LiDAR data were used to assign elevations to drains in the model. The main variables needed to simulate drains are the drain elevation and drain conductance. Drain elevations were initially set at 3 ft below ground surface based on air photos and the field survey. These elevations were adjusted during steady-state calibration. Based on air photos, a width of 20 ft was applied to all drains. The DRN package calculates conductance the same as the RIV package, and we again assigned initial K_v as 10% of the initial estimate of aquifer horizontal hydraulic conductivity. These values were later adjusted during model calibration.

Evapotranspiration

The MODFLOW EVT package simulated riparian evapotranspiration (ET_r) as a flux equal to the portion of groundwater consumed by riparian vegetation. Evapotranspiration from agricultural fields is not simulated by ET package; ET is already accounted for in irrigation recharge calculations (appendix A). The ET_r flux depends on the head in the cell and on three user-specified variables: maximum extinction depth, surface elevation, and maximum ET_r rates. The extinction depth was set to 10 ft below ground surface, which is an estimate of the root depth (Shah and others, 2007). The surface elevation for each cell was set equal to the top elevation, which was interpolated from a DEM. Riparian vegetation was limited to the dominant three types in the area, mesic forest, riparian, and riparian grass; the extent of each was estimated from air photos and the LANDFIRE vegetation types database (USGS, 2016). Evapotranspiration is simulated during the growing season, April through September, with maximum ET rates in July. Maximum ET rates varied based on the vegetation type (fig. 9, table 4). The initial ET rates reported in table 4 were set at 50% of the rates cited in the groundwater budget section because ET only occurs for about half of each year (Johns, 1989; Lautz, 2008). ET rates were varied during model calibration. In cells that contain more than one type of vegetation, the ET rate was calculated

Table 3. MODFLOW River Package reaches.

Surface-Water Feature	Number of Reaches	Reaches
Jefferson River	35	#1 to #35
Fish Creek	1	#49
Slaughterhouse Slough	1	#50
Jefferson Slough	7	#51 to #57
Whitetail Creek	3	#58 to #60
Pipestone Creek	3	#61 to #63

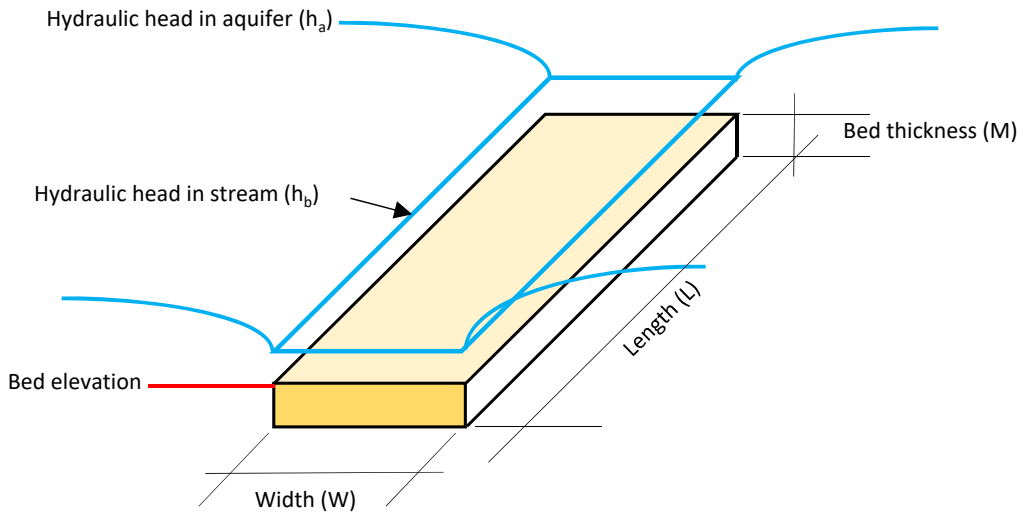

Figure 10. Model river/drain schematics. In drain cells, there is no flow when the head in the aquifer is below or at bed elevation. In river cells, water flows to or from the river cell depending on the head difference between the aquifer and the stream.

as the sum of each vegetation type rate multiplied by its fraction of the cell. ET input in the transient model reflected changes in evapotranspiration rates over time (appendix A).

Specified-Flux Boundaries

Specified-flux boundaries add or remove a prescribed amount of water. MODFLOW 2000 also implements some specified flux boundaries as injection/extraction wells using the WEL package. In the Whitehall model, the WEL package was used to represent (1) alluvial groundwater flow into and out of the model, (2) groundwater influx entering the model through bedrock, (3) lateral groundwater recharge (inflow), (4) leakage from irrigation canals, and (5) evaporation from ponds (figs. 6A, 6B). The WEL package was implemented to simulate alluvial flow because the General Head Boundary package (GHB) requires more information to estimate a conductance term and it is logistically easier to include all boundary fluxes in one package. Recharge was modeled as a specified flux boundary with the recharge, RCH, package (fig. 11).

Alluvial Groundwater Influx and Outflux

Groundwater flows into and out of the model area through the alluvium. Groundwater flows through the alluvium at the southern boundary, and through the alluvium along Pipestone and Whitetail Creeks. Groundwater flows out through the alluvium at the northeast boundary (fig. 6B).

Based on Darcy flow calculations (Groundwater Budget section and appendix A), the total alluvial influx was set to 1,188 acre-ft/yr. Similarly, groundwater outflux was set to 410 acre-ft/yr (205 acre-ft/yr through the alluvium and 205 acre-ft/yr through Renova Formation). We placed 108 injection wells in layer 1 to supply the alluvial groundwater influx, including 75 wells in the main valley, 17 wells along the Pipestone section, and 16 for the Whitetail section.

Table 4. Evapotranspiration rates in non-irrigated areas.

Vegetation	Depth (ft)	ET Rate (in/yr)*	Adjusted ET Rate (50%) (in/yr.)	Area (acres)	Total ET Rate (acre-ft/yr)
Mesic Forest	10	3.1	1.5	180	23
Riparian	10	22.5	11.2	1,013	948
Riparian Grass	10	3.1	1.5	1,416	180

*Rates are based on Lautz (2008) and on Butler and Bobst (2017).

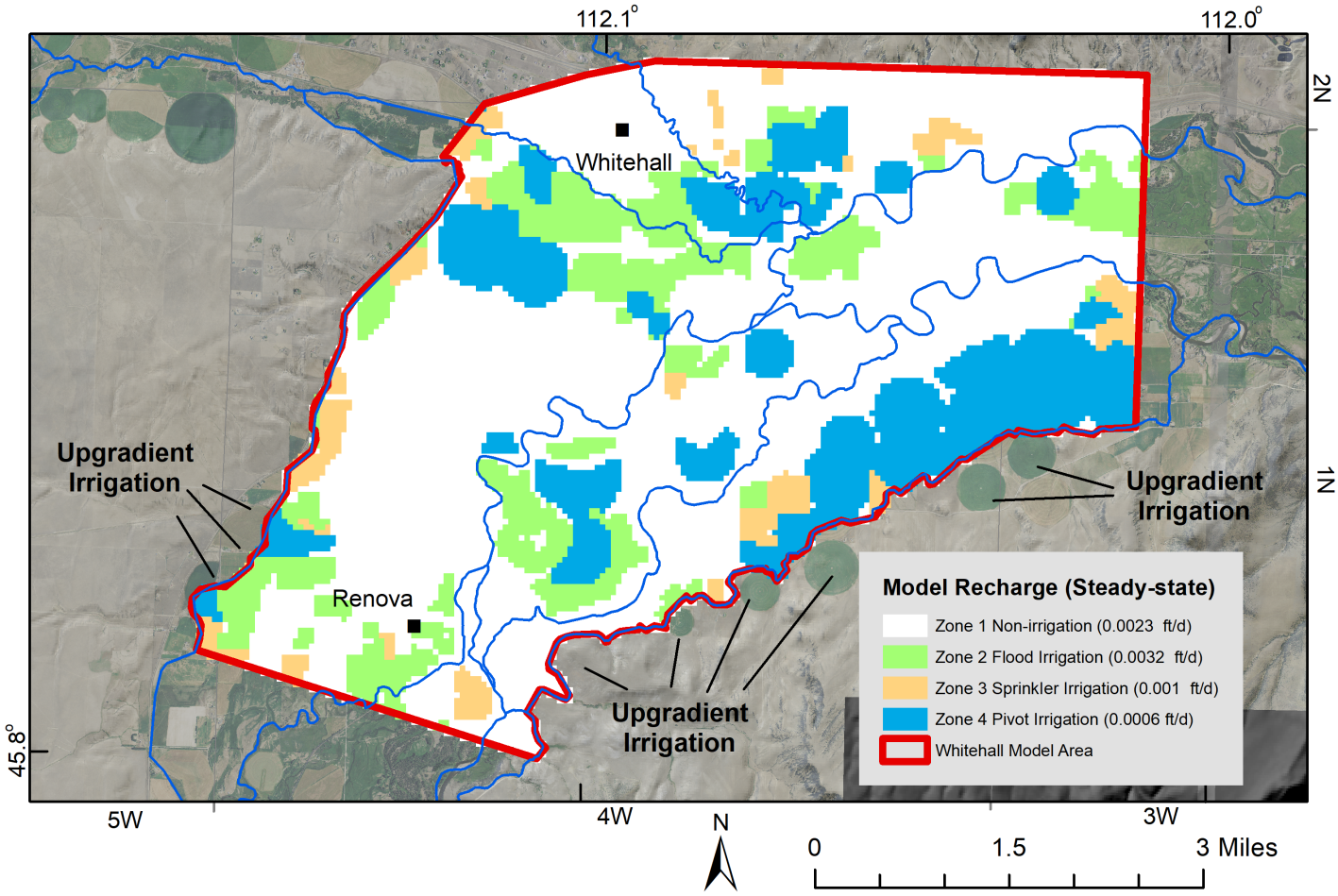

Figure 11. Four recharge zones represent areas with non-irrigated recharge, flood-irrigated recharge, sprinkler-irrigated recharge, and pivot-irrigated recharge.

An additional 109 wells were placed in layer 2 to provide the deeper influx through the Renova Formation, including 76 wells in the main valley, 17 wells along the Pipestone section, and 16 for the Whitetail section. Groundwater outflux at the northeastern boundary is simulated by 84 extraction wells, with 42 wells in each model layer.

Bedrock/Tertiary Influx

We identified four areas along the northern model boundary as a likely source of groundwater influx from bedrock and Renova Formation deposits (figs. 6A, 6B), with total estimated influx of 77 acre-ft/yr. This influx is divided among 234 injection wells, with 117 wells in each layer.

Canal Leakage, Lateral Groundwater (GWlat), and Upgradient Irrigation Recharge

Specified flux boundaries established along the Jefferson and Parrot Canals represent the combined water flowing to the model from canal leakage, lateral groundwater influx, and upgradient irrigation recharge from outside the model domain (figs. 6A, 6B, and 11). Both the Jefferson and Parrot Canal boundaries were divided into segments to simulate spatial variation of upgradient irrigated fields (appendix A).

The leakage rates for Jefferson and Parrot Canals were set to 1.31 cfs/mi in the transient model, based on the annual rate calculated for both canals (Groundwater Budget section and appendix A). The canals operate about 6 mo each year, during the irrigation season of April through October, and this leakage rate was applied only during that time in the transient model (table C1, appendix C). The annual average rate applied in the steady-state model is 50% of the calculated leakage, 0.66 cfs/mi. Injection wells placed along Jefferson and Parrot Canals in layer 1 simulate canal leakage, and include 152 injection wells along Jefferson Canal and 222 wells along Parrot Canal (appendix A).

Lateral groundwater influx ($GW_{lat\text{-}in}$) along the edges of the model occurs through the Renova Formation and through bedrock. At an estimated rate of 215 acre-ft/yr, this flow is added as uniform flux split

between model layer 1 and model layer 2, through the 152 injection wells along Jefferson Canal and in the 222 wells along Parrot Canal (appendices A and C). The total flow was subject to change in the transient calibration (tables C1 and C2, appendix C).

Upgradient groundwater recharge from irrigated fields outside of the model domain (fig. 11) was added along the canals with the injection wells used to simulate canal leakage in layer 1. The flux from the outside irrigation recharge is applied only during the irrigation season, and varies monthly. The flow was estimated with the same recharge rates applied to irrigated areas within the model boundaries, depending on irrigation type (pivot, flood, and sprinkler) and irrigated area (air photo). Recharge from outside irrigation is assumed readily available at the boundaries (canals), without consideration of the distance of this recharge from the boundary, because water-level data were not available upgradient of the irrigation canals. The annual outside irrigation recharge was estimated to be 374 acre-ft/yr. In the groundwater budget, irrigation recharge was a combination of outside irrigation flow plus irrigation recharge in areas inside the model domain (appendix A).

Recharge

Within the model domain, we applied irrigation recharge as a specified-flux boundary using the RCH package (fig. 11). The RCH package applies flux in units of length over time (L/T) and is applied in this model over areas designated as irrigated fields. The areas were derived from the Statewide Final Land Unit classification database [Montana Department of Revenue (MDOR), 2012], and field visits. The annual total amounts of irrigation recharge were 3,136 acre-ft by flood, 447 acre-ft by sprinkler, and 882 acre-ft by pivot (appendix A). Application rates in the steady-state model are listed in table 5. For surficial distribution of irrigation recharge, we considered three recharge zones to represent the three irrigation methods (fig. 11). A fourth zone designated non-irrigation recharge was added (8,317 acre-ft/yr) and is discussed later in this report (table 5, fig. 11).

Pumping Wells

MODFLOW's WEL package simulates four types of wells in the model. These include domestic, livestock, irrigation, and public water supply (PWS) wells.

Domestic well consumptive use was calculated using the rates determined for the North Hills, located north of Helena, Montana, based on 15 yr of water-use records (Waren and others, 2013). We expect domestic water-use rates to be similar in the North Hills and Whitehall areas as they both lie within intermontane valley settings in western Montana. The average annual consumptive use was 435 gallons per day (gpd) per residence (58.15 ft^3/d). There were 307 homes identified in the Whitehall study area that are not connected to public water supplies. Five PWS wells in the area serve individual businesses, and we assumed water use for these wells at rates similar to that of domestic wells. Thus, the annual consumption for domestic and non-municipal PWS wells was estimated to be about 152 acre-ft/yr.

Twenty-five wells within the model domain are livestock wells, and we assigned a withdrawal rate of 693 gpd per well based on a method provided by Butler and Bobst (2017). Assuming that all livestock water is consumptively used, livestock consume 19.4 acre-ft/yr of groundwater.

Based on GWIC data, water-rights information, and aerial photographs, there are 22 active irrigation wells in the study area. Withdrawal rates for irrigation wells were based on permitted volumes. Since irrigation water returned to the aquifer is already accounted for by simulating irrigation recharge, the withdrawal rate for irrigation wells was considered the consumptive use rate. The estimated total annual groundwater withdrawal by irrigation wells was 511 acre-ft/yr.

There are seven active PWS wells in the model area. Two of these supply the town of Whitehall, and five supply individual businesses. The individual business wells are described above, with domestic wells. Using per capita water use data from Boulder, Montana (Butler and Bobst, 2017), the withdrawal rate for the Whitehall wells is estimated at 605 acre-ft/yr. This volume is consumptively used, since the sewer system does not discharge to groundwater.

Well withdrawals within the model area total 1,287 acre-ft/yr, with about 40% irrigation, 47% public water supply, 12% domestic water, and 1% livestock water.

Ponds

Fifty-eight ponds in the model area remove groundwater from the aquifer through evaporation. Based on calculated free water surface evaporation

Table 5. Steady-state model irrigation recharge.

		IWR Monthly Recharge Rates* (in)			IWR Monthly Recharge Rates* (ft)			IWR Daily Recharge Rates (ft/d)			Steady-State Model Recharge Rates** (ft/d)			
	Days	Flood	Sprinkler	Pivot	Flood	Sprinkler	Pivot	Flood	Sprinkler	Pivot	Flood	Sprinkler	Pivot	Non-irrigation
January	31	0	0	0	0.00	0.00	0.00	0.00000	0.00000	0.00000	0.00319	0.001	0.00059	0.0023
February	28	0	0	0	0.00	0.00	0.00	0.00000	0.00000	0.00000	0.00319	0.001	0.00059	0.0023
March	31	0	0	0	0.00	0.00	0.00	0.00000	0.00000	0.00000	0.00319	0.001	0.00059	0.0023
April	30	1.32	0.50	0.24	0.11	0.04	0.02	0.00367	0.00139	0.00067	0.00319	0.001	0.00059	0.0023
May	31	5.72	2.16	1.03	0.48	0.18	0.09	0.01538	0.00581	0.00277	0.00319	0.001	0.00059	0.0023
June	30	5.63	2.13	1.01	0.47	0.18	0.08	0.01564	0.00592	0.00281	0.00319	0.001	0.00059	0.0023
July	31	3.84	1.45	0.69	0.32	0.12	0.06	0.01032	0.00390	0.00185	0.00319	0.001	0.00059	0.0023
August	31	2.51	0.95	0.45	0.21	0.08	0.04	0.00675	0.00255	0.00121	0.00319	0.001	0.00059	0.0023
September	30	2.36	0.89	0.42	0.20	0.07	0.04	0.00656	0.00247	0.00117	0.00319	0.001	0.00059	0.0023
October	31	2.65	1.00	0.48	0.22	0.08	0.04	0.00712	0.00269	0.00129	0.00319	0.001	0.00059	0.0023
November	30	0	0	0	0.00	0.00	0.00	0.00000	0.00000	0.00000	0.00319	0.001	0.00059	0.0023
December	31	0	0	0	0.00	0.00	0.00	0.00000	0.00000	0.00000	0.00319	0.001	0.00059	0.0023
Annual	365	24.03	9.08	4.32	2.00	0.76	0.36							

*For additional details see appendix A.
**Adjusted rate to account for partial grid cell recharge, to maintain water-budget recharge in the preliminary (conceptual) budget.

rate of 3.29 ft/yr, evaporation consumes about 306 acre-ft/yr of groundwater (appendix A). In the model, 287 extraction wells in model layer 1 simulate pond evaporation, with the number of wells per pond depending on the pond's areal extent.

No-Flow

No-flow boundaries are a type of specified-flux boundary where there is no flow into or out of the cell. Referred to as inactive cells, these boundaries surround the model's perimeter specified-flux boundaries. Assigning no-flow boundaries to portions of the grid beyond the area of interest removes these cells from the numerical solution and can improve model run times. As shown in figure 5, the potentiometric lines near the southeast region and the northeast edge of the model are mostly perpendicular to the model boundary. This implies little or no flow across these regions of the model boundary. Therefore, we assigned no-flow boundaries in these areas (fig. 6B).

MODEL CALIBRATION

Model calibration involves making systematic changes to the model's parameters in order to match field measurements (e.g., groundwater elevations) within some acceptable error. The ultimate goal of model calibration is to identify a set of model parameters that make the model useful to predict future system behavior with confidence. One challenge in model calibration is the non-uniqueness problem, wherein different combinations of model parameters produce an equally good match to field measurements, producing another calibrated model. For this model, we used field data and published values for hydraulic conductivities, calculated canal leakage rates, and surveyed river stations and river stages. This reduces the possibility of producing non-unique solutions and supports accurate representation of site-specific conditions.

Steady-State Calibration

A steady-state model simulates the groundwater flow system in equilibrium with boundary stresses, including surface-water flows. The goal of the steady-state calibration was to adjust model parameters, within a reasonable range, to simulate the average groundwater head distribution, while keeping the water budget similar to estimated values. A steady-state simulation can be useful in predicting the ultimate impact to the groundwater flow system from anticipated future stress, assessing the total groundwater flow budget, and estimating hydraulic conductivity and stream and drain conductance independently from storage parameters (Doherty and Hunt, 2010).

Calibration Targets

Calibration targets included observed groundwater elevations from the monitoring well network. The targets were split into two groups. MBMG staff surveyed and monitored 16 wells from June 2013 to October 2015, with a range of 4 to 23 measurements per well, with 300 total measurements. Hourly water-level records were available from several wells equipped with recording pressure transducers. A second group of 30 wells had only one static water-level measurement reported by the driller at the time of construction, and were not surveyed. The first group of wells was assigned a calibration weight of 1 while the second group was given a weight of 0.1. At non-surveyed sites land-surface elevations were determined using LiDAR data, if available, or the USGS DEM (10 m). Based on well construction logs, we placed 10 wells in layer 1 (4 from group one and 6 from group two) and 36 wells in layer 2 (12 from group one and 24 from group two; figs. 12A, 12B).

To estimate a water level for each well to be used for steady-state calibration, monthly average values were calculated and then averaged for the years 2013, 2014, and 2015 (table 6). The water levels reported from construction of the group 2 wells were also used as steady-state targets with the lower weight, as described above (figs. 12A, 12B).

Calibration Methods

The steady-state model was calibrated to produce groundwater heads that reasonably matched observed water levels at selected target wells (minimizing the residuals). As part of the calibration method, we divided the active portions of both model layers into zones, generally following the geologic setting (fig. 3). Ten zones developed for the calibration process are assigned to one or more areas within the model. We assigned initial horizontal and vertical conductivities (K_h and K_v) to each zone (figs. 4A, 4B). The calibration process involved manually adjusting K_h and K_v in all zones. Within each zone, K_h and K_v were kept uniformly constant, i.e., they do not vary within each zone.

Table 6. Model: Groundwater targets.

Well Id (GWIC)	X Coordinate* (ft)	Y Coordinate* (ft)	Layer	Average Monthly Water-Level Elevation (ft)	Weight	Group*
237722	1295038.9	579560.2	2	4381.9	1	1
48626	1298658.9	581071.0	2	4372.9	1	1
156080	1291125.6	582183.8	2	4398.6	1	1
48577	1312035.3	587126.3	2	4341.5	1	1
280978	1319445.9	588235.0	2	4344.1	1	1
48569	1309160.8	591114.5	2	4338.1	1	1
171688	1295278.5	591407.9	2	4371.1	1	1
277285	1316053.7	591677.2	1	4327.3	1	1
277282	1302749.7	592295.2	1	4351.5	1	1
279262	1314330.0	593617.7	2	4329.3	1	1
277286	1328206.3	596185.1	1	4301.0	1	1
48522	1301044.5	599560.4	2	4362.6	1	1
48378	1328090.3	599747.3	2	4300.8	1	1
48521	1300948.6	602004.0	2	4368.5	1	1
48477	1309531.1	602209.6	1	4342.0	1	1
247793	1312690.0	602715.6	2	4331.0	1	1
48381	1327169.4	598520.5	2	4299.0	0.1	2
48386	1326485.5	596641.4	2	4289.2	0.1	2
48424	1323539.1	590043.7	1	4346.0	0.1	2
48461	1309806.7	600225.2	2	4339.7	0.1	2
48527	1299432.8	598225.2	1	4401.3	0.1	2
48547	1306968.5	597327.9	2	4343.8	0.1	2
48590	1301419.9	589591.5	1	4353.3	0.1	2
48603	1295330.0	587759.9	2	4328.1	0.1	2
48605	1295865.7	583150.6	2	4372.8	0.1	2
48611	1297698.0	583581.9	2	4369.5	0.1	2
48616	1298502.7	582407.9	2	4365.7	0.1	2
48623	1302493.2	580949.3	1	4369.2	0.1	2
48681	1290237.5	581782.2	2	4410.7	0.1	2
120988	1315771.3	600688.6	1	4323.7	0.1	2
126672	1309543.9	597228.5	2	4331.7	0.1	2
127059	1314788.5	603048.2	2	4274.0	0.1	2
134915	1309242.5	584013.7	2	4370.8	0.1	2
143492	1296818.3	581472.1	2	4371.3	0.1	2
144711	1295034.9	588788.8	2	4367.4	0.1	2
153805	1295523.2	581535.2	2	4371.8	0.1	2
170414	1327797.4	593885.8	2	4325.4	0.1	2
202071	1309319.5	594486.2	2	4330.0	0.1	2
203498	1310301.5	586298.6	2	4323.7	0.1	2
209419	1317132.0	600644.1	2	4310.0	0.1	2
211036	1307466.0	601309.4	1	4345.5	0.1	2
218151	1317417.8	598970.0	2	4321.0	0.1	2
221498	1300173.3	580694.7	2	4368.3	0.1	2
230659	1318289.4	591561.7	2	4323.3	0.1	2
252255	1307272.6	593631.2	2	4335.5	0.1	2
258872	1298332.8	587999.1	2	4351.8	0.1	2

*Coordinate system: NAD 1983, State Plane Montana FIPS 2500 Intl. Feet

**Group: 1, wells with multiple water levels; 2, domestic wells with a single water level.

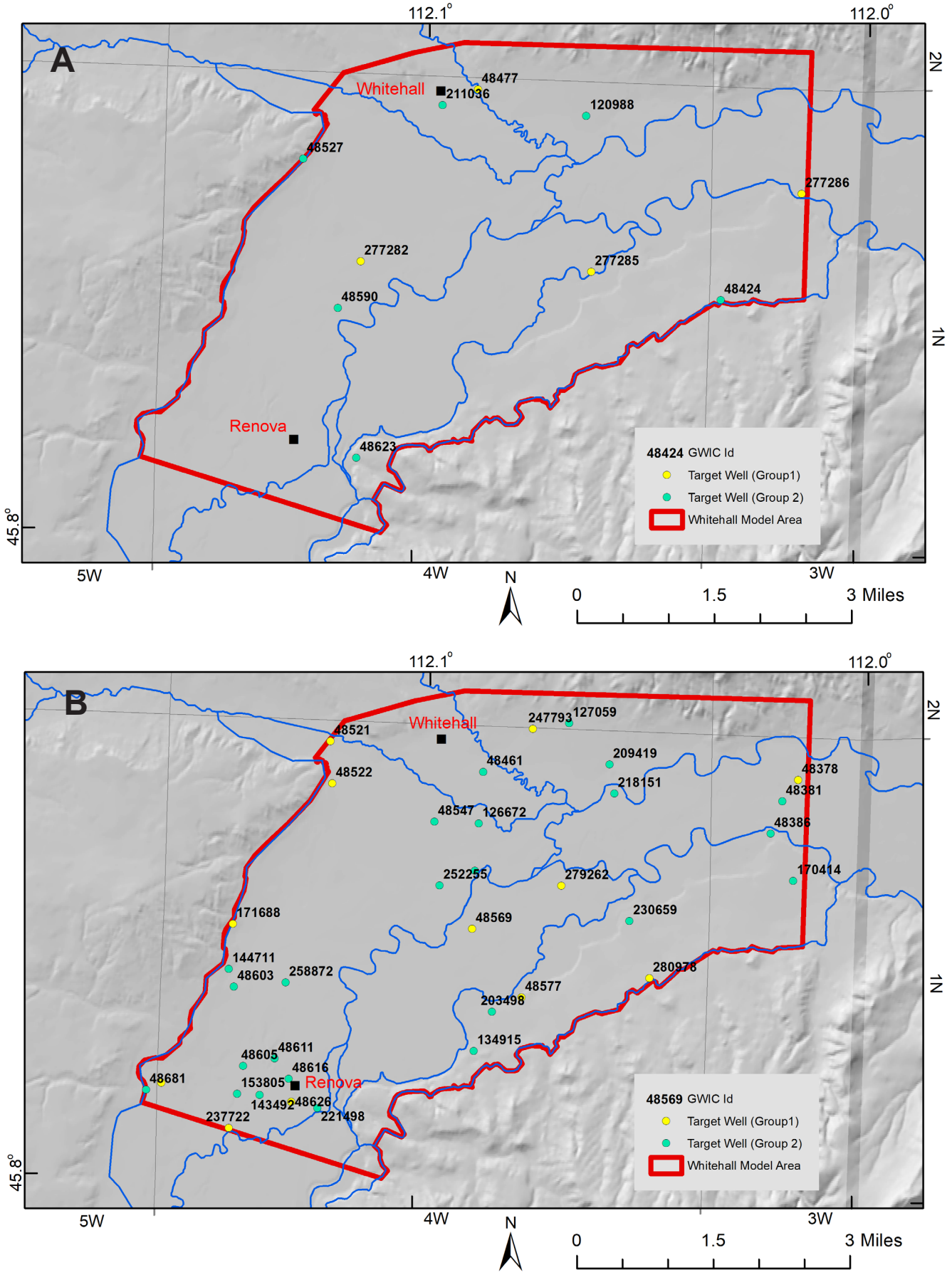

Figure 12. (A) Steady-state calibration depended on 10 wells placed in the upper model layer (layer 1). Annual average of groundwater elevations in group 1 wells (given 100% weight) and one measurement from group 2 wells (given a 10% weight). (B) Steady-state calibration based on the annual average of groundwater elevations in 36 wells placed in model layer 2.

For steady-state calibration, five primary zones in layer 1 included two zones for the alluvium, one zone for bench sediments, one zone for the Renova Formation, and one for bedrock outcrop. A sixth zone, Zone 10, was added and assigned to Pipestone and Whitetail Creeks (fig. 13A). The six hydraulic conductivity zones in model layer 2 represent variations in the Renova Formation and bedrock (fig. 13B). Additional zones were added in some areas of layer 2 to improve the calibration (figs. 13A, 13B).

The calibration criterion for groundwater heads was set as a ±10 ft head residual (observed minus modeled), which, as recommended by Anderson and others (2015), was approximately 10% of the range of observed groundwater elevations within the model area (table 7). Head error statistics were used to evaluate model calibration, including the square root of the average squared residuals—also known as the root mean square error (RMS), the residual mean error (ME), and the mean of the absolute value of the residual error (MAE). The model inflows and outflows were compared to the estimated water budget, and the distribution of aquifer properties was evaluated relative to the geologic model.

During calibration, pumping rates at the target wells were set to zero to avoid simulating drawdown at their locations, since water elevations were measured under static conditions. In order to maintain water balance and avoid instability in the model solution, the cumulative amount of water pumped by the target wells was added evenly to pumping rates at the remaining 246 non-target domestic wells.

For the steady-state calibration, we estimated the river stage by capitalizing on the September 2016 survey and on the available 2014 data. The September 2016 survey was the most recent and complete survey, and covered 16 monitoring stations (where stage and discharge are measured) and 35 surveyed points on the Jefferson River. Compared to 2013 and 2015, the year 2014 has the most stage and discharge data for the Jefferson River. However, September is typically a low-flow month, and river stage in September 2016 is expected to be lower than the average stage (i.e., September flows and stages do not represent the average annual river conditions). For this reason, we estimated the average annual river stage, at any station, by adding an offset calculated from 2014 data to the September 2016 surveyed stages (appendix B).

Calibration Results

The head residuals (figs. 14A, 14B) and potentiometric surface (figs. 15A, 15B) present a reasonably calibrated steady-state simulation. The effect of surface-water bodies on groundwater is clear: the network of drains and minor channels generally gain groundwater. The Jefferson River, the sloughs, and other streams show a mix of gaining and losing conditions. The steady-state calibration results show a close match between observed and modeled heads (figs. 14A, 14B, 16A). Qualitatively, the simulated potentiometric contours show the effect of the drains and the river gaining and losing reaches, consistent with the conceptual model.

Computed weighted head residuals from the target wells were all below the 10 ft criteria. Only three wells had residuals greater than 5 ft: one in layer 1 (GWIC 48477) and two in layer 2 (GWIC 247793 and 27059). Of the 46 targets, 23 of the residuals (50%) were less than 1 ft, 20 residuals (43%) were between 1 and 5 ft, and 3 residuals (7%) were between 5 and 7.5 ft (table 8). The ME was 0.11 ft, the RMS was 2.3 ft, and the absolute mean error MAE was 1.6 ft (table 9).

The final calibrated distribution of the hydraulic conductivity zones followed the geologic model (fig. 3). Table 10 summarizes the initial estimates and final calibrated hydraulic conductivities for the steady-state model. All vertical hydraulic conductivities were initially set to 10% of the K_h and adjusted during calibration. Vertical hydraulic conductivity remained within the 10% of the K_h range in all hydrogeologic units except the Renova Formation, where the ratio was reduced to a lower ratio of 1%.

The mass balance (water budget) for the Whitehall calibrated steady-state model was comparable to the estimated conceptual mass balance. The initial steady-state model without non-irrigation recharge matched well with the preliminary budget. Total inflow and outflow values for the initial steady-state model were within 5% of the preliminary water-budget estimates (table 11A). However, during transient calibration it became clear that non-irrigation recharge was needed, so the steady-state model was rerun with this added recharge. The overall steady-state calibration was slightly improved, but the water budget has changed due to the additional recharge that resulted in more groundwater outflux to natural surface-water features.

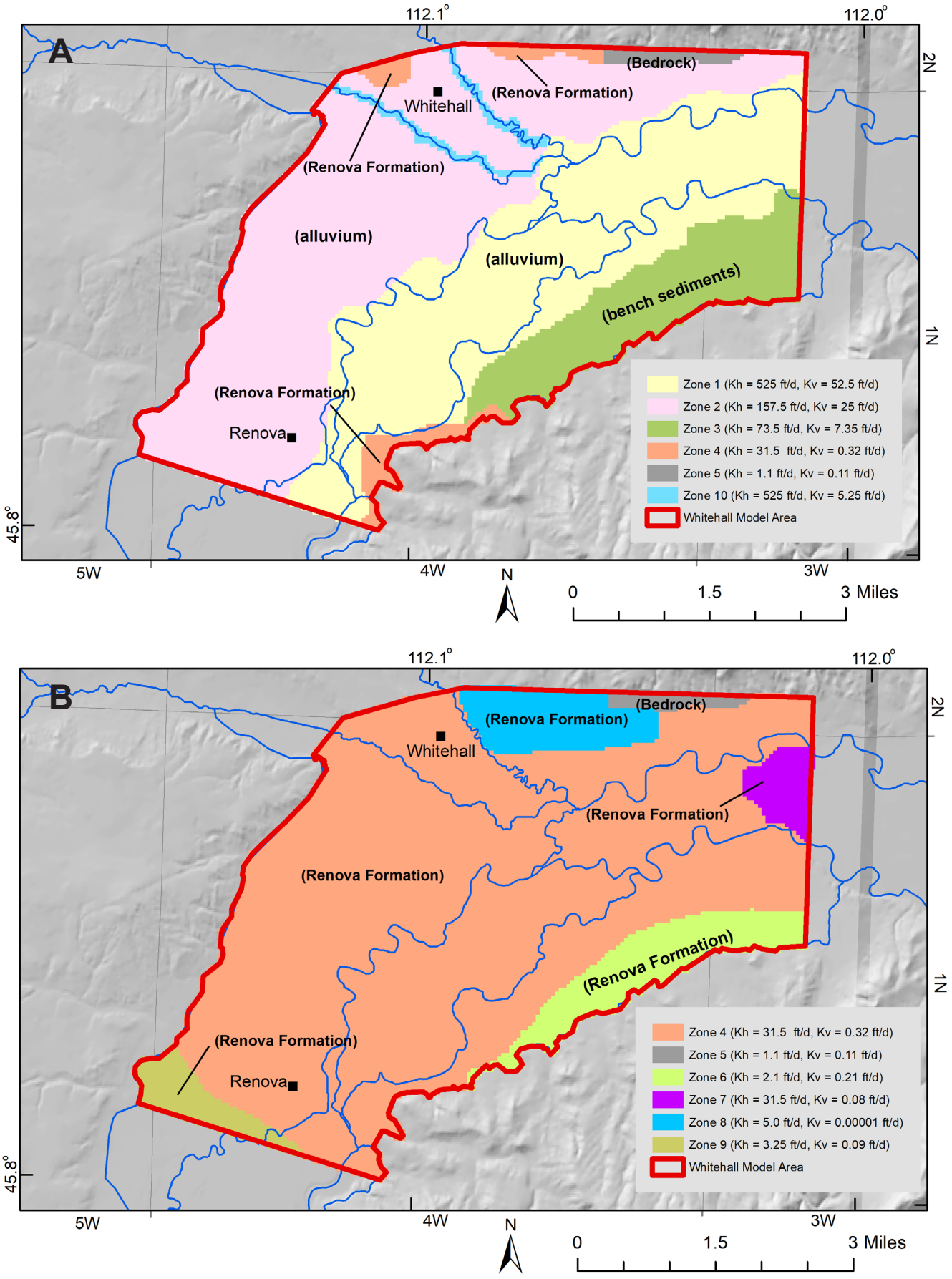

Figure 13. (A) Steady-state calibration. Six hydraulic conductivity zones in layer 1 represent the alluvium (zones 1 and 2), bench sediments (zone 3), Renova Formation (zone 4), bedrock outcrop (zone 5), and Pipestone and Whitetail streams (zone 10). (B) Steady-state calibration. Six hydraulic conductivity zones in model layer 2 represent variation of hydraulic conductivity in the deeper Renova formation (zones 4, 6, 7, 8, and 9), and bedrock (zone 5).

Table 7. Model: Groundwater targets (calibration limits).

Target Group	Maximum Water-Level Elevation (ft)	Minimum Water-Level Elevation (ft)	Range Water-Level Elevation (ft)	Maximum Calibration Error (10% of range) (ft)
Group 1	4398.6	4300.8	97.8	9.8
Group 2	4410.7	4274.0	136.7	13.7
Group 1 & 2	4410.7	4274.0	136.7	13.7
All Layer 1	4401.3	4301.0	100.3	10.0
All Layer 2	4410.7	4274.0	136.7	13.7

Table 11B and figure 16B show the adjusted steady-state model water budget in comparison to the conceptual water budget.

The steady-state water budget indicates that surface water is the primary source of water to the groundwater system and is also the primary location for groundwater discharge. Eighty-four percent of the model's groundwater influx comes from natural surface-water bodies, e.g., losses from the Jefferson River, Slaughterhouse and Jefferson Slough, etc. (excluding canal leakage and irrigation recharge). About ninety-seven percent of the model's groundwater outflux discharges to natural surface-water bodies as stream gains and as flux to secondary canals (drains; fig. 16B).

Transient Calibration

Transient model calibration aims to adjust the model's time-dependent parameters (e.g., storage coefficients) and boundary inflows so that the model reasonably responds to temporal changes in boundary conditions and/or applied stresses. The steady-state calibrated model produced a set of heads and boundary conditions that establish the initial conditions in the transient model.

In this model, we adjusted aquifer storage properties, which include specific yield (S_y) for the unconfined upper layer, and specific storage (S_s) in layer 2. Eight zones represented the distribution of S_y and S_s in both model layers (figs. 17A, 17B). Storage parameters were varied during the transient calibration, keeping their values uniform within each zone. The variations were within the limits appropriate for the geologic units (e.g., bedrock versus alluvium; tables 10, 12). Additional adjustments included changes to river stage, riverbed conductance, irrigation canal seepage, lateral groundwater influx, irrigation recharge, and hydraulic conductivity in limited areas near some wells. The steady-state model was re-run with these limited hydraulic conductivity adjustments and the non-irrigation recharge.

Calibration Targets

Sixteen well targets had data suitable for the transient calibration. Water levels were measured in these wells from July 2013 to October 2015. Four of the wells were in layer 1 and 12 were in layer 2 (table 13). The transient calibration aimed to match the monthly average water-level elevation in target wells.

Calibration Methods

Stress Periods

In the transient simulation (beyond the first stress period), boundary flux rates were varied to replicate seasonal variation and changes in pumping rates between April 2013 and December 2015. These included changes in recharge rate, canal seepage, lateral groundwater flux, irrigation recharge, evapotranspiration, river stages, and pumping from irrigation, domestic, and PWS wells. However, the alluvial flux (Darcy flow) across the southern and northeastern boundaries remained constant at their steady-state rates throughout the transient simulation.

Aquifer Storage Estimation

In the layer property flow (LPF) package, the layer type specified in this model was type 1 for layer 1 (i.e., LAYTYP = 1). This is a convertible layer type; MOD-

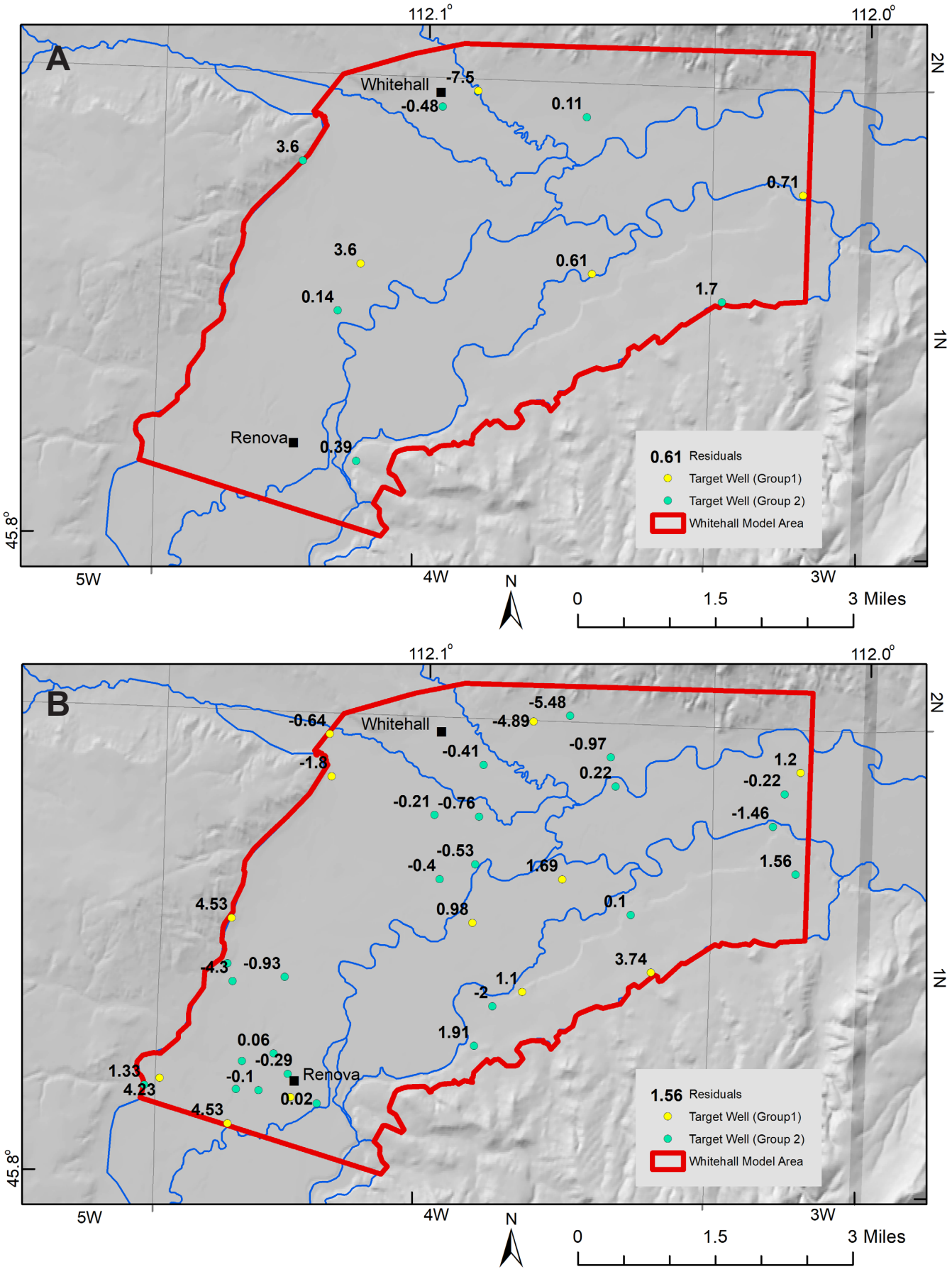

Figure 14. (A) Steady-state calibration. Residual (ft) in model layer 1. Residuals are the difference between observed groundwater levels and simulated groundwater levels at target wells. (B) Steady-state calibration. Residual (ft) in model layer 2.

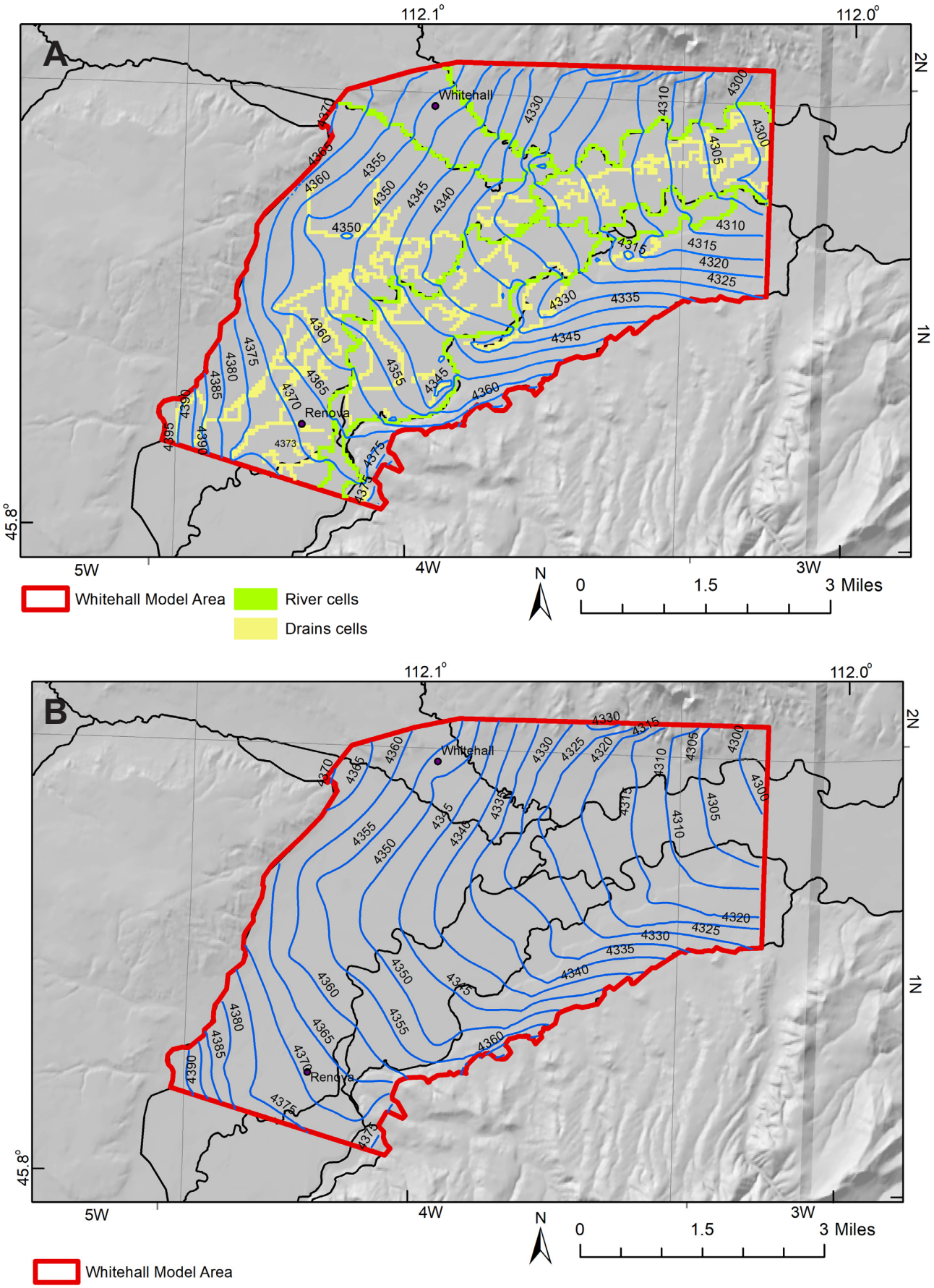

Figure 15. (A) Simulated potentiometric surface in layer 1 of the steady-state model shows similarity with the measured potentiometric surface in figure 5 and the interaction between surface-water features and groundwater in the floodplain and alluvial units. (B) Simulated potentiometric surface in layer 2 from the steady-state model shows the general flow direction in the deeper water-bearing Tertiary sediments.

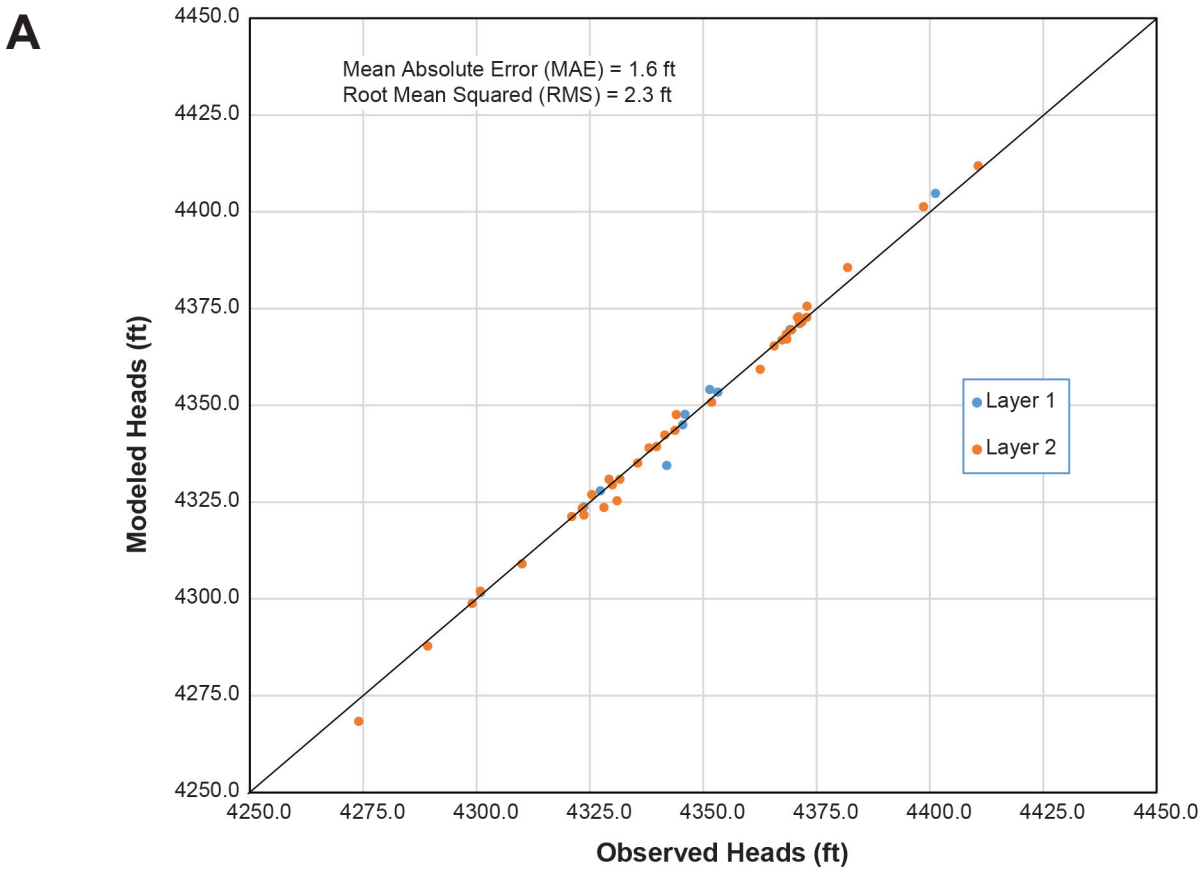

Figure 16. (A) Steady-state calibration—modeled vs. observed Heads (layer 1 and layer 2). (Figure 16B is on the next page.)

B

Whitehall Conceptual Model

Net Surface Water Gain (ac-ft/yr)

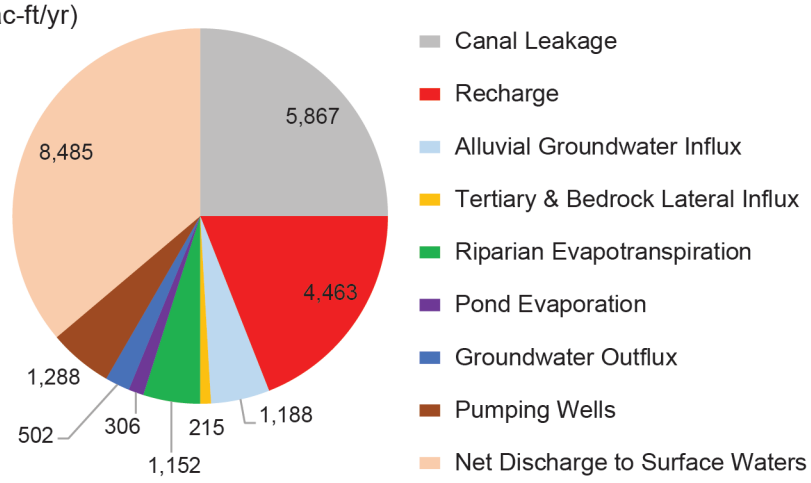

Whitehall Steady-State Model

Net Surface Water Gain (ac-ft/yr)

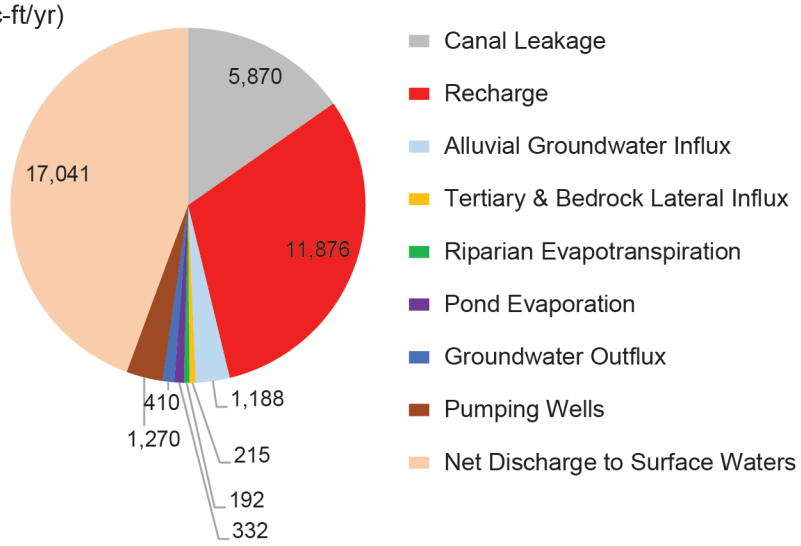

Whitehall Steady-State Model

Gross Surface Water Gains and Losses
(flux= 58,240 ac-ft/yr)

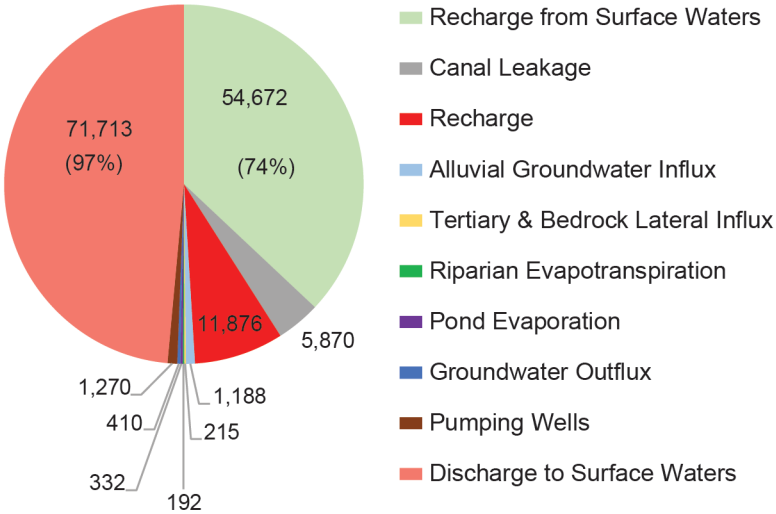

Figure 16. (B) Steady-state model groundwater-budget. Mass balance is comparable for both steady-state and conceptual models. Seventy four percent of model's inflows come from surface water and about ninety seven percent of model's outflows discharge to surface water.

Table 8. Steady-state calibration: Groundwater head residuals.

Name	Layer	Observed Head (ft)	Computed Head (ft)	Weight	Group	Residual* (ft)
277285	1	4327.3	4326.7	1	1	0.6
277282	1	4351.5	4347.9	1	1	2.6
277286	1	4301.0	4300.2	1	1	0.7
48477	1	4342.0	4349.4	1	1	-7.5
48424	1	4346.0	4329.2	0.1	2	1.7
48527	1	4401.3	4364.8	0.1	2	3.5
48590	1	4353.3	4351.9	0.1	2	0.1
48623	1	4369.2	4365.4	0.1	2	0.4
120988	1	4323.7	4322.6	0.1	2	0.0
211036	1	4345.5	4350.3	0.1	2	-0.6
237722	2	4381.9	4377.3	1	1	3.7
48626	2	4372.9	4369.7	1	1	2.7
156080	2	4398.6	4394.4	1	1	2.7
48577	2	4341.5	4340.4	1	1	0.8
280978	2	4344.1	4340.3	1	1	3.5
48569	2	4338.1	4337.1	1	1	0.9
171688	2	4371.1	4366.5	1	1	1.8
279262	2	4329.3	4327.6	1	1	1.6
48522	2	4362.6	4364.4	1	1	-3.3
48378	2	4300.8	4299.6	1	1	1.1
48521	2	4368.5	4369.1	1	1	-1.4
247793	2	4331.0	4335.9	1	1	-5.7
48381	2	4299.0	4301.2	0.1	2	-0.2
48386	2	4289.2	4303.8	0.1	2	-1.5
48461	2	4339.7	4343.8	0.1	2	-0.4
48547	2	4343.8	4345.9	0.1	2	-0.3
48603	2	4328.1	4371.1	0.1	2	-4.5
48605	2	4372.8	4373.5	0.1	2	-0.1
48611	2	4369.5	4368.9	0.1	2	0.0
48616	2	4365.7	4368.6	0.1	2	-0.4
48681	2	4410.7	4397.4	0.1	2	1.1
126672	2	4331.7	4339.2	0.1	2	-0.8
127059	2	4274.0	4328.8	0.1	2	-5.6
134915	2	4370.8	4351.7	0.1	2	1.9
143492	2	4371.3	4372.3	0.1	2	-0.2
144711	2	4367.4	4370.7	0.1	2	-0.5
153805	2	4371.8	4374.4	0.1	2	-0.3
170414	2	4325.4	4309.8	0.1	2	1.5
202071	2	4330.0	4335.3	0.1	2	-0.5
203498	2	4323.7	4343.7	0.1	2	-2.0
209419	2	4310.0	4319.7	0.1	2	-1.0
218151	2	4321.0	4318.9	0.1	2	0.2
221498	2	4368.3	4368.1	0.1	2	0.0
230659	2	4323.3	4322.3	0.1	2	0.1
252255	2	4335.5	4339.5	0.1	2	-0.4
258872	2	4351.8	4361.2	0.1	2	-1.0

*Residual = observed – computed.

Table 9. Steady-state calibration statistics.

Statistics	(ft)
Residual Mean	0.11
Absolute Residual Mean	1.60
Residual Std. Deviation	2.29
Sum of Squares	241.96
RMS Error	2.29
Min. Residual	-7.49
Max. Residual	3.70
Number of Observations	46
Range in Observations	136.7
10% of Range	13.7

Table 10. Initial and calibrated hydraulic conductivity values.

Hydrogeologic Unit	Horizontal Hydraulic Conductivity Kh (ft/d)			Vertical Hydraulic Conductivity K_v (ft/d)	
	Aquifer Test	Initial Estimate*	Steady-State Calibration**	Initial Estimate*	Steady-State Calibration**
Alluvium	NT	(150–500)	(157.5–525)	(15– 50)	(5.25–52.5)
Bench Sediments	NT	70	73.5	7	7.35
Renova	(27–382)	(30–80)	(2.1–31.5)	(3–8)	(0.00001–.32)
Bedrock	NT	1	1.1	0.1	0.1

Note. NT, formation was not tested.
*For surficial distribution see figs. 4A, 4B.
**For surficial distribution see figs. 13A, 13B.

Table 11A. Groundwater budget comparison between the preliminary (conceptual) and steady-state models.

Conceptual Model		Steady-State Model		Sum Error (Conceptual & Steady-State Models)
	acre-ft/yr		acre-ft/yr	
Alluvial Groundwater Influx	1,188	Alluvial Groundwater Influx	1,188	
Tertiary & Bedrock Lateral Influx	215	Tertiary & Bedrock Lateral Influx	215	
Canal Leakage	5,867	Canal Leakage	5,870	
Irrigation Recharge	4,463	Irrigation Recharge	3,932	
Total	11,733	Total	11,205	5%
Groundwater Outflux	502	Groundwater Outflux	410	
Riparian Evapotranspiration	1,152	Riparian Evapotranspiration	192	
Net Discharge to Surface Waters*	8,485	Net Discharge to Surface Waters*	8,977	
Pumping Wells	1,288	Pumping Wells	1,270	
Pond Evaporation	306	Pond Evaporation	332	
Total	11,733	Total	11,181	5%

*Recharge = irrigation + non-irrigation.
Note. Model gross recharge from surface waters = 54,672 acre-ft/yr. Model gross discharge to surface waters = 67,217 acre-ft/yr. Difference = 8,977 acre-ft/yr.

Table 11B. Groundwater budget comparison between the preliminary (conceptual) and steady-state models (with on-irrigation recharge).

Conceptual Model		Steady-State Model		Sum Error (Conceptual & Steady-State Models)
	acre-ft/yr		acre-ft/yr	
Alluvial Groundwater Influx	1,188	Alluvial Groundwater Influx	1,188	
Tertiary & Bedrock Lateral Influx	215	Tertiary & Bedrock Lateral Influx	215	
Canal Leakage	5,867	Canal Leakage	5,870	
Irrigation Recharge	4,463	Recharge *	11,876	
Total	11,733	Total	19,149	63%
Groundwater Outflux	502	Groundwater Outflux	410	
Riparian Evapotranspiration	1,152	Riparian Evapotranspiration	185	
Net Discharge to Surface Waters*	8,485	Net Discharge to Surface Waters*	17,041	
Pumping Wells	1,288	Pumping Wells	1,270	
Pond Evaporation	306	Pond Evaporation	332	
Total	11,733	Total	19,238	64%

*Recharge = irrigation + non-irrigation.
Note. Model gross recharge from surface waters = 58,240 acre-ft/yr. Model gross discharge to surface waters = 71,713 acre-ft/yr. Difference = 17,041 acre-ft/yr.

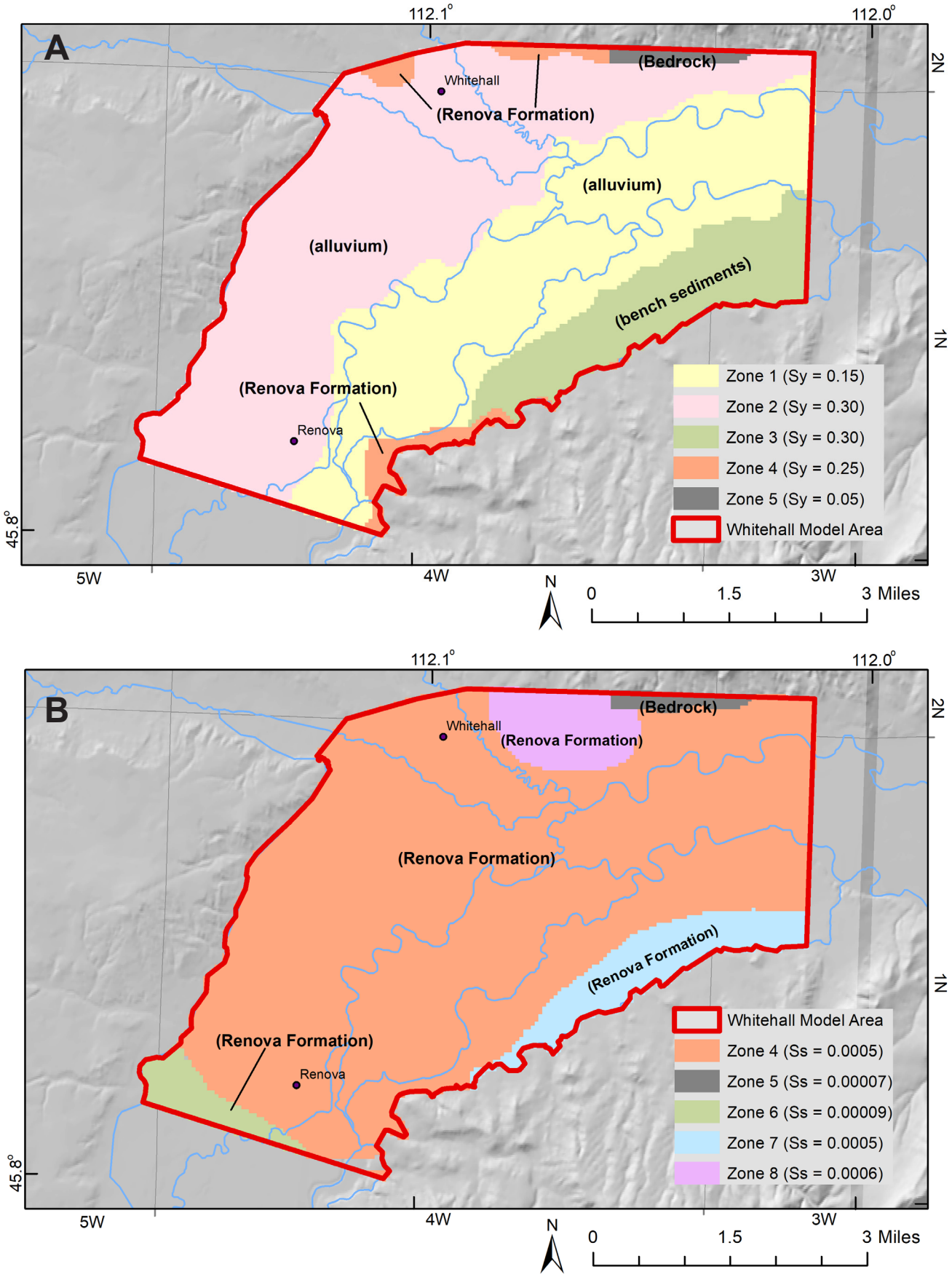

Figure 17. (A) Calibration of the transient model included adjustment of the specific yield in (Sy) in layer 1. (B) Calibration of the transient model included adjustment of specific storage (Ss) in layer 2.

Table 12. Transient model—initial and calibrated storage coefficients.

Hydrogeologic Unit	Specific Yield (S_y)			Specific Storage (S_s)		
	Aquifer Test	Initial Estimate	Calibration*	Aquifer Test	Initial Estimate	Calibration*
Alluvium	NT	0.2	(0.15–0.3)	NT	Unconfined, no S_s	Unconfined, no S_s
Bench Sediments	NT	0.2	(0.25–0.3)	NA	Unconfined, no S_s	Unconfined, no S_s
Renova	NA	NA	Confined layer no S_y	(1x 10^{-5} -1 x 10^{-4})**	1 x 10^{-4}	(7 x 10^{-5} - 6 x 10^{-4})
Bedrock	NT	NA	Confined layer no S_y	NT	1 x 10^{-5}	7 x 10^{-5}

Note. NA, not applicable; aquifer test solution was for leaky confined conditions. NT, formation was not tested.
*For surficial distribution see figs. 17A, 17B.
**Specific storage (S_s) is based on aquifer test storage coefficient (S) divided by saturated thickness.

FLOW uses either specific yield (S_y) or specific storage (S_s) exclusively to calculate the change in storage within a cell depending on whether the conditions are confined (S_s) or unconfined (S_y). Layer 2 was specified as confined (LAYTYP = 0), where only S_s is used to calculate changes in storage.

For the transient calibration, both S_y and S_s coefficients were estimated through trial and error, by manually changing storage coefficients assigned to each zone (figs. 17A, 17B). The model contains eight zones, which generally match the geologic model pattern. Initial and calibrated estimates are listed in table 12.

We used the Nash Sutcliffe coefficient of efficiency (Nash and Sutcliffe, 1970) for target wells (fig. 18) to quantify the fit between simulated and measured heads. The Nash Sutcliffe coefficient (NS) ranges from -∞ to 1; a positive NS means a good fit (1 is the best fit), while negative NS indicates poor matching (Anderson and others, 2015). A detailed example of the NS calculation is in appendix D.

Recharge Estimation

Four recharge rates were assigned to four discrete areas (zones), 1, 2, 3, and 4, to simulate non-irrigation recharge, flood irrigation, sprinkler irrigation, and central pivot irrigation, respectively (fig. 11). During transient calibration, the average rates for the three irrigation types were changed using multipliers to adjust the monthly rates (table 14, fig. 19, and appendix A). The application of non-irrigation recharge was necessary during transient calibration. This recharge in non-irrigated areas simulates precipitation recharge during warm months, and recharge from small secondary natural channels (streams) that fill with water flowing from the Jefferson River during high-flow months; this surface water then infiltrates to groundwater.

Evapotranspiration Estimation

Evapotranspiration rates (ET) used in the steady-state model (fig. 9) for both riparian woody plants and riparian grasses and mesic forest were the basis for the transient simulation. These rates vary monthly, using multipliers to reflect seasonal variations in ET (Butler and Bobst, 2017). Since the steady-state ET rate is based on an annual rate, the transient model ET rate was roughly doubled for the warm months (April–September) to apply the same annual amount of ET (table 15). During calibration, the ET rate for October was reduced by 50% of the steady-state value.

Canal Seepage and Lateral Groundwater Recharge

Simulations of canal seepage and upgradient irrigation recharge were adjusted during the irrigation season (April–October). Multipliers were applied to modify monthly injection rates in the specified flux boundaries at the east side boundary (Parrot Canal) and the west side boundary (Jefferson Canal). Lateral groundwater influx was initially kept constant but subsequently slightly adjusted along some reaches during the transient calibration (appendix A).

Jefferson River and Other Streams

River stages varied monthly in the transient model. The monthly stages were calculated using the September 2016 surveyed stages, in the Jefferson River

Table 13. Monthly groundwater elevations (msl, ft) used transient model calibration.

	Target Wells (GWIC)															
	237722	48626	156080	48577	280978	48569	171688	277285	277282	279262	277286	48522	48378	48521	48477	247793
No. of Measurements*	22	22	22	21	4	21	22	21	21	8	21	12	22	17	21	23
Month/Year																
Jun-13	-	-	-	-	-	-	-	-	-	-	-	-	-	-	4341.0	-
Jul-13	4382.3	4373.2	4402.2	4342.9	-	4337.7	4374.7	-	-	-	-	-	4301.1	-	4340.3	4329.6
Aug-13	4381.9	4373.2	4401.4	4342.6	-	4337.3	4374.8	-	-	-	-	-	4301.2	-	4339.5	4328.8
Sep-13	4382.6	4373.3	4400.8	4343.2	-	4338.1	4374.9	-	-	-	-	4365.6	4301.7	4369.0	4340.0	4328.8
Oct-13	4381.6	4372.8	4399.8	4343.0	-	4338.1	4372.7	-	-	-	-	4364.7	4301.4	4369.3	4340.8	4329.6
Nov-13	4381.2	4372.7	4398.2	4341.1	-	4338.1	4370.7	-	-	-	-	-	4300.7	4368.9	4341.7	4330.4
Dec-13	4381.2	4372.8	4397.3	4341.1	-	4338.1	4369.7	-	-	-	-	4361.9	4300.1	4368.8	4342.1	4330.8
Jan-14	4381.1	4372.8	4396.4	4340.1	-	4338.0	4369.3	-	-	-	-	-	4299.9	4367.7	4342.6	4331.3
Feb-14	4381.0	-	4395.7	4340.1	-	4338.0	4368.8	4327.6	4351.9	-	4301.2	4360.3	4299.6	4368.4	-	4331.5
Mar-14	4381.6	4373.0	4395.7	4339.7	-	4338.2	4369.0	4327.1	4352.0	-	4300.8	-	-	4368.4	4342.2	4332.0
Apr-14	4381.2	4372.6	-	4339.9	-	4338.3	4368.5	4328.1	4351.6	-	4301.8	4359.9	4300.3	4368.2	4342.0	4332.0
May-14	4383.1	4373.3	4400.5	4342.1	-	4338.5	4370.0	4329.6	4351.5	-	4303.2	4361.6	4299.9	4368.9	4341.5	4331.7
Jun-14	4383.3	4373.4	4400.5	-	-	4338.9	4372.7	4329.8	4351.5	-	4303.3	-	4302.9	-	4341.2	4330.7
Jul-14	4382.5	4372.9	4399.8	-	-	-	4373.9	4327.3	4351.4	-	4300.9	4364.3	4301.9	4366.7	4340.5	4330.2
Aug-14	4382.9	4373.4	4400.7	-	-	-	-	4326.2	4351.3	-	4299.9	4365.0	4302.7	-	4340.9	4329.4
Sep-14	4382.7	4373.0	4401.2	4342.8	-	4338.3	4375.0	4326.5	4351.8	4329.0	4300.1	4365.3	4301.5	-	4341.1	4329.7
Oct-14	4381.4	4372.8	4399.4	4343.4	-	4338.6	4372.7	4327.2	4351.7	4329.2	4300.7	-	4300.7	4368.9	-	4330.1
Nov-14	4381.4	4372.7	4398.2	4341.8	-	4338.5	4371.0	4327.8	4351.7	4329.3	4301.8	-	4300.3	4368.9	4341.3	4330.7
Dec-14	4381.4	4372.9	4397.5	4340.9	-	4338.5	4370.3	4327.3	4351.7	4329.4	4300.8	4361.7	4300.3	4368.8	4341.5	4331.1
Jan-15	4381.3	4372.8	4396.7	4340.8	-	4338.2	4369.4	4327.9	4351.6	4329.5	4301.8	-	4299.6	4368.6	4341.5	4331.4
Feb-15	4381.2	4372.8	4396.2	4340.0	4343.6	4338.2	4369.2	4327.1	4351.4		4300.7	-	4300.2	4368.4	4341.5	4331.6
Mar-15	4381.0	4372.7	4395.9	4339.5		4338.1	4368.7	4327.4	4351.4	4329.1	4301.0	4360.0	4299.9	4368.2	4341.2	4331.8
Apr-15	4381.4	4372.6	4395.4	4339.5	4342.1	4338.1	4368.3	4327.3	4351.4	4329.2	4301.0	-	4300.0	4368.2	4339.8	4331.9
May-15		4373.0	4400.0	4342.3	4342.2	4338.3	4369.3	4328.2	4351.5	4329.4	4301.8	4360.5	4302.6			4331.6
Jun-15	-	-	-	-	-	-	-	4327.8	4351.3	-	4301.3	-	-	-	-	-
Jul-15	-	-	-	-	-	-	-	4325.9	4350.8	-	4299.5	-	-	-	-	-
Aug-15	-	-	-	-	-	-	-	4325.4	4351.1	-	4299.1	-	-	-	-	-
Sep-15	-	-	-	4342.7	4347.0	-	-	4325.9	4351.4	-	4299.5	-	-	-	-	-
Oct-15	-	-	-		-	-	-	4326.6	4351.2	-	4300.1	-	-	-	-	-

*Total measurements from all wells = 300.

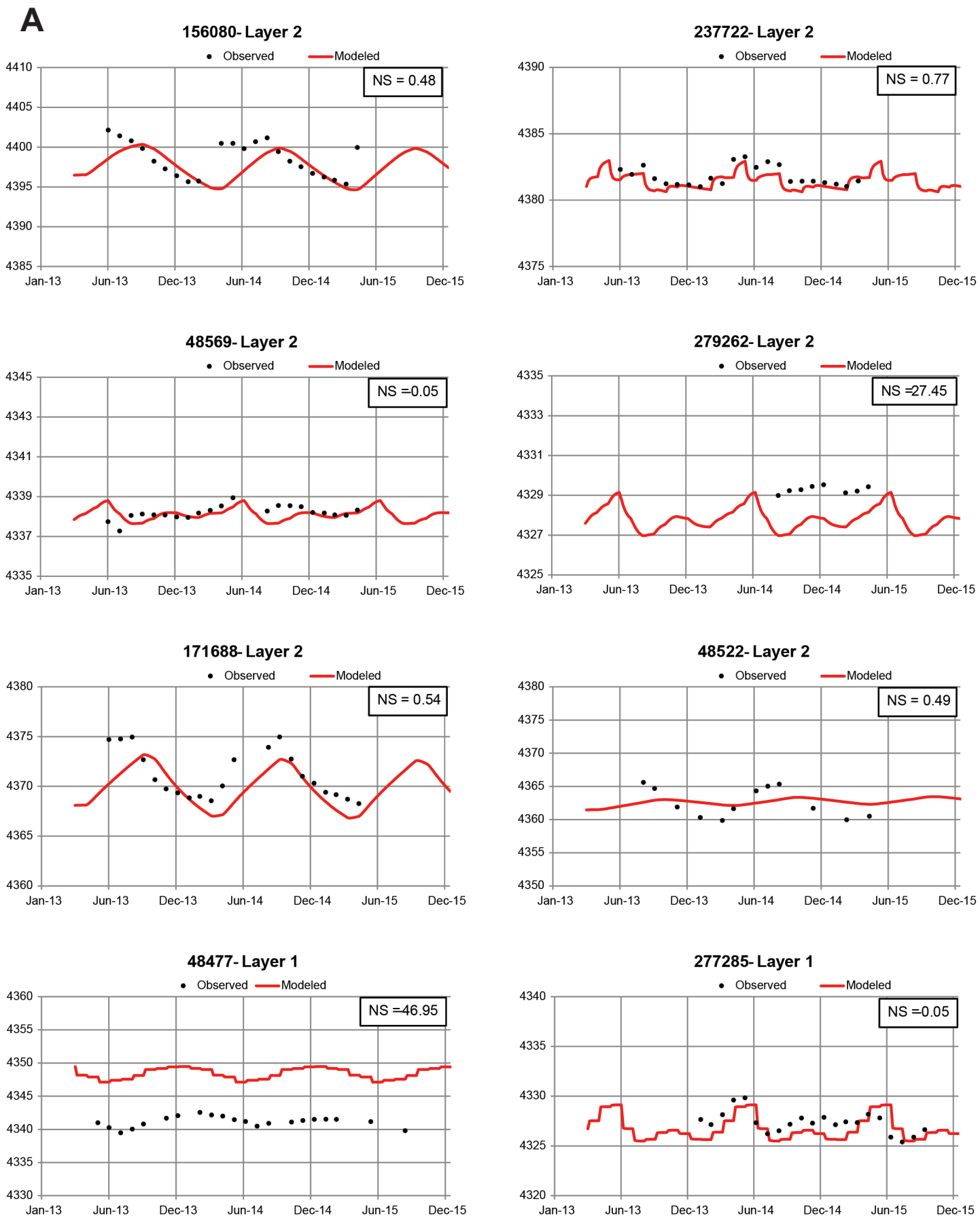

Figure 18. The transient model was calibrated to groundwater elevations at target wells (April 2013–December 2015). The model simulated the dynamics of the groundwater system, seasonality, and irrigation recharge effects in most target wells in both model layers. Quantitatively, nine hydrographs (56%) have a positive Nash Sutcliffe coefficient (NS = >0), two hydrographs (11%) show a good

B

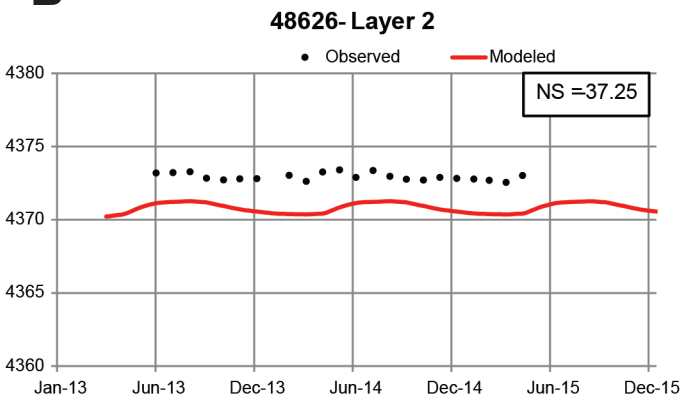

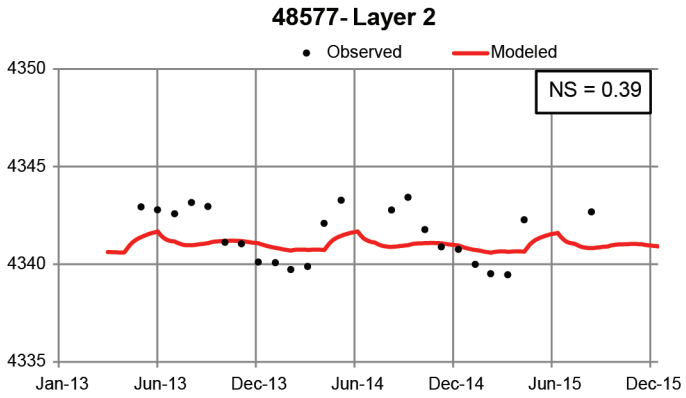

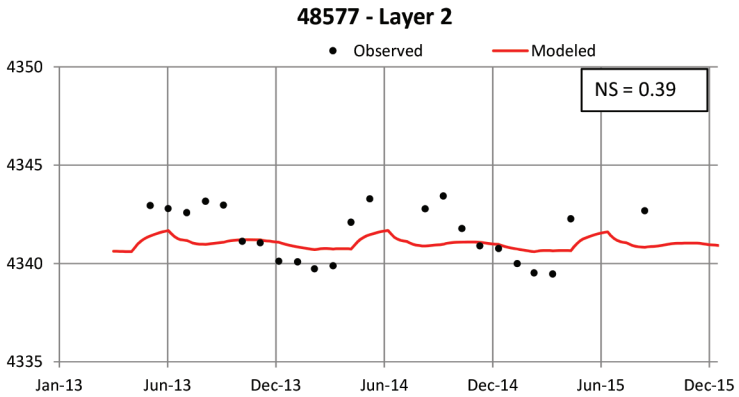

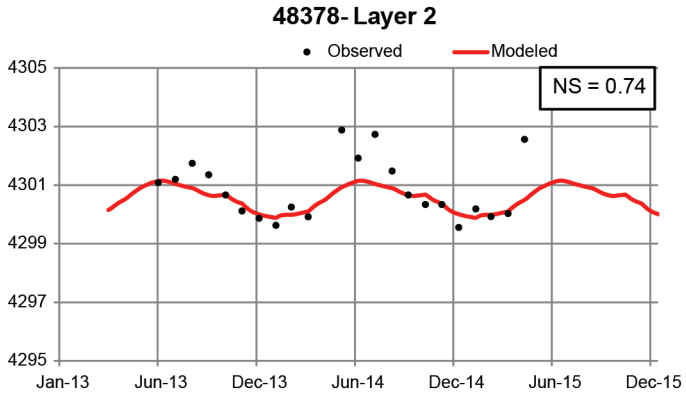

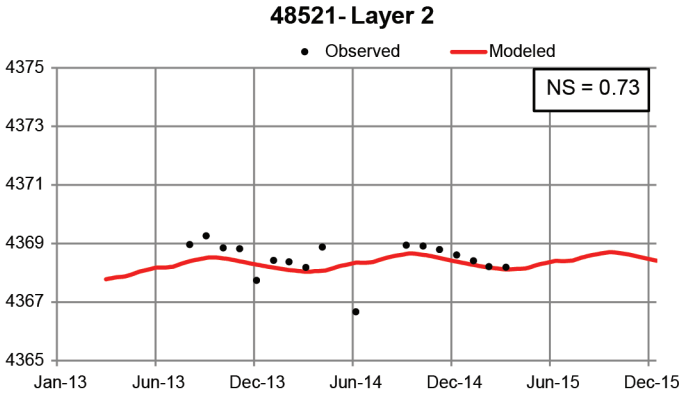

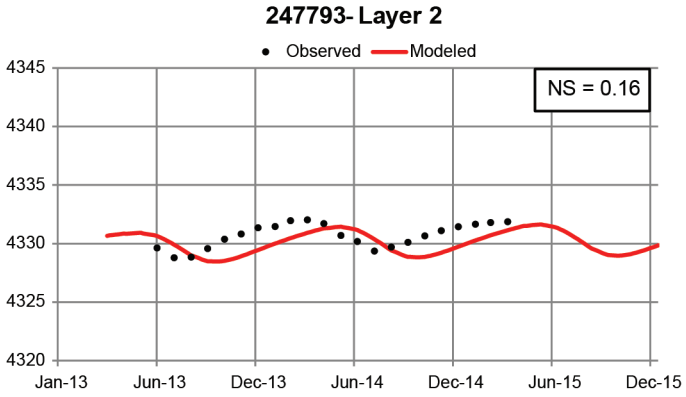

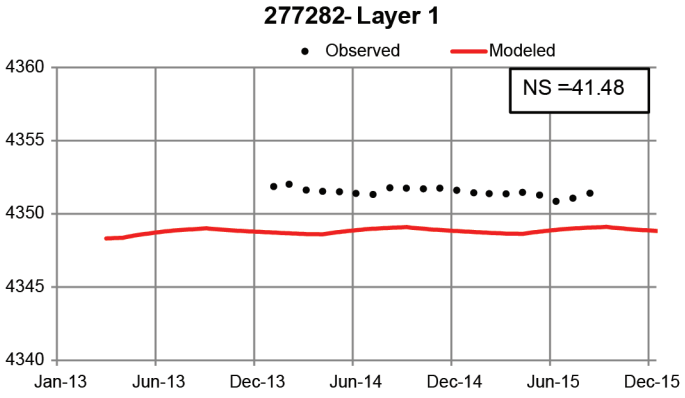

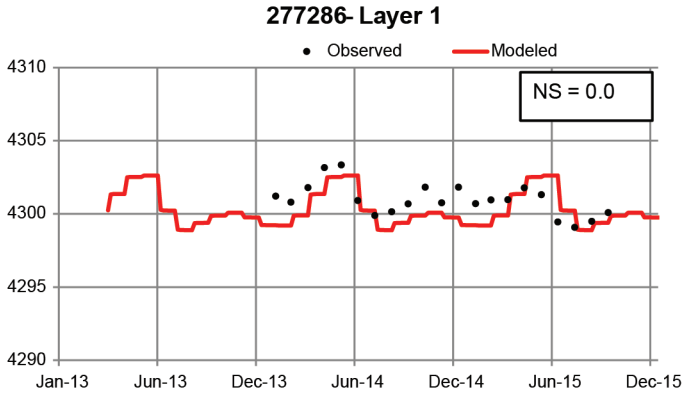

match, although have very small negative NS (277285 and 277286), and five hydrographs (23%) have poor matching (NS <0). Improving the fitting for targets with poor matching was not possible without altering the rest of the model calibration.

Table 14. Transient model—calibrated irrigation recharge.

Month	Zone 1 Non-Irrigation (ft/d)	Zone 2 Flood (ft/d)	Zone 3 Sprinkler (ft/d)	Zone 4 Pivot (ft/d)
Jan	0	0	0	0
Feb	0	0	0	0
Mar	0	0	0	0
Apr	9.560E-04	3.187E-03	1.000E-03	5.901E-04
May	3.824E-03	6.373E-03	2.001E-03	1.180E-03
June	3.824E-03	6.373E-03	2.001E-03	1.180E-03
July	3.824E-03	6.373E-03	2.001E-03	1.180E-03
Aug	3.824E-03	6.373E-03	2.001E-03	1.180E-03
Sept	3.824E-03	6.373E-03	2.001E-03	1.180E-03
Oct	9.560E-04	3.187E-03	1.000E-03	5.901E-04
Nov	0	0	0	0
Dec	0	0	0	0

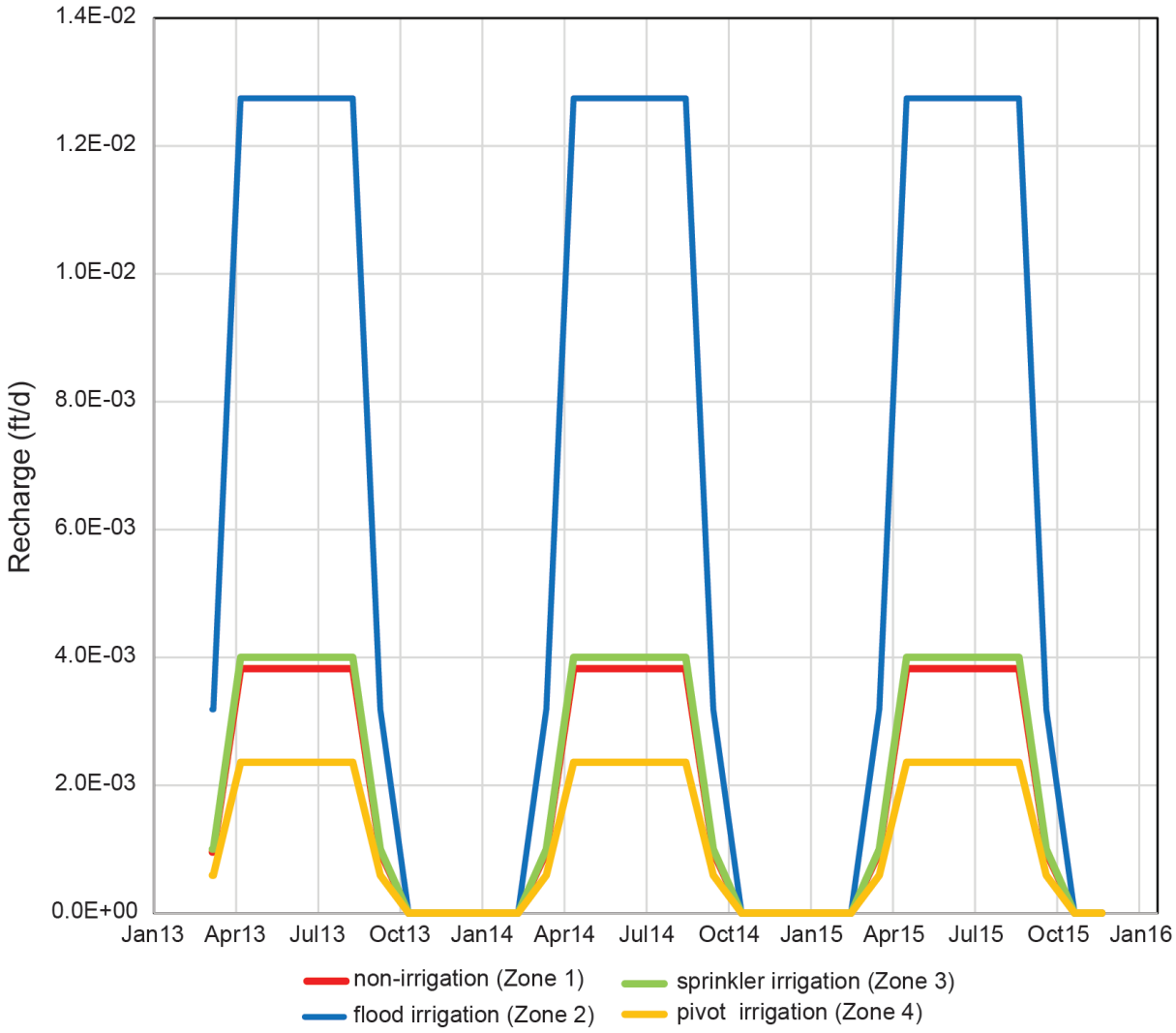

Figure 19. Transient model recharge rates. Four recharge zones in the model (see figure 11) supplied irrigation and non-irrigation recharge to model layer 1. Recharge rates varied throughout the irrigation season (from April through September).

Table 15. Transient model—evapotranspiration multipliers.

Month	ET Multiplier
Jan	0
Feb	0
Mar	1
Apr	2
May	2
June	2
July	2
Aug	2
Sept	1
Oct	0.5
Nov	0
Dec	0

and other streams, and monthly offsets from 2014 data (see Steady-State Calibration section). Appendix B provides more details about the computation of the monthly offset calculation. The calculated stage values were interpolated to assign stages at the other river cells representing the Jefferson River and other streams. During calibration, the monthly offsets at some river reaches were adjusted to improve the match between observed and simulated heads at target wells.

Calibration Results

The calibrated transient model simulated head changes with time that generally followed measured water levels (hydrographs) in target wells (fig. 18). We observed the following from the target well hydrographs and their locations (figs. 12A, 12B, 18):

1. The model produced an overall reasonable transient calibration. It simulates the dynamics of the groundwater system, and captures seasonality and irrigation recharge effects in most target wells in both model layers.

2. In figure 18, more than half of the targets show a good fit (56%) between the simulated and measured values (positive NS); five hydrographs have noticeable poor matching (279262, 48626, 280978, 48477, and 277282), and two wells with good match have negative but near zero NS values: well 277285 (layer 1) and well 48569 (layer 2). Improving the fit at targets with a poor match was not possible without altering the rest of the model calibration.

3. Well 48477 is located very close to Whitetail Creek (fig. 14A) and has the highest absolute residual (7.5 ft). It appears that the water level in this well is controlled by changes in Whitetail Creek. Target well 280978, completed in layer 2, has only four data points, and is located very close to the Parrot Canal (fig. 12B). Improving the match at this well would have required changing canal leakage rates beyond field estimates.

4. In general, the distance from surface water affects the simulated heads in wells completed in layer 1. For example, wells 277285 and 277286, located 80 ft and 90 ft, respectively, from the Jefferson River, showed a greater change in groundwater elevations in response to changes in river stage compared to well 277282, located 2,020 ft from the Jefferson River (figs. 12A, 18).

SENSITIVITY ANALYSIS

A calibrated groundwater model contains the best estimates of the hydrogeologic system parameters that produce results in good agreement with target values, or other calibration criteria. The objective of the sensitivity analysis is to "quantify the uncertainty of the calibrated model caused by uncertainty of aquifer pa-

rameters measurements, applied stresses, and boundary conditions" (Anderson and others, 2015). Sensitivity analysis involves running the calibrated model many times while varying model parameters or boundary stresses, one by one, over a reasonable range while observing changes in model response (e.g., simulated heads) and/or calibration criteria (e.g., RMS error).

The Whitehall model sensitivity analysis tested the model's sensitivity to changes in horizontal and vertical hydraulic conductivity in all zones; river conductance and river stage in the Jefferson River, Jefferson Slough, Slaughterhouse Slough, Pipestone Creek, and Whitetail Creek; drain stage and conductance at all drains; and recharge. In addition, model sensitivity to canal leakage, evapotranspiration rates, groundwater influx and outflux across model boundaries, and pond evaporation rates were tested. The analysis was limited to the steady-state simulation to test sensitivity under average long-term conditions. The analysis involved modifying the calibrated steady-state model, referred to as the base run, using the selected parameters (table 16). For each parameter incremental change, a unique model was executed, resulting in 1,070 model runs (table 16). The calibration statistics RMS and RSS were documented for each run.

Using the statistics RMS and RSS, the model is most sensitive to changes in river stage, horizontal hydraulic conductivity, and to a lesser degree to non-irrigation recharge in zone 1 (fig. 20). Changes in river stage affect the model because the river provides a large volume of water to the aquifer (fig. 16B). The results indicate that if river stage error is increased by 100% (multiplier = 2) or more, the model RMS will increase proportionally (very sensitive). However, while the model is sensitive to river stage, the stage measurements were surveyed to 0.01 ft and uncertainty in stage measurements is very low. Note that one of the reasons we run sensitivity analysis is to assess the adequacy of the measurement methods and accuracy of field data. The model sensitivity to river stage points to the critical interaction between surface water and groundwater, and the role of surface water as the main driver in the flow system and overall water budget.

MODEL PREDICTIONS

The model was developed to evaluate changing land-use scenarios on the hydrogeologic system. Seven predictive scenarios simulated the effect of residential growth effects on groundwater and surface-water availability. The evaluation was focused on changes in groundwater levels, and on stream depletion in the Jefferson River, Slaughterhouse Slough, Jefferson Slough, Pipestone Creek, Whitetail Creek, and their secondary channels.

Stream depletion results from reduced groundwa-

Table 16. Sensitivity analysis—parameters and multipliers.

Parameter	Reaches/Zones	Multipliers					No. of Model Runs
K_h (all zones)	15 zones	0.1	0.5	1	2	10	75
K_v (all zones)	15 zones	0.1	0.5	1	2	10	75
River Conductance (all reaches)	50 reaches	0.1	0.5	1	2	10	250
River Stage (all reaches)	50 stages	0.1	0.5	1	2	10	250
Drain Heads (all reaches)	26 reaches	0.1	0.5	1	2	10	130
Drain Conductance (all reaches)	26 reaches	0.1	0.5	1	2	10	130
Canal Leakage*	8 reaches	0.1	0.5	1	2	10	40
Groundwater Influx*	16 reaches	0.1	0.5	1	2	10	80
Groundwater Outflux*	2 reaches	0.1	0.5	1	2	10	10
Evaporation Ponds*	1 reach	0.1	0.5	1	2	10	5
Irrigation Recharge (all zones)	4 zones	0.1	0.5	1	2	10	20
ET Rates	Single matrix	0.1	0.5	1	2	10	5

Note. Number of runs, number of zones (reaches) x 5 (multipliers).
*Specified heads: (1) injection wells (groundwater influx and canal leakage), (2) extraction wells (groundwater outflux and evaporation ponds).

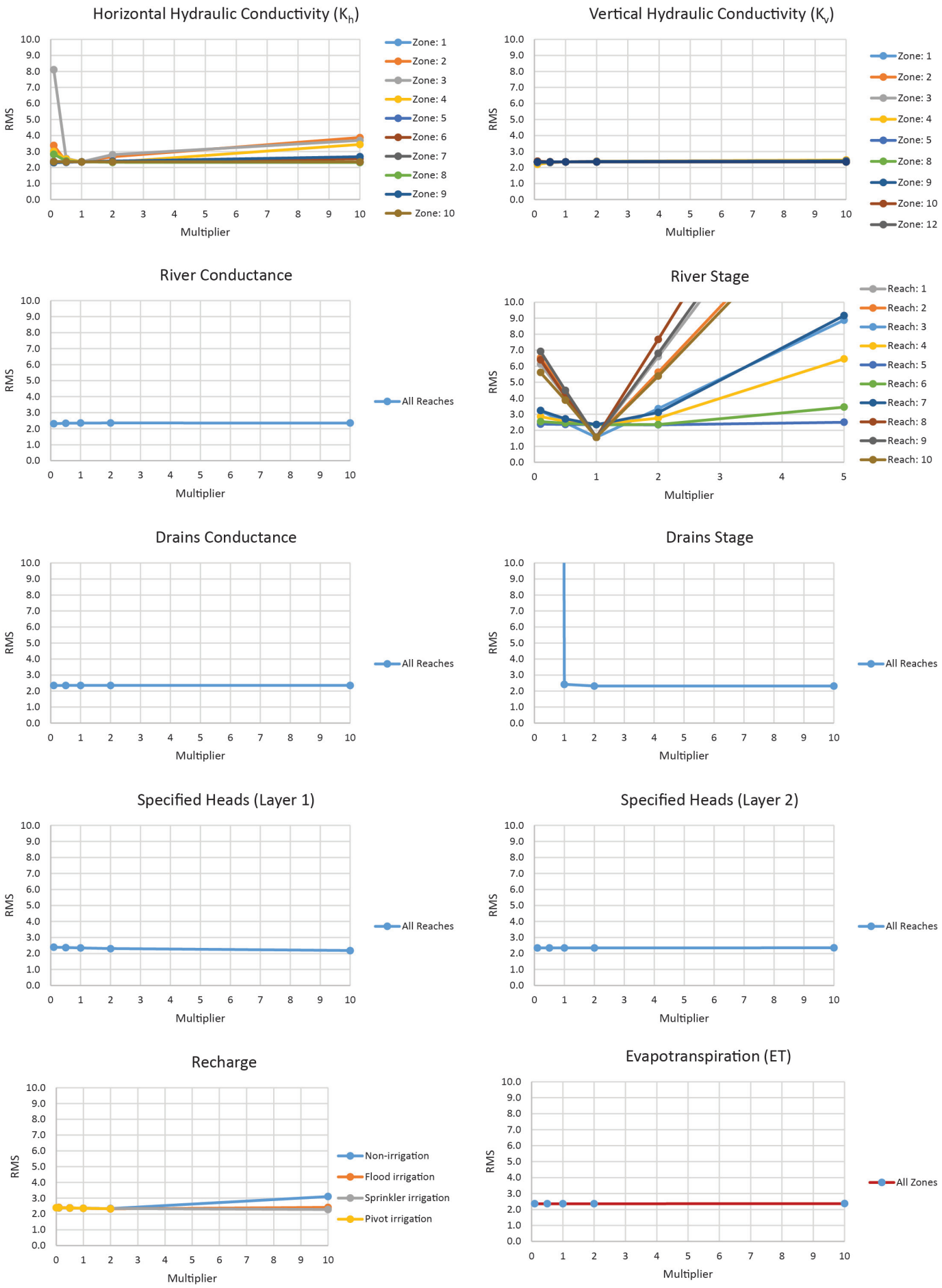

Figure 20. The sensitivity analysis showed greatest sensitivity to changes in hydraulic conductivity and river stage, and to a lesser degree to non-irrigation recharge.

ter discharge to water bodies, which may be related to changes in land use, i.e., converting irrigated areas to non-irrigated and /or new residential subdivisions (increased groundwater withdrawals). Six scenarios simulated groundwater withdrawals with new subdivisions developed in non-irrigated areas, and one scenario (scenario 2) evaluated a new subdivision in an irrigated area. Recharge zones 5, 6, and 7 were added to help simulate the effect of changing irrigated areas to non-irrigated.

The predictive scenarios are evaluated using results from August because this late summer month is characterized by low surface-water flows, high evapotranspiration rates, and high groundwater consumption rates. A base case scenario, referred to as scenario 0, extends the transient model run time for 10 yr, to December 31, 2025, with no change in irrigation practices or pumping.

Scenarios 1 through 4 simulate subdivisions with 23 homes on 10-acre lots (table 17). Scenario 1 models a subdivision on the bench north of the Jefferson Slough in a non-irrigated area, with pumping from bench sediments in layer 1 (fig. 21). Scenario 2 is the same as scenario 1, except that the subdivision lies within an irrigated area, therefore, the scenario simulates changes in pumping and irrigation recharge. Due to model instability when we removed all irrigation recharge from the developed area, recharge was reduced to 10% of the pre-development rate. Scenario 3 simulates a subdivision between the Jefferson River and the Slaughterhouse Slough, in a non-irrigated area (fig. 21), with pumping from the alluvium in layer 1. Scenario 4 is the same as scenario 3, except that pumping is deeper, in the Renova formation of layer 2.

Scenarios 5 through 7 are located between the Jefferson River and the Parrot Canal (fig. 21), with pumping from the Renova Formation in layer 2. These scenarios simulate effects of increasing housing density. Scenario 5 includes 5 homes on 20-acre lots, scenario 6 models 10 homes on 10-acre lots, and scenario 7 models 20 homes on 5-acre lots (table 17).

Scenarios are compared by the reduction in groundwater discharge to surface-water features (stream depletion) and changes in groundwater elevations. Changes in groundwater discharge were calculated as the difference between the discharge to a surface-water reach in scenario 0 and the discharge to that reach in the other scenarios. The effect on groundwater elevations was examined on a cell-by-cell basis by comparing heads obtained from scenario 0 to heads from the other scenarios.

All simulations ran from January 2013 to December 2025, to allow the model to capture seasonality of the flow regime in order to simulate the long-term effects of these changes. The 2015 time-dependent stresses, such as non-irrigation-recharge, boundary fluxes, canal leakage, and evapotranspiration are repeated in each year. MODFLOW produces results for every time step, including groundwater drawdown and groundwater discharge to surface water.

Table 17. Model predictive scenarios—overall effects.

		Maximum Stream Flow Depletion (August 2025)						
		Stream Depletion (all)						
Scenario	Description	Pumping from Layer	Total Lot Area (acre)	ft^3/d	cfs	gpm	gpm/home	Overall Reduction from scenario 0 (%)
0	Base model (no added homes and no change in land use)							
1	23 homes—Non-Irrigated Bench	1	230	1,770	0.020	9.2	0.4	0.02%
2	23 homes—Irrigated Bench (reduced irrigation recharge by 90%)	1	230	18,325	0.212	95.2	4.1	0.24%
3	23 homes—Non-Irrigated Alluvium	1	230	3,680	0.043	19.1	0.8	0.05%
4	23 homes—Non-Irrigated Renova	2	230	3,720	0.043	19.3	0.8	0.05%
5	5 homes—Non-Irrigated Renova	2	100	700	0.008	3.6	0.7	0.01%
6	10 homes—Non-Irrigated Renova	2	100	1,395	0.016	7.2	0.7	0.02%
7	20 homes—Non-Irrigated Renova	2	100	2,754	0.032	14.3	0.7	0.04%

Note. The annual average pumping rate is 0.3 gpm/home.

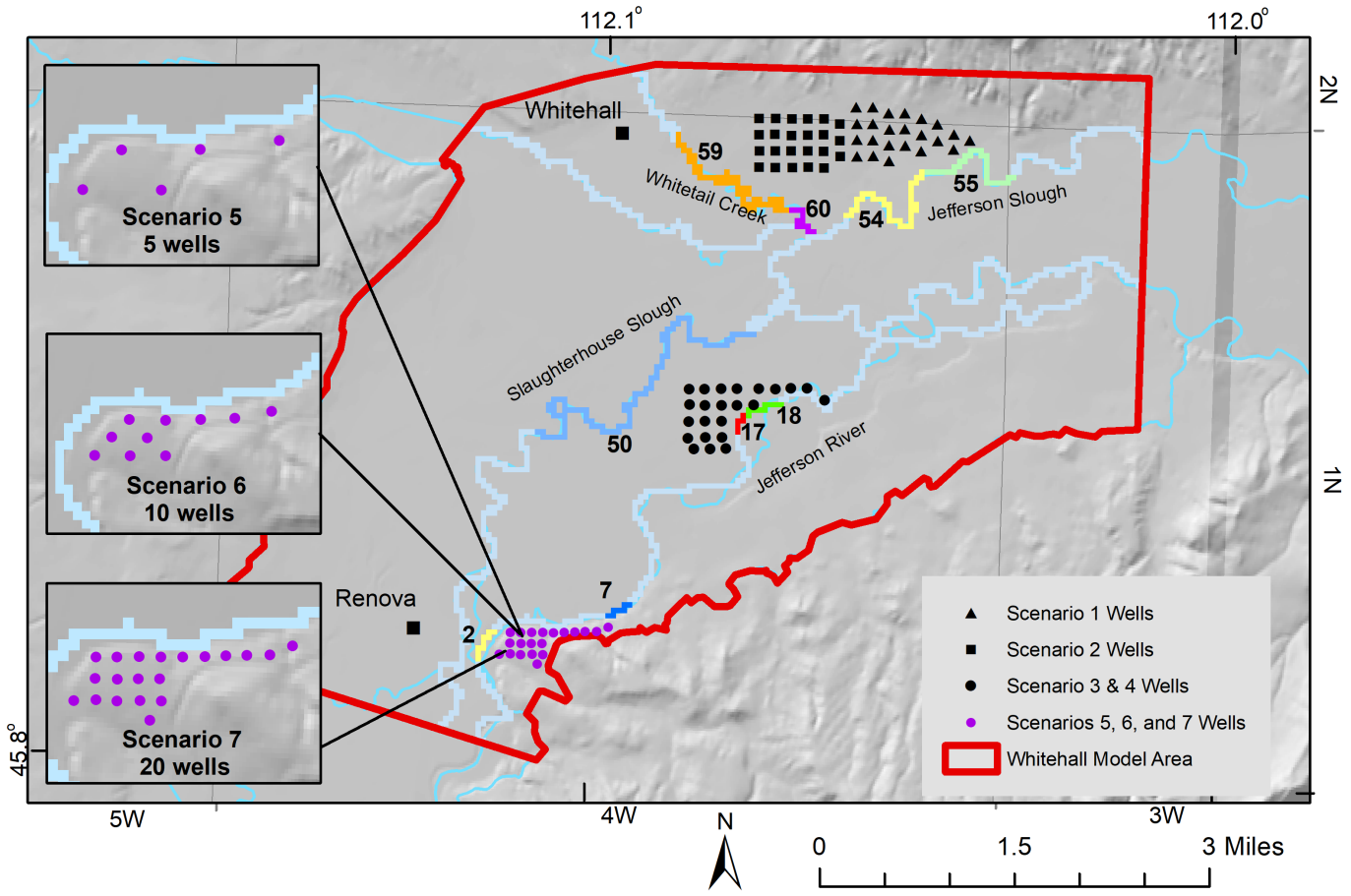

Figure 21. The effects of increased groundwater development were evaluated by simulating pumping from seven hypothetical subdivision scenarios. The affected reaches are shown in color with their model reach numbers.

MODEL RESULTS

The most stream depletion during August 2025 resulted from scenario 2 (fig. 22A), and totaled 18,325 ft^3/d (0.21 cfs). This is a 0.24% reduction from scenario 0 (table 17). In scenarios 5, 6, and 7, stream depletion was directly proportional to the number of pumping wells (fig. 22B).

We also looked at scenario results at surface-water reaches close to the simulated subdivisions. Effects on groundwater levels were evaluated using 1 ft of drawdown as a marker and stream depletion was examined at the reach or reaches with the greatest change. The main findings are as follows:

Scenario 1: Drawdown in the subdivision area was minimal, at less than 1 ft. Stream depletion was slight, and was limited to Jefferson Slough reaches 54 and 55 (fig. 21). The highest depletion rate in August 2025 was about 825 ft^3/d (0.01 cfs) in reach 55 in Jefferson Slough, a 2% reduction in that reach from scenario 0 (fig. 23, table 18).

Scenario 2: Drawdown exceeded 1 ft in layer 1 near the simulated subdivision (fig. 24A). The largest stream depletions occurred in Jefferson Slough reaches 54 and 55, and in Whitetail Creek reaches 59 and 60 (fig. 21). The highest stream depletion rate in August 2025 was about 10,000 ft^3/d (0.12 cfs) in Whitetail Creek reach 59, a 41% reduction from scenario 0 (table 18).

Scenario 3: Drawdown was less than 1 ft in the subdivision area. Stream depletion was highest in Jefferson River reaches 10 to 22 (fig. 25) and in Slaughterhouse Slough reach 50 (figs. 21, 25). The highest depletion rate in August 2025 was about 1,500 ft^3/d (0.017 cfs) in Jefferson River reach 17, a 3% reduction from scenario 0 (table 18).

Scenario 4: Drawdown was less than 1 ft. As in scenario 3, some stream depletion occurred in Jefferson River reaches 10 to 22 (figs. 21, 26) and in Slaughterhouse Slough reach 50. Since pumping in this scenario is from the deeper Renova Formation, the stream depletion rates were lower than scenario 3. The highest depletion rate in August 2025 was about 1,200

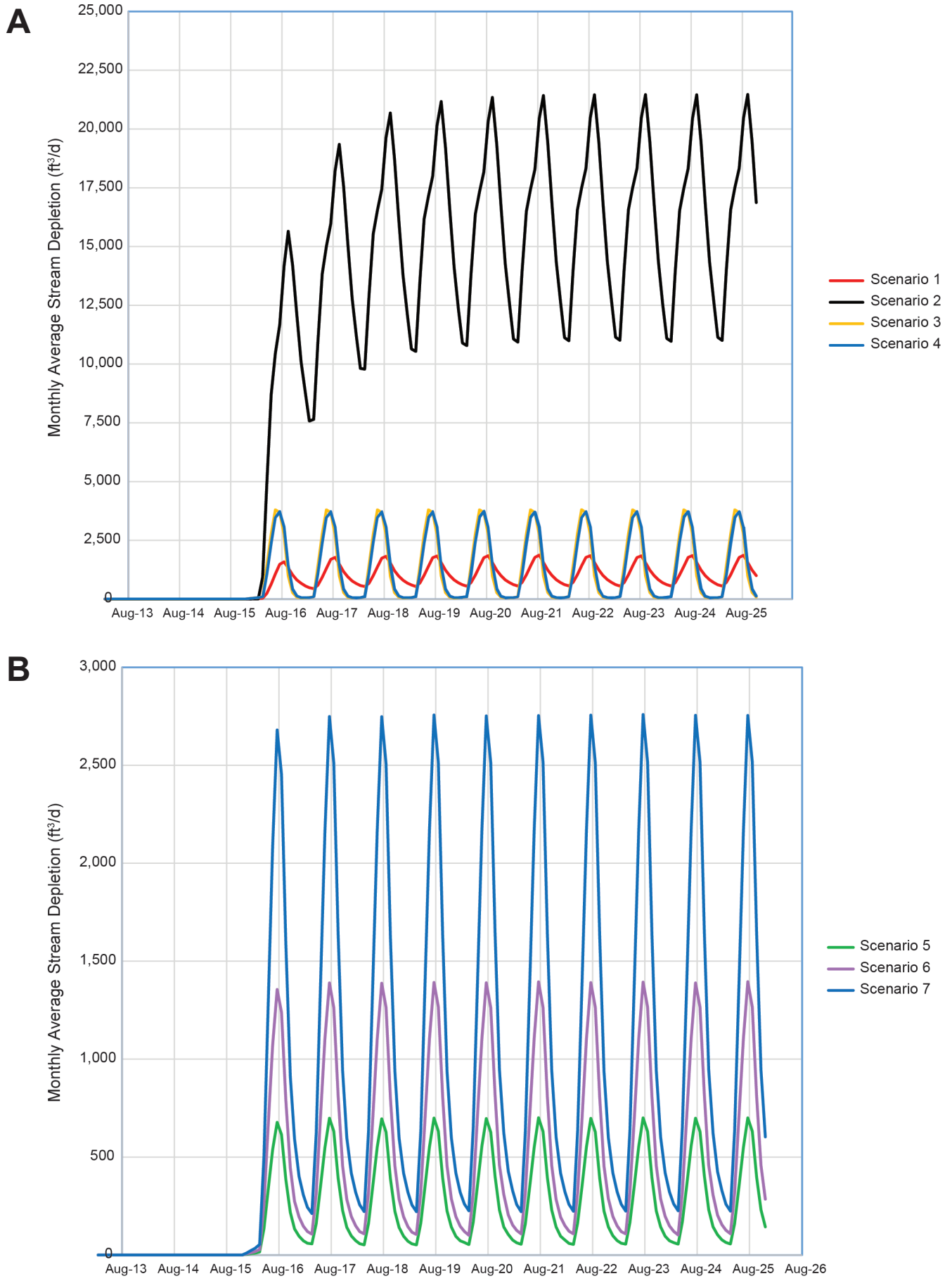

Figure 22. (A) Scenarios 1 through 4. The greatest stream depletion occurred under scenario 2. The stream depletion caused by scenarios 3 and 4 was nearly identical. (B) Scenarios 5 through 7. These scenarios show that the amount of stream depletion increased as the number of wells and total pumping increased.

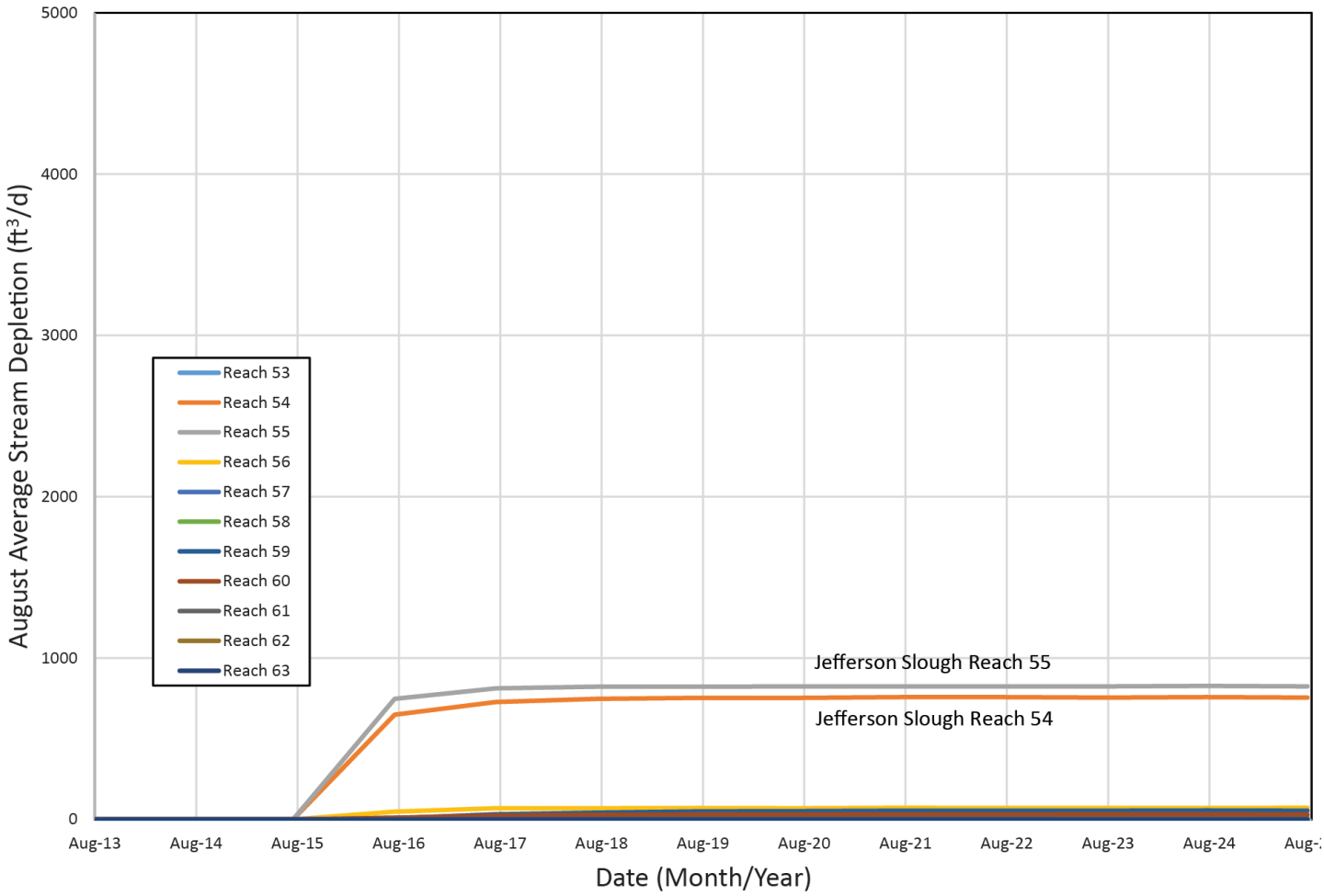

Figure 23. Scenario 1 stream depletion. Pumping from 23 domestic wells in layer 1 has the most effect on reaches 54 and 55 of Jefferson Slough.

Table 18. Model predictive scenarios results—local effects.

Maximum Stream Flow Depletion (August 2025)								
		Stream Depletion						
Scenario	Description	ft³/d	cfs	gpm	gpm/home	Stream	Reaches	Maximum Reduction from Scenario 0 (%)
0	Base Case—No development and no change in land use	0	0	0	0	NA	NA	
1	23 homes—Non-Irrigated Bench	825	0.01	4.3	0.2	Jefferson Slough	55	2%
2	23 homes—Irrigated Bench (reduced irrigation recharge by 90%)	10,000	0.12	51.9	2.3	Whitetail Creek	59	41%
3	23 homes—Non-Irrigated Alluvium	1,497	0.017	7.8	0.3	Jefferson River	17	3%
4	23 homes—Non-Irrigated Renova	1,207	0.014	6.3	0.3	Jefferson River	19	2%
5	5 homes—Non-Irrigated Renova	96	0.001	0.5	0.1	Jefferson River	2	1%
6	10 homes—Non-Irrigated Renova	196	0.002	1.0	0.1	Jefferson River	2	3%
7	20 homes—Non-Irrigated Renova	400	0.005	2.1	0.1	Jefferson River	4	6%

Note. The annual average pumping rate is 0.3 gpm/home.

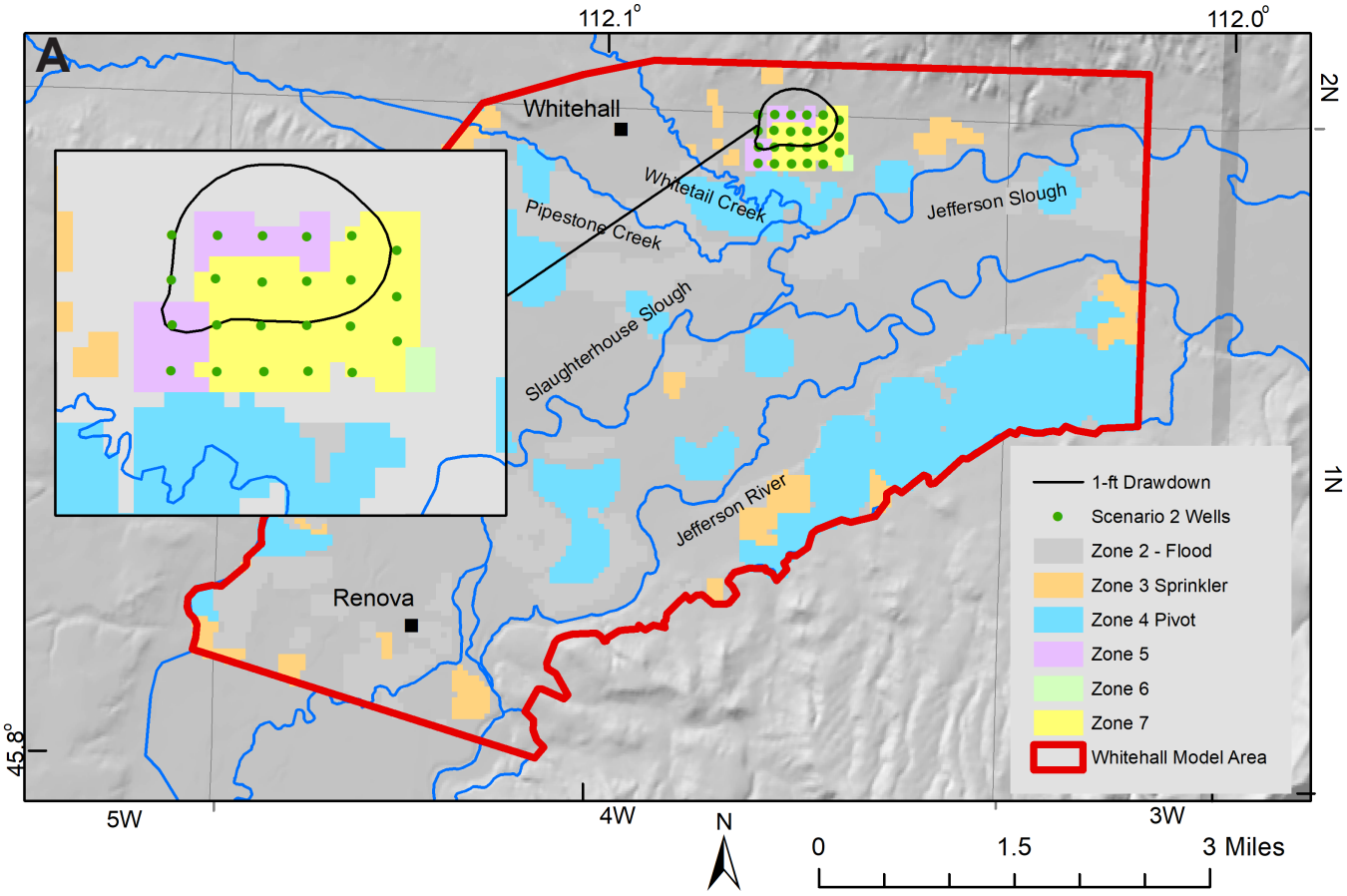

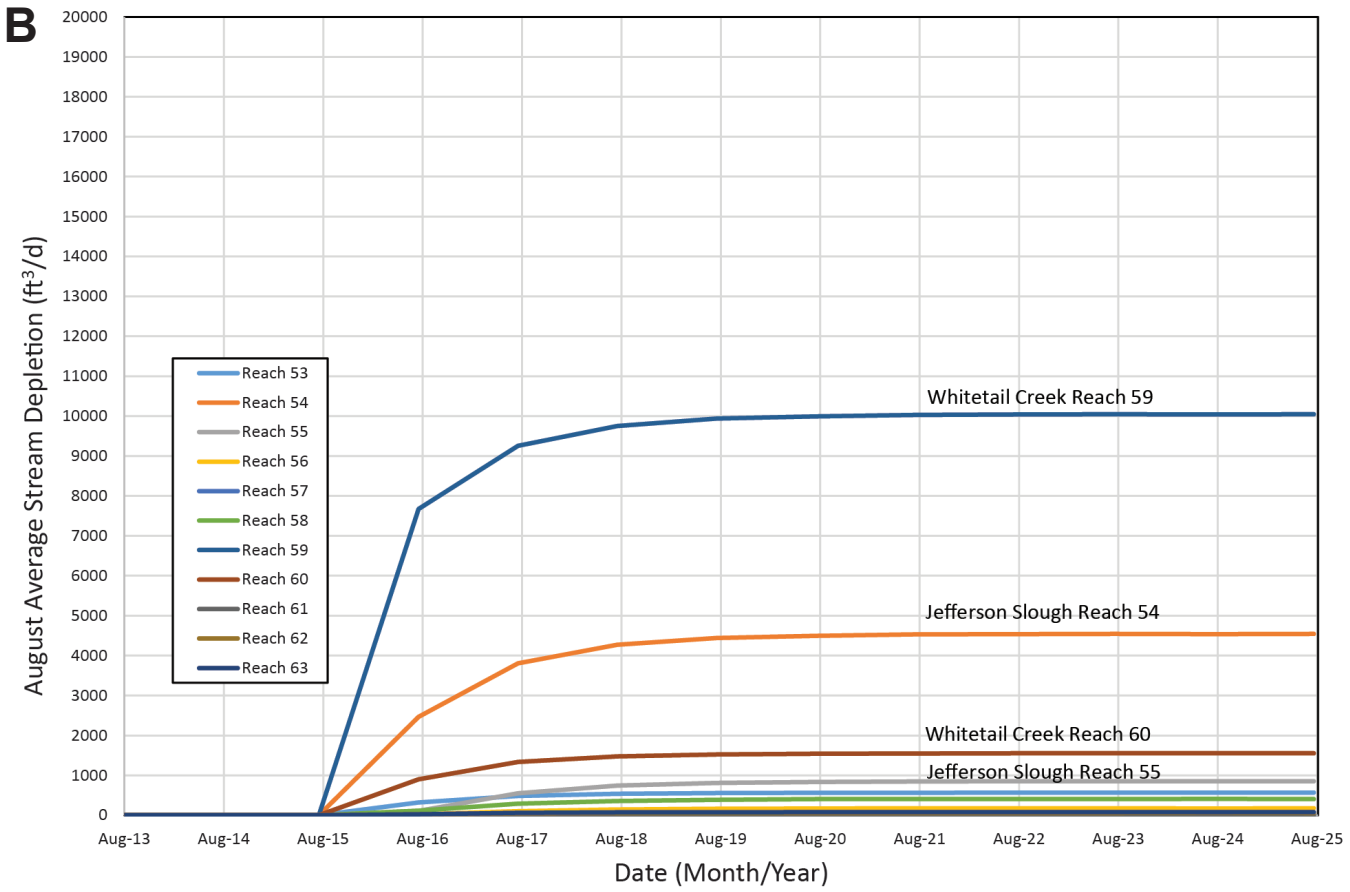

Figure 24. (A) Scenario 2 includes reducing irrigation recharge by 90% and adding pumping in layer 1 from 23 domestic wells from the proposed subdivision, results in 1 ft of drawdown at the subdivision. (B) Scenario 2 (pumping 23 domestic wells in layer 1). With time, the maximum late summer stream depletion was in Whitetail Creek (reach 59), Jefferson Slough (reach 54), Whitetail Creek (reach 60), and Jefferson Slough (reach 55).

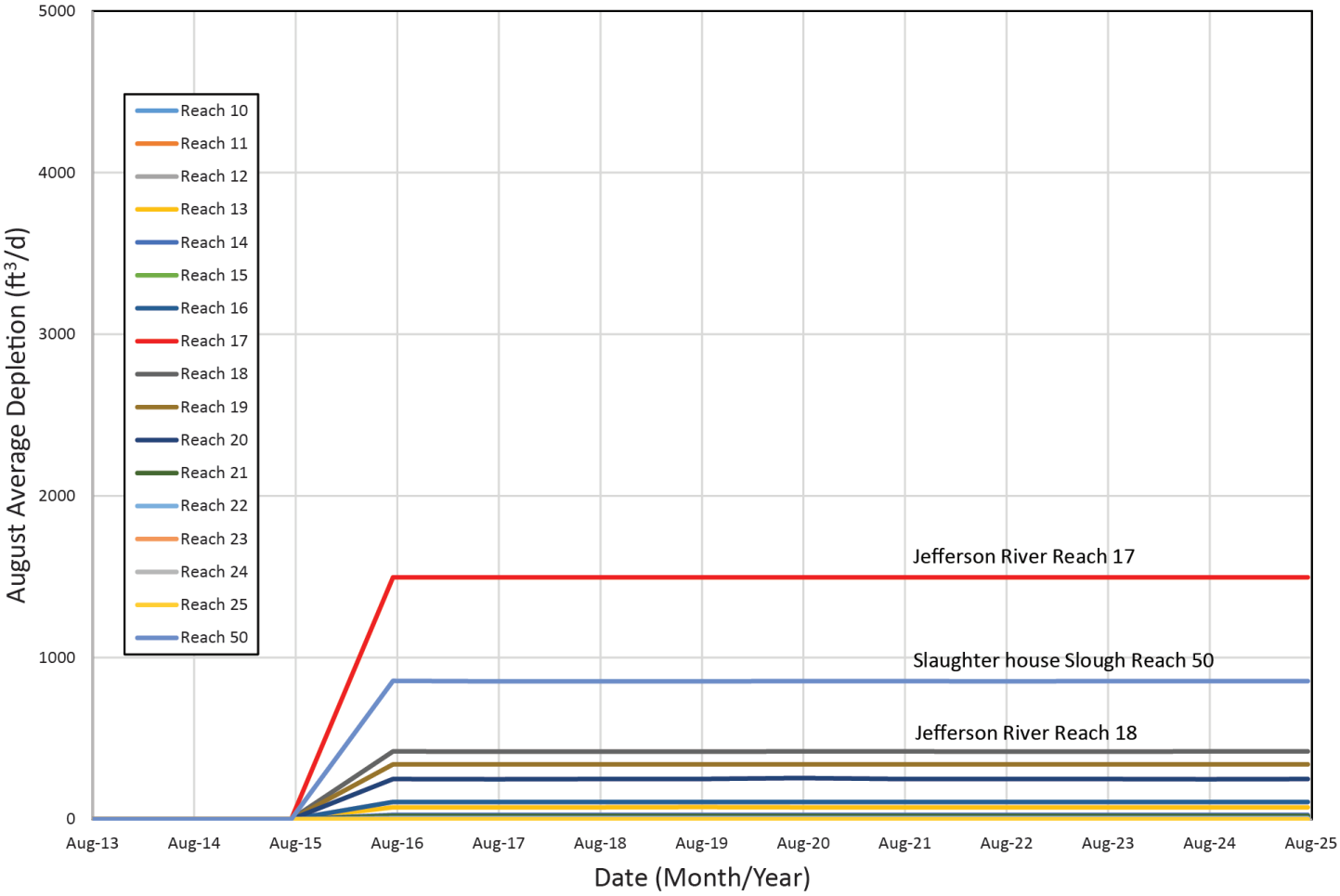

Figure 25. Scenario 3 (pumping 23 domestic wells in layer 1). With time, the maximum stream depletion in August was in Jefferson River (reach 17), Slaughterhouse Slough (reach 50), and Jefferson River (reach 18).

ft³/d (0.014 cfs) in Jefferson River reach 17, a 2% reduction from scenario 0 (table 18).

Scenario 5: Drawdown was less than 1 ft. Stream depletion was limited to Jefferson River reaches 1 to 10 (figs. 21, 27). The highest depletion rate in August 2025 was 96 ft³/d (0.001 cfs) in Jefferson River reach 2 (fig. 21), a 1% reduction from scenario 0 (table 18).

Scenario 6: Drawdown was less than 1 ft. Some stream depletion occurred in Jefferson River reaches 1 to 9 (fig. 28). With 10 wells, this scenario doubles the number of pumping wells in scenario 5, and increased depletion. The highest depletion rate in August 2025 was 196 ft³/d (0.002 cfs) in Jefferson River reach 2, a 3% reduction from scenario 0 (table 18).

Scenario 7: Drawdown was less than 1 ft. Stream depletion was limited to Jefferson River reaches 1 to 10 (fig. 29). At 20 wells, this scenario doubles the pumping in scenario 6, and the depletion also doubles. The highest depletion rate in August 2025 was about 400 ft³/d (0.005 cfs) in Jefferson River reach 4, a 6% reduction from scenario 0 (table 18).

Scenarios 5–7 simulate additional pumping near the Parrot Canal, which is modeled as a specified flux boundary. Because the flux from this boundary cannot change in response to increased pumping, the model may overestimate stream depletion resulting from these scenarios. In reality, pumping from these scenarios could increase flux through the aquifer under the canal.

Model results (tables 17, 18; fig. 21) show that pumping from non-irrigated areas of bench sediments produced low depletion rates (scenarios 1, 5, 6, and 7). Development that involved a reduction in recharge along with an increase in pumping (scenario 2) created the largest effects. Placing subdivision wells close to surface water resulted in similar depletion rates, regardless of the stressed formation; pumping from the layer 1 alluvium (scenario 3) and from the layer 2 Renova Formation (scenario 4) produced 1,497 ft³/d and 1,207 ft³/d depletion rate, respectively. Placing subdivision wells near surface water at a location close to a model hydraulic boundary reduced stream deple-

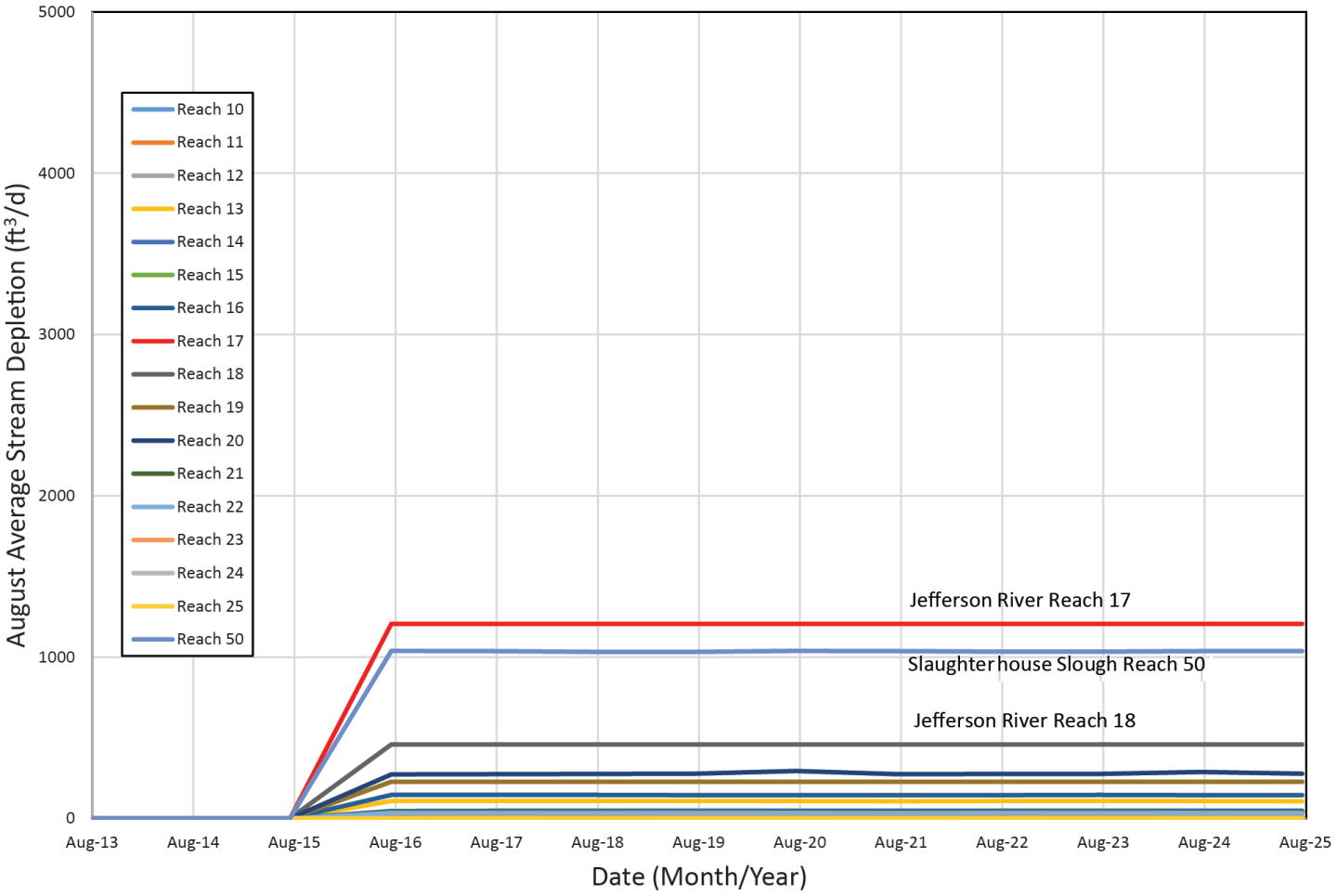

Figure 26. Scenario 4 (pumping 23 domestic wells in layer 2). With time, the maximum stream depletion in August was in Jefferson River (reach 17), Slaughterhouse Slough (reach 50), and in Jefferson River (reach 18).

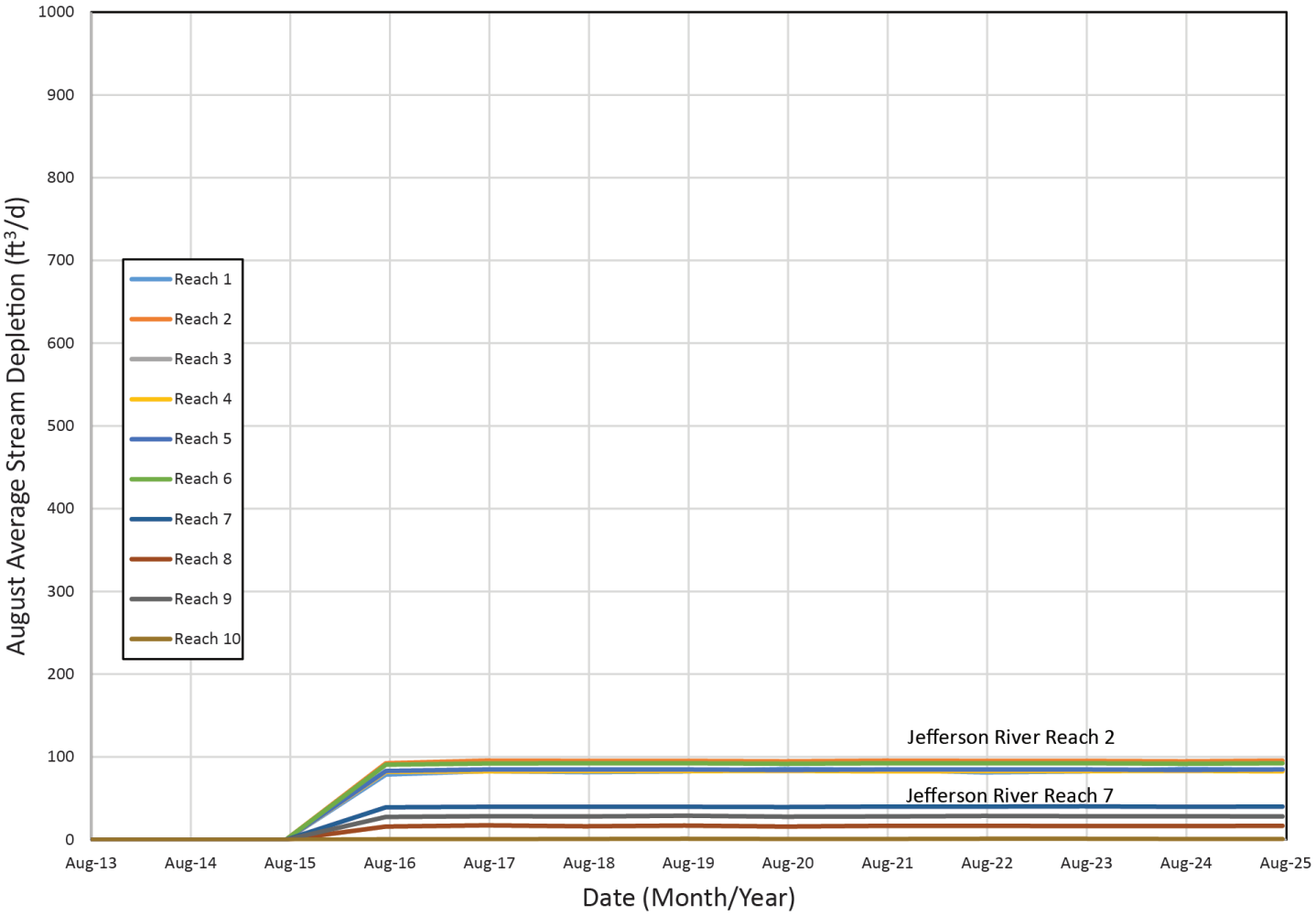

Figure 27. Scenario 5 (pumping 5 domestic wells in layer 2). With time, maximum stream depletion in August was in Jefferson River (reach 2 and reach 7).

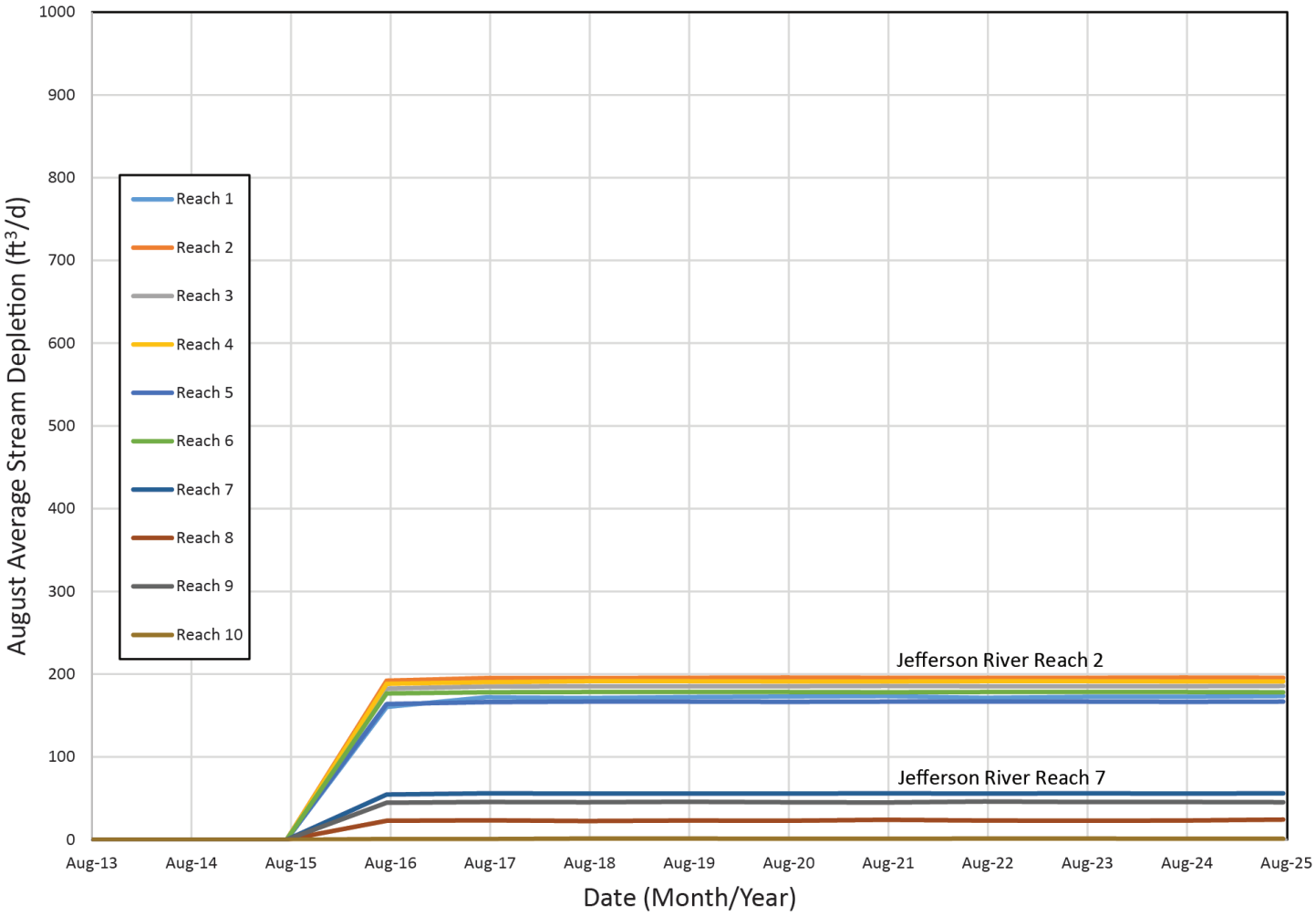

Figure 28. Scenario 6 (pumping 10 domestic wells in layer 2). With time, the maximum stream depletion in August was in Jefferson River (reach 2 and reach 7).

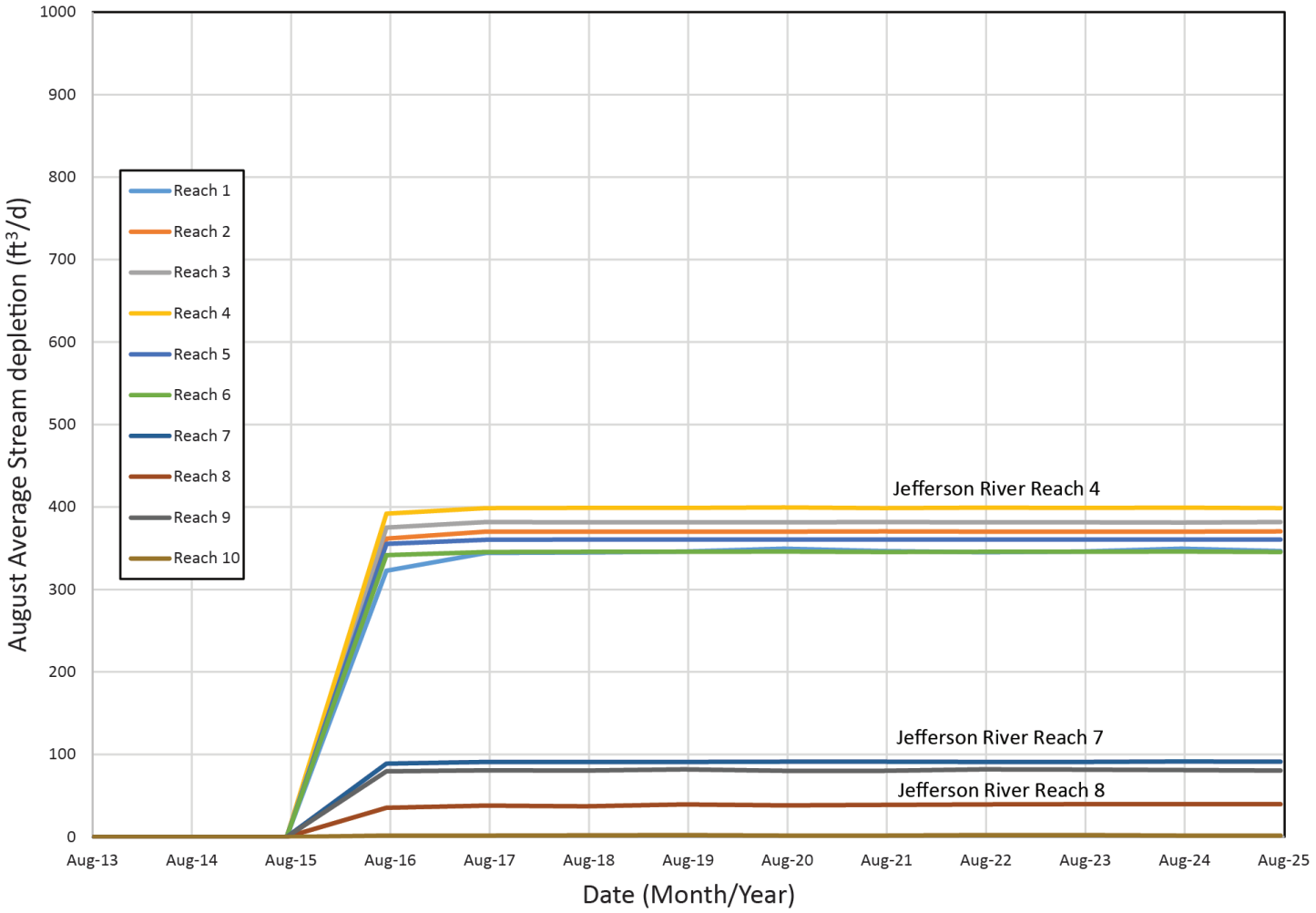

Figure 29. Scenario 7 (pumping 20 domestic wells in layer 2). With time, maximum stream depletion in August was in Jefferson River (reach 4, reach 7, and reach 8).

tion. In scenario 7 (fig. 21) 20 wells pumping from the deeper formation (layer 2) but close to the Jefferson River caused only 400 ft^3/d of stream depletion in August, about one-third the depletion produced by 23 wells placed in the same model layer in scenario 4.

UNCERTAINTY ANALYSIS

Model predictions are subject to two broad sources of uncertainty: (1) uncertainty associated with the model itself, and (2) uncertainty associated with specifications of future conditions (Anderson and others, 2015).

The first source of uncertainty originates from the following:

- Error in field measurements of certain parameters. Thus, uncertainty in predictions stemming from error in calibration of these parameters can be reduced but not eliminated.
- Failure to capture the complexity of the natural setting relevant to the prediction. Error results from the conceptual model or from the spatial and temporal simplifications made during model construction and calibration.

The second source of uncertainty occurs when predictions include an estimate of future stresses and properties (e.g., recharge rates affected by climate change), and future non-hydrogeologic conditions, such as political, economic, and societal actions that will affect hydrologic stresses (e.g., conversion from agricultural land use to residential development).

In this study, we focused on the first source of uncertainties, including those caused by errors in field parameter estimates and by the simplifications of spatial and temporal parameters in model construction and calibration. The scenarios provided the range of effects on groundwater/surface-water interactions caused by increased pumping at hypothetical subdivisions.

We employed an uncertainty analysis that is similar to the scenario modeling method presented by Anderson and others (2015). The model parameters selected for uncertainty analysis were based on sensitivity analysis, and on the uncertainty in the measurement of some model parameters (e.g., canal seepage). Five parameters were selected as the most likely to affect predictions: (1) horizontal hydraulic conductivity (K_h in all zones), (2) vertical hydraulic conductivity (K_v all zones), (3) lateral groundwater inflow (GW_{lat}; all boundaries with a GW_{lat} component), (4) irrigation canal leakage (Jefferson and Parrot Canals), and (5) aquifer storage coefficients (all zones). We used minimum and maximum multipliers to produce extreme effects.

For this analysis, we focused on scenario 2, because it produced the largest stream depletion which occurred in reach 59 of Whitetail Creek in August 2025. This is a conservative approach because it evaluates uncertainty associated with the greatest simulated change.

Staring with the base run (scenario 0), we changed the five parameters twice, using high and low multipliers, generating 10 model runs (table 19). Each simulation time extended over 12 yr, from April 2013 to December 2025. Groundwater flux to surface-water bodies in August of each year was recorded for the 10 simulations. Next, we completed 10 runs of scenario 2, using the same five uncertainty parameters, multipliers, and time frame employed with the base run (table 19). Similarly, the predicted groundwater flux to rivers and drains during the month of August in each year was recorded (fig. 30).

The difference in stream depletion at reach 59 of Whitetail Creek in August 2025 between the base run with changes in one of the uncertainty parameters and that produced by scenario 2 (modified with the same changed uncertainty parameter) is the error in prediction associated with that particular uncertainty parameter (appendix E).

At Whitetail reach 59, using five parameters and two multipliers, ten prediction errors were estimated for every August from 2016 to 2025. Figure 31 shows the assembled errors as percentage of the model's prediction of stream depletion. This collection of prediction errors defines an envelope of uncertainty around the model's prediction (Anderson and others, 2015).

The Whitehall model prediction error (fig. 31) stabilizes as time progresses. The error ranged from about 23% (scenario 2, storage coefficient times 0.1) to 80%, with most values showing between 23 and 50% uncertainty. To put this in practical terms, if the model shows a reduction in streamflow of 10 cfs with 50% uncertainty, the expected effect lies between 5 cfs and 15 cfs. Since this model shows a maximum

Table 19. Model uncertainty analysis—parameters and multipliers.

Uncertainty Parameters	Uncertainty Multipliers		Number of Model Runs	
	Base Run	Scenario 2	Base Run	Scenario 2
K_h (all zones)	0.1, 2	0.1, 2	2	2
K_v (all zones)	0.1, 2	0.1, 2	2	2
Lateral Groundwater Influx (all zones)	0.75, 1.25	0.75, 1.25	2	2
Canal Leakage (all segments)	0.75, 1.25	0.75, 1.25	2	2
Storage Coefficients (all zones)	0.1, 10	0.1, 10	2	3
		Total	10	10

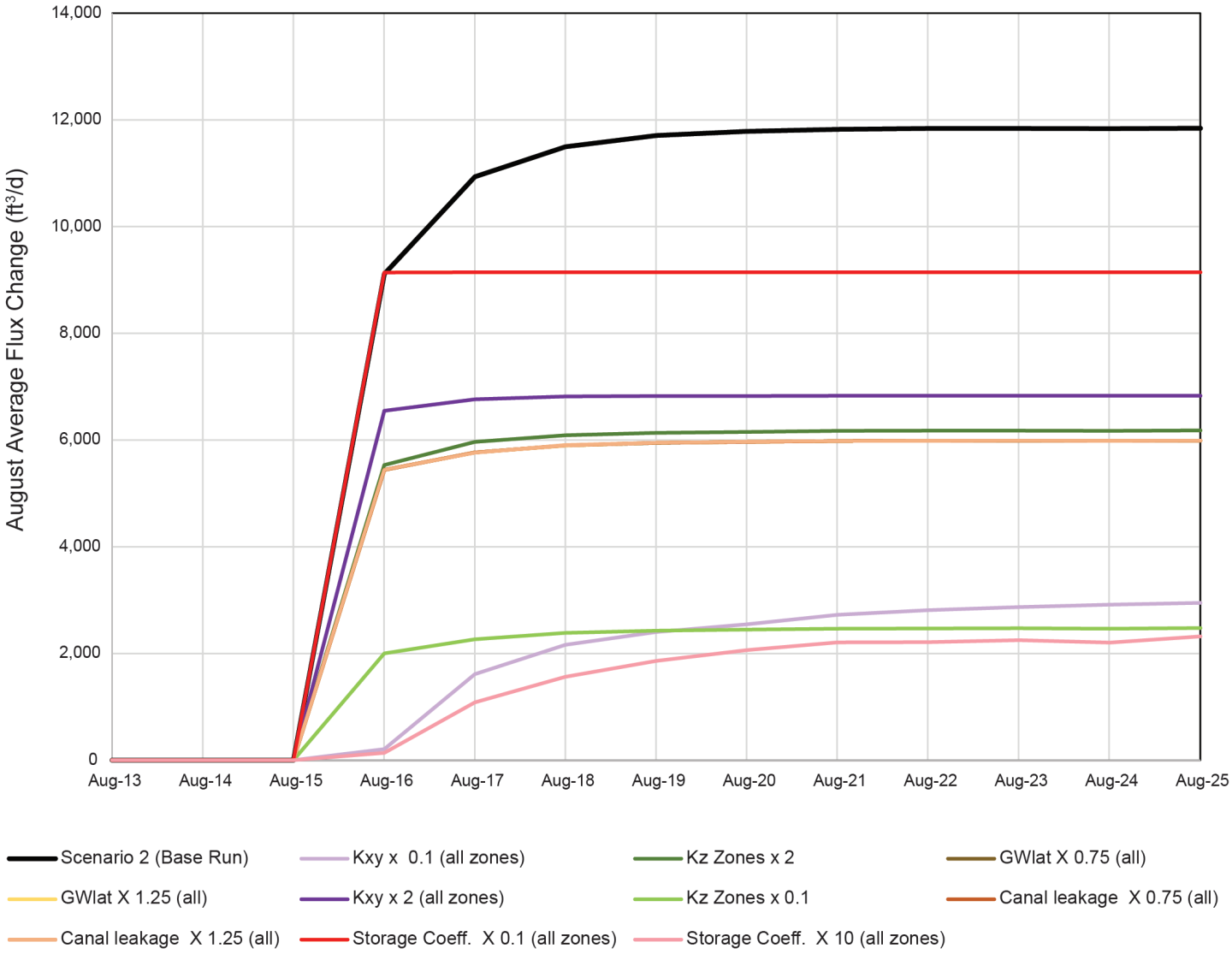

Figure 30. Model uncertainty analysis. The month of August net flux in Whitetail Creek at reach 59 (scenario 2 conditions) indicates that stream depletion in August became more stable over time. Deviation from the base run depletion (black) varied with changes in tested parameters and multipliers.

stream depletion of 0.12 cfs (scenario 2), a 50% error in prediction uncertainty suggests that the actual maximum depletion would likely be between 0.06 and 0.24 cfs.

MODEL LIMITATIONS

The Whitehall groundwater flow model implements and quantifies the conceptual model, and may be used to evaluate the effects of development on groundwater and surface-water flows, especially in late summer conditions. However, the model limitations include scale and parameter uncertainty.

The scale of the model encompasses the Whitehall area and is not designed to account for large basin flow beyond the model domain. For example, it is not suitable to estimate a water budget for a much larger area. At the other extreme, groundwater/surface-water interactions cannot be resolved at a finer scale than the model cell size, of 220 ft x 220 ft. The simulated 100 ft thickness of the Renova Formation likely underrepresents the total flux through the entire thickness of the Renova Formation. However, this limitation is unlikely to affect the groundwater/surface-water interactions in the upper alluvium water-bearing formations, the focus of this modeling effort.

Results for scenarios 5–7 may overestimate stream depletion due to the proximity of a specified flux boundary to the area of increased pumping. Although a recognized limitation of the model structure, the physical setting of the study area, at the edge of the mountain front, precluded moving this model boundary farther from the area of interest.

Uncertainty analysis identified which parameters limit model results. Model predictions are sensitive to

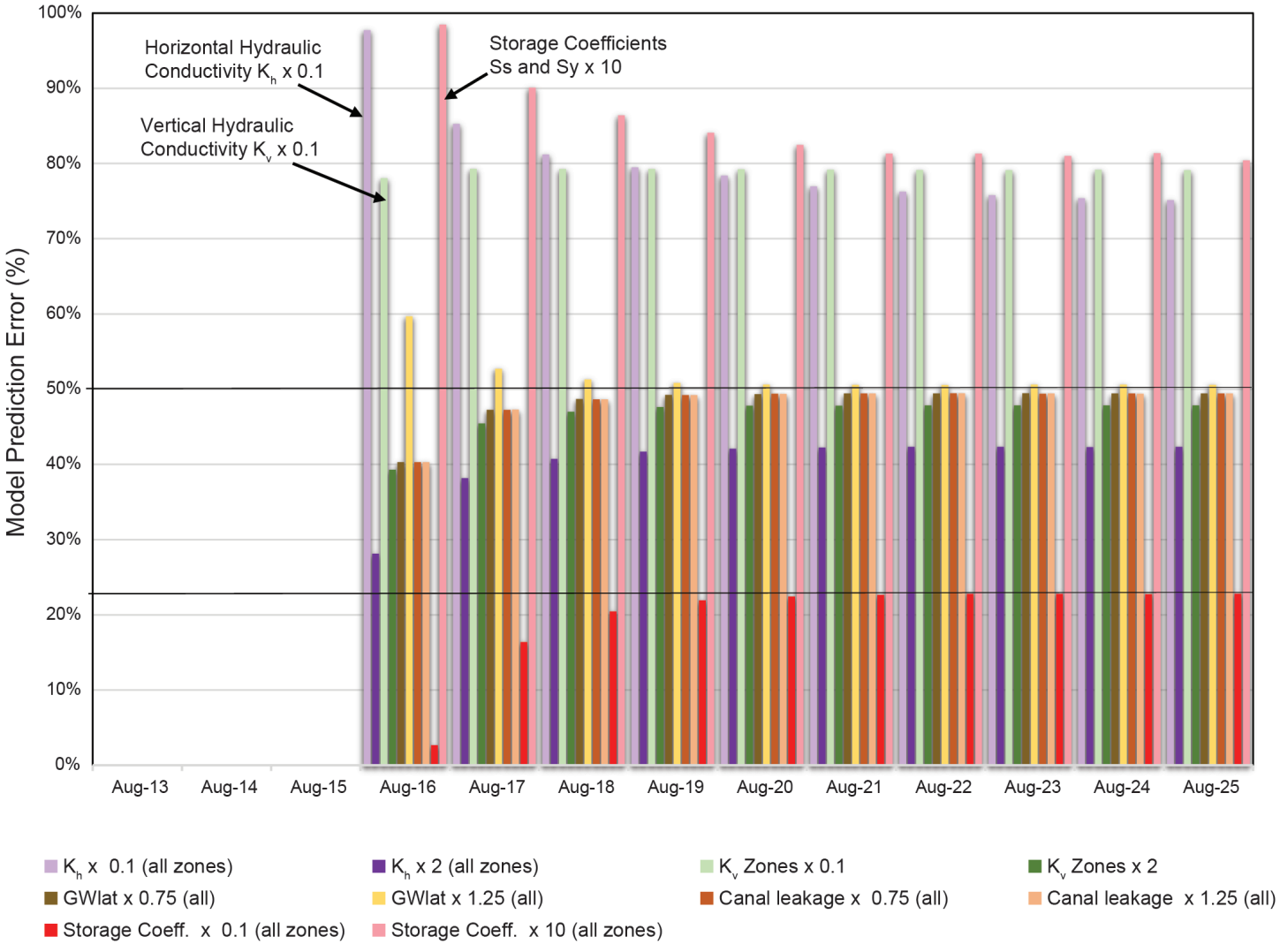

Figure 31. Model uncertainty analysis. The model's uncertainty—prediction error—focused on errors in predicting late summer (August) stream depletion at the most affected stream, Whitetail Creek (reach 59) under scenario 2 conditions. The error ranged from 23% (scenario 2, storage coefficient times 0.1) to about 80%, with most values lay between 23% and 50% uncertainty.

hydraulic conductivity, lateral groundwater flux, canal leakage, and storage coefficients (figs. 30, 31). The estimate of uncertainty error presented above helps to overcome this limitation.

MODEL RECOMMENDATIONS

More survey data in Slaughterhouse and Jefferson Sloughs and in Whitehall and Pipestone Creeks would enhance simulation of groundwater/surface-water interactions, which are sensitive to elevation. LiDAR coverage recently acquired for this area could be incorporated into the model to improve estimates of surface elevations.

SUMMARY AND CONCLUSIONS

As development of land and water resources increase, development of either resource is likely to affect the quantity and quality of the other (Winter and others, 1999). The Whitehall area modeling study focused on simulating groundwater and surface-water interactions and forecasting stream depletion due to the changes in groundwater consumption that result from the development of new subdivisions in both irrigated and non-irrigated areas. The model considers both increases in groundwater consumption and reductions in irrigation recharge.

The calibrated model results matched with measured groundwater elevations, generated a balanced water budget that agreed well with the estimated water budget for the conceptual model, and maintained parameter values reasonably close to the estimated aquifer properties. The transient simulation demonstrated the model's ability to capture the seasonality of water-level changes, yielding good fits of simulated hydrographs to data.

Extending the transient model for an additional 10 yr facilitated testing seven hypothetical scenarios. The scenarios evaluate stream depletion related to pumping from subdivisions, especially during the late summer low-flow period. Results suggest that adding pumping from 23 homes would cause stream depletion ranging from 0.01 to 0.14 cfs, or 2 to 48% of groundwater discharge to the stream reach in late summer. The greatest depletion rate occurred with subdivisions placed on previously irrigated lands (scenario 2), because a reduction in agricultural irrigation was also simulated. The greatest depletion was to Whitetail Creek along reach 59.

The model simulated low stream depletion rates (<0.15 cfs) caused by a reduction in groundwater flux under extreme conditions. The conditions included late summer low flow, high temperatures, elimination of irrigation recharge, and increased groundwater consumption (scenario 2). Such low rates are difficult to accurately measure in the field. Even with the ±50% uncertainty associated with the model's predictions, depletion will be less than 0.25 cfs. This is a low flow compared to the 14 cfs average daily discharge measured in August 2014 (Whitetail Creek at Mouth, GWIC 287492). However, as demonstrated in scenarios 5, 6, and 7, increasing the number of homes in a subdivision, or increasing the number of subdivisions, will proportionally increase local stream depletion if additional pumping is in close proximity to surface-water bodies.

The highest stream depletion in the Whitehall area occurs at approximately the same time as pumping peaks from the unconsolidated Quaternary and Tertiary deposits. This is due to the close coupling between surface waters and groundwater. As shown in the groundwater budget (fig. 16B), most of the water passing through the unconsolidated aquifer is received from, and returns to, surface waters. Over the long term, the amount of stream depletion must equal consumptive water use. The ways that groundwater is used have a direct effect on stream flows, so there is a direct tradeoff between consumptive water use and stream flows. This tradeoff should be taken into consideration when making development decisions that can affect water resources.

REFERENCES

Anderson, M.P., Woessner, W.W., and Hunt, R.J., 2015, Applied groundwater modeling: Simulation of flow and advective transport: San Diego, Calif., Academic Press, 381 p.

ASTM, 2010, D5447-04, Standard guide for application of a groundwater flow model to a site-specific problem: West Conshohocken, Pa., ASTM International.

ASTM, 2014, D5979-96, Standard guide for conceptualization and characterization of groundwater systems: West Conshohocken, Pa., ASTM International.

Bobst, A., Butler, J., and Carlson, L., 2016, Hydrogeologic investigation of the Boulder River Valley,

Jefferson County, Montana, interpretive report: Montana Bureau of Mines and Geology Open-File Report 682, 92 p.

Bobst, A., and Gebril, A. in prep., Hydrologic investigation of the Upper Jefferson River Valley

Madison and Jefferson Counties, Montana Waterloo groundwater modeling report: Montana Bureau of Mines and Geology Open-File Report.

Bobst, A.L., and Gebril, A., 2020, Aquifer tests in the Upper Jefferson Valley: Montana Bureau of Mines and Geology: Open-File Report 727, 52 p.

Brancheau, N.L., 2015, Hydrogeologic evaluation of the Waterloo area in the Upper Jefferson River Valley, Montana: Butte, Montana Tech, Master's thesis.

Butler, J., and Bobst, A., 2017, Hydrogeologic investigation of the Boulder Valley, Jefferson County, Montana: Groundwater modeling report: Montana Bureau of Mines and Geology Open-File Report 688, 131 p.

Doherty, J.E., and Hunt, R.J., 2010, Approaches to highly parameterized inversion-A guide to using PEST for groundwater-model calibration: U.S. Geological Survey Scientific Investigations Report 2010-5169, 37 p.

Dugan, J.T., and Peckenpaugh, J.M., 1985, Effects of climate, vegetation, and soils on consumptive water use and groundwater recharge in the Central Midwest Regional Aquifer System, Mid-Continent United States: U.S. Geological Survey Water Resources Investigations Report 85-4236, 78 p.

Environmental Simulations Incorporated, 2011, Guide to using Groundwater Vistas, Version 6.77 Build9, 213 p.

Freeze, R.A., and Cherry, J.A., 1979, Groundwater: Upper Saddle River, N.J., Prentice-Hall, Inc.

Groundwater Information Center (GWIC), 2019, http://mbmggwic.mtech.edu/ [Accessed August 2019].

Hackett, O.M., Stermitz, F., Boner, F.C., and Krieger, R.A., 1960, Geology and ground-water resources of the Gallatin Valley, Gallatin County, Montana: U.S. Government Printing Office.

Harbaugh, A.W., Banta, E.R., Hill, M.C., and McDonald, M.G., 2000, MODFLOW-2000: The U.S. Geological Survey modular ground-water model-user guide to modularization concepts and the ground-water flow process: U.S. Geological Survey Open-File Report 00-92, p. 121. Hackett

Jensen, M.E., 2010, Estimating evaporation from water surfaces: Proceedings of the CSU/ARS Evapotranspiration Workshop, p. 1–27.

Johns, E., ed., 1989, Water use by naturally occurring vegetation, including an annotated bibliography: New York, American Society of Civil Engineers, 216 p.

Kendy, E., and Tresch, R.E., 1996, Geographic, geologic, and hydrologic summaries of intermontane basins of the northern Rocky Mountains, Montana: U.S. Geological Survey Water-Resources Investigations Report 96-4025.

Lautz, L.K., 2008, Estimating groundwater evapotranspiration rates using diurnal water-table fluctuations in a semi-arid riparian zone: Hydrogeology Journal, v. 16, p. 483–497.

MesoWest & Synoptic Data, MesoWest.utah.edu, https://mesowest.utah.edu [Accessed July 2020].

Montana Department of Natural Resources and Conservation (MT-DNRC), 2011, DNRC general water-use requirements, presented by the DNRC Water Resources Division to the Water Policy Interim Committee on September 13, 2011.

Montana Department of Revenue (MDOR), 2012, Revenue Final Land Unit Classification [Accessed October 2012].

Montana Fish Wildlife and Parks Department (MTFWP), 2012, Montana Statewide Fisheries Management Plan, 2013–2018: 478 p.

Nash, J.E., and Sutcliffe, J.V., 1970, River flow forecasting thorough conceptual models. Part I. A discussion of principles: Journal of Hydrology, v. 10, p. 287–290.

NRCS, 1993, NRCS National engineering handbook (NEH), Part 623, Chapter 2: Irrigation water requirements: U.S. Department of Agriculture.

NRCS, 2003, IWR program guide, https://www.nrcs.usda.gov/Internet/FSE_DOCUMENTS/nrcs144p2_013838.pdf [Accessed August 2019].

NRCS, 2019, NRCS web soil survey, https://websoilsurvey.sc.egov.usda.gov/App/WebSoilSurvey.aspx [Accessed August 2019].

National Oceanic and Atmospheric Administration

(NOAA), 2011, NOAA's 1981–2010 climate normals, http://www.ncdc.noaa.gov/oa/climate/normals/usnormals.html [Accessed March 4, 2013].

Noble, R.A., Bergantino, R.N., Patton, T.W., Sholes, B.C., Daniel, F., and Scofield, J., 1982, Occurrence and characteristics of groundwater in Montana: MBMG Open-File Report 99, 214 p.

PRISM Climate Group, 2014, Oregon State University, from PRISM Climate Data: http://www.prism.oregonstate.edu/ [Accessed July 23, 2014].

Shah, N., Nachabe, M., and Ross, M., 2007, Extinction depth and evapotranspiration from ground water under selected land covers: Groundwater, v. 45, no. 3, p. 329–338.

Sterling, R., and Neibling, W.H., 1994, Final report of the Water Conservation Task Force: Boise, Idaho Department of Water Resources.

Sweet, M.D., Oyler, J., Jencso, K., Running, S., and Ballantyne, A., 2015, Climate atlas of Montana: Montana Forest and Conservation Experiment Station, http://www.climate.umt.edu/atlas/default.php [Accessed September 9, 2015].

U.S. Geological Survey (USGS), 2013, 1/3-arc second national elevation dataset, https://viewer.nationalmap.gov/basic/ [Accessed February 2020].

U.S. Geological Survey (USGS), 2016, LANDFIRE database, Wildland Fire Science, Earth Resources Observation and Science Center, U.S. Geological Survey, https://www.landfire.gov/viewer/ [Accessed December 2017].

Vuke, S.M., Coppinger, W.W., and Cox, B.E., 2004, Geologic map of Cenozoic deposits in the Upper Jefferson Valley, southwestern Montana: Montana Bureau of Mines and Geology Open-File Report 505, 35 p., 1 sheet, scale 1:50,000.

Waren, K.B., Bobst, A.L., Swierc, J.E., and Madison, J.D., 2013, Hydrologic investigation of the North Hills Study area, Lewis and Clark County, Montana, groundwater modeling report: Montana Bureau of Mines and Geology Open-File Report 628, 90 p.

Water & Environmental Technologies (WET), 2006, Ground water study of the Waterloo area: Butte, Water & Environmental Technologies.

Watershed Sciences, Inc. (WSI), 2013, Jefferson Slough–Pipestone Creek LiDAR survey: Prepared for Confluence Consulting, Technical Data Report, 18 p.

Winter, T.C., Harvey, J.W., Frank, O.L., and Alley, W.M., 1999, Groundwater and surface water: A single resource: U.S. Geological Survey Circular 1139.

APPENDIX A:
PRELIMINARY WATER BUDGET

PRELIMINARY WATER BUDGET

A preliminary water budget was developed for the Whitehall area to aid in model construction and ensure that the amount of water entering and leaving the model through the boundaries was reasonable. This budget was based on monitoring data, aquifer tests, well logs, literature values, and GIS analysis of soil, climate, vegetation, land-use, and water rights data. For each component best estimates (BE) minimum estimates (MinE) and maximum estimates (MaxE) were calculated to characterize the likely range. The BE values were used to develop the numerical model, and the values were modified during the model calibration process.

1. Alluvial Groundwater Inflow (GWin-al)

Groundwater flowed into the model area in three locations: (1) at the south end of the model through the Jefferson River alluvium; (2) in the northwest portion of the model through the Pipestone Creek alluvium; and (3) in the northwest portion of the model through the Whitetail Creek alluvium (fig. A1). Inflow through alluvium was calculated using the Darcy Flux Equation:

$$Q = KAI,$$

where Q is groundwater inflow (ft^3/d); K is hydraulic conductivity of the aquifer (ft/d); A is saturated cross-sectional area of the alluvial aquifer at the boundary (ft^2); and I is hydraulic gradient across the boundary (ft/ft or unitless).

Table A1. Flow through the alluvium was estimated using Darcy's Law.

	K (ft/d)								Q (ac-ft/yr)		
	BE	MinE	MaxE	Length (ft)	Sat Tk (ft)	A (ft^2) L x T	I (ft/ft)	BE Q (ft^3/d)	BE	MinE	Max E
Jefferson River alluvium	100	75	250	13,169	40	526,760	0.0017	89,549	751	563	1,877
Pipestone Creek alluvium	50	25	100	2,455	40	98,200	0.0052	25,532	214	107	428
Whitetail Creek alluvium	50	25	100	2,913	30	87,390	0.0061	26,654	223	112	447
						TOTAL Alluvial Groundwater Inflow		141,735	1,188	782	2,752

Note. K, estimated from aquifer tests conducted for this study; sediment descriptions from water well logs and literature values. A, based on the geologic model for this study. I, calculated using observed water levels from April 2015.

Table A2. Monthly alluvial inflow (acre-ft).

	Jan	Feb	Mar	Apr	May	Jun	Jul	Aug	Sep	Oct	Nov	Dec	Total
Days	31	28.25	31	30	31	30	31	31	30	31	30	31	365.25
BE	101	92	101	98	101	98	101	101	98	101	98	101	1,188
MinE	66	60	66	64	66	64	66	66	64	66	64	66	782
MaxE	234	213	234	226	234	226	234	234	226	234	226	234	2,752

Note. The total annual BE inflow values (table A1) were divided by 365.25 and multiplied by the days in a month to get monthly amounts.

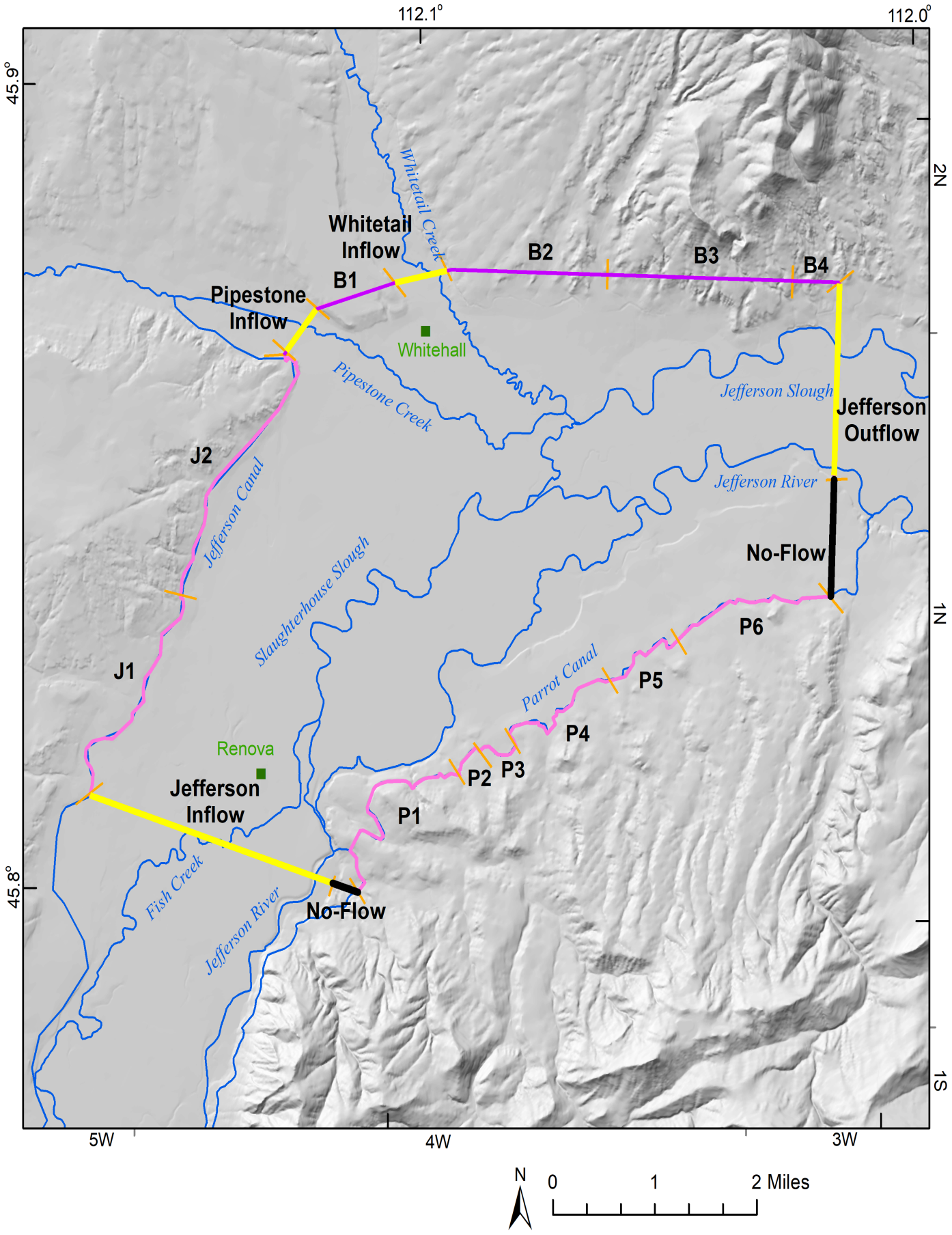

Figure A1. Groundwater inflow and outflow occur along the edges of the model domain. Alluvial inflow occurs along the yellow segments at the southern end of the model area, and along Pipestone and Whitetail Creeks. Lateral groundwater inflow occurs along the numbered segments. Alluvial outflow occurs along the yellow segment on the east side.

2. Lateral Groundwater Inflow (GWin-lat)

Groundwater inflow along the lateral edges of the model occurred through the Tertiary Renova Formation, and through bedrock. Both of these materials are less permeable than the alluvium. The groundwater inflow was calculated using the Darcy Flux Equation (see Alluvial Groundwater Inflow section), and by breaking the lateral boundaries into 12 segments (fig. A1). Two segments underlie the Jefferson Canal, four correspond to the Tertiary and bedrock materials along the northern edge of the model domain, and six underlie the Parrot Canal.

Table A3. Lateral groundwater inflow calculated using the Darcy Flux Equation.

Segment	K (ft/d)			Width	Sat Tk	Area	I	BE Q	Q (ac-ft/yr)		
	BE	MinE	MaxE	(ft)	(ft)	(ft^2)	(ft/ft)	(ft^3/d)	BE	MinE	MaxE
J1	1.0	0.1	5.0	11,986	40	479,440	0.0082	3,923	33	3.3	164
J2	1.0	0.1	5.0	14,309	40	572,360	0.0084	4,806	40	4.0	202
B1	1.0	0.1	5.0	4,268	40	170,720	0.0045	768	6	0.6	32
B2	1.0	0.1	5.0	8,078	40	323,120	0.0181	5,842	49	4.9	245
B3	0.1	0.1	0.5	9,576	40	383,040	0.0235	902	8	3.8	38
B4	1.0	0.1	5.0	2,448	40	97,920	0.0240	2,348	20	2.0	98
P1	1.0	0.1	5.0	12,384	40	495,360	0.0035	1,749	15	1.5	73
P2	1.0	0.1	5.0	2,097	40	83,880	0.0035	296	2	0.2	12
P3	1.0	0.1	5.0	2,302	40	92,080	0.0035	325	3	0.3	14
P4	1.0	0.1	5.0	7,994	40	319,760	0.0035	1,129	9	0.9	47
P5	1.0	0.1	5.0	5,021	40	200,840	0.0052	1,046	9	0.9	44
P6	1.0	0.1	5.0	9,168	40	366,720	0.0069	2,516	21	2.1	105
								TOTAL	215	25	1,075

Table A4. Monthly lateral groundwater inflow.

	Jan	Feb	Mar	Apr	May	Jun	Jul	Aug	Sep	Oct	Nov	Dec	Total
Days	31	28.25	31	30	31	30	31	31	30	31	30	31	365.25
BE	18	17	18	18	18	18	18	18	18	18	18	18	215
MinE	2	2	2	2	2	2	2	2	2	2	2	2	25
MaxE	91	83	91	88	91	88	91	91	88	91	88	91	1,075

Note. The total annual BE inflow values (table A3) were divided by 365.25 and multiplied by the days in a month.

3. Canal Leakage (CL)

The Parrot and Jefferson Canals leak water to the underlying aquifer from mid-April to mid-October. An overall average leakage rate of 1.31 cfs/mi was estimated from monitoring the Parrot Canal (Bobst and Gebril, in prep.). The canals were separated into the same segments used to calculate lateral groundwater inflow (fig. A1).

Table A5. Annual canal leakage.

Segment	Leakage Rate (cfs/mi)			Miles	BE cfs	BE ft^3/d	Days on per year	BE Leakage (ft^3/yr)	Leakage (ac-ft/yr)		
	BE	MinE	MaxE						BE	MinE	MaxE
P1	1.31	1.00	1.62	2.35	3.1	265,982	184	48,807,770	1,120	855	1,386
P2	1.31	1.00	1.62	0.40	0.5	45,274	184	8,307,706	191	146	236
P3	1.31	1.00	1.62	0.44	0.6	49,801	184	9,138,476	210	160	259
P4	1.31	1.00	1.62	1.51	2.0	170,908	184	31,361,589	720	550	890
P5	1.31	1.00	1.62	0.95	1.2	107,525	184	19,730,801	453	346	560
P6	1.31	1.00	1.62	1.74	2.3	196,940	184	36,138,519	830	633	1,026
J1	1.31	1.00	1.62	2.27	3.0	256,928	184	47,146,229	1,082	826	1,338
J2	1.31	1.00	1.62	2.71	3.6	306,729	184	56,284,705	1,292	986	1,598
								TOTAL*	5,898	5,339	6,457

*Total MinE and MaxE values are based on root sum of squares error propagation.

For the monthly water budget, the annual value was divided based on a time-weighted split while the canals were on.

Table A6. Monthly canal leakage.

	Jan	Feb	Mar	Apr	May	Jun	Jul	Aug	Sep	Oct	Nov	Dec	Total
Days on	0	0	0	15	31	30	31	31	30	16	0	0	184
BE	0	0	0	482	996	964	996	996	964	498	0	0	5,898
MinE	0	0	0	436	902	873	902	902	873	451	0	0	5,339
MaxE	0	0	0	528	1,091	1,056	1,091	1,091	1,056	545	0	0	6,457

4. Irrigation Recharge (IR)

When more water is applied to fields than the crops can use, the excess may evaporate, runoff, infiltrate and be stored within the root zone, or infiltrate through the root zone to create groundwater recharge (i.e., irrigation recharge). Irrigation recharge that occurred within the model domain was assigned as groundwater recharge within the model. The modeled area is also affected by irrigation that occurs upgradient from the Parrot and Jefferson Canals. This upgradient irrigation recharge was applied at the segmented specified flux boundaries at the edges of the model domain (fig. A1), along with lateral groundwater inflow and canal leakage.

The NRCS's Irrigation Water Requirements (IWR) program was used to calculate the amount of irrigation recharge (NRCS, 1993; 2019). IWR considers soil types, crop type, irrigation method, and climate. Sandy loam is the predominant soil type within the study area (NRCS, 2012). Alfalfa is the main irrigated crop; based on landowner interviews and field observations, alfalfa was planted on about 70% of irrigated lands near Waterloo. The irrigated acres and irrigation type were determined by using the MT Department of Revenue's Final Land Use (FLU) Classification coverage (obtained from http://geoinfo.msl.mt.gov/) with modifications based on field observations and aerial photographs. Irrigation efficiency was set at 25% for flood, 65% for sprinkler, and 80% for pivot (NRCS, 1993; 2003; Sterling and Neibling, 1994).

Table A7. Whitehall Model Summary of Irrigated Acres.

Irrigation Type	Total	In Model	Upgradient
Flood	1568	1550	18
Sprinkler	604	423	181
Pivot	2405	1846	559

Table A8. Summary of IWR calculated irrigation recharge rates (ft).

	Flood	Sprinkler	Pivot
Jan	0	0	0
Feb	0	0	0
Mar	0	0	0
Apr	0.11	0.04	0.02
May	0.48	0.18	0.09
Jun	0.47	0.18	0.08
Jul	0.32	0.12	0.06
Aug	0.21	0.08	0.04
Sep	0.20	0.07	0.04
Oct	0.22	0.08	0.04
Nov	0	0	0
Dec	0	0	0
TOTAL	2.00	0.76	0.36

Table A9. Irrigation recharge summary.

Irrigation Type	Acres		Jan	Feb	Mar	Apr	May	Jun	Jul	Aug	Sep	Oct	Nov	Dec	Total
In Model															
Flood	1,566	BE	0	0	0	172	746	735	501	328	308	346	0	0	3,136
		MinE	0	0	0	149	647	637	434	284	267	300	0	0	2,718
		MaxE	0	0	0	195	846	833	568	371	349	392	0	0	3,554
Sprinkler	591	BE	0	0	0	25	106	105	71	47	44	49	0	0	447
		MinE	0	0	0	18	76	75	51	33	31	35	0	0	319
		MaxE	0	0	0	28	122	120	82	53	50	56	0	0	511
Pivot	2,451	BE	0	0	0	49	210	206	141	92	86	98	0	0	882
		MinE	0	0	0	37	158	155	106	69	64	74	0	0	662
		MaxE	0	0	0	74	316	309	211	138	129	147	0	0	1,324
Upgradient															
Flood	18	BE	0	0	0	2	9	8	6	4	4	4	0	0	36
		MinE	0	0	0	2	7	7	5	3	3	3	0	0	31
		MaxE	0	0	0	2	10	10	7	4	4	5	0	0	41
Sprinkler	181	BE	0	0	0	8	33	32	22	14	13	15	0	0	137
		MinE	0	0	0	5	23	23	16	10	10	11	0	0	98
		MaxE	0	0	0	9	37	37	25	16	15	17	0	0	157
Pivot	559	BE	0	0	0	11	48	47	32	21	20	22	0	0	201
		MinE	0	0	0	8	36	35	24	16	15	17	0	0	151
		MaxE	0	0	0	17	72	71	48	31	29	34	0	0	302
TOTAL*	5,366	BE	0	0	0	267	1,152	1,134	773	505	474	535	0	0	4,840
		MinE	0	0	0	239	1,035	1,018	694	454	426	480	0	0	4,346
		MaxE	0	0	0	294	1,270	1,249	852	557	523	589	0	0	5,334

*Total MinE and MaxE values based on root sum of squares error propagation.

5. Alluvial Groundwater Outflow (GWout)

Groundwater outflow occurs through the alluvium on the eastern side of the model domain (fig. A1). The groundwater outflow was calculated using the Darcy Flux Equation (see Alluvial Groundwater Inflow section).

Table A10. Summary of groundwater outflow calculations.

	K (ft/d)	Width (ft)	Sat Tk (ft)	Area (ft^2)	I (ft/ft)	Q (ft^3/d)	Q (ac-ft/yr)
BE	100	6,437	40	257,480	0.0019	48,921	410
MinE	75	6,437	40	257,480	0.0019	36,691	308
MaxE	250	6,437	40	257,480	0.0019	122,303	1,026

These values were proportioned by month based on a time-weighted split.

Table A11. Monthly alluvial groundwater outflow.

	Jan	Feb	Mar	Apr	May	Jun	Jul	Aug	Sep	Oct	Nov	Dec	Total
Days	31	28.25	31	30	31	30	31	31	30	31	30	31	365.25
BE	35	32	35	34	35	34	35	35	34	35	34	35	410
MinE	26	24	26	25	26	25	26	26	25	26	25	26	308
MaxE	87	79	87	84	87	84	87	87	84	87	84	87	1,026

6. Pond Evaporation (PE)

There are 58 groundwater fed ponds within the Whitehall area. These include abandoned gravel pits and cutoff meander bends. These ponds were digitized in a GIS system, and have a total area of 93 acres. Jensen (2010) showed that water surface evaporation can be reliably estimated by using the evapotranspiration rate for grass and then multiplying that value by 1.1. Weather data from the RAWS weather station near Whitehall (NWS station 243204) during 2014 were used for to calculate grass ET values using the RefET program (Allen, 2000). Calculated grass ET in 2014 totaled 35.9 in (2.99 ft), so the calculated water surface evaporation rate was about 39.5 in (3.29 ft). Applying this to the 93 acres of ponds results in a total of 306 acre-ft/yr.

Table A12. Summary of pond evaporation (93 acres).

Month	RefET Grass ET (ft)[1]	Evap Rate (ft)[2]	Pond Evap (ac-ft)[3]		
			BE	MinE[4]	MaxE[4]
Jan	0	0	0	0	0
Feb	0	0	0	0	0
Mar	0	0	0	0	0
Apr	0.40	0.44	41	39	43
May	0.49	0.54	50	48	53
Jun	0.52	0.58	54	51	56
Jul	0.67	0.74	69	65	72
Aug	0.51	0.56	52	49	54
Sep	0.39	0.43	40	38	42
Oct	0	0	0	0	0
Nov	0	0	0	0	0
Dec	0	0	0	0	0
Annual Total	2.99	3.29	306	291	321

[1]RefET Grass ET (Allen, 2000) used weather data from RAWS weather station near Whitehall (NWS station 243204) during 2014.
[2]Evaporation Rate = RefET Grass ET x 1.1.
[3]Pond Evaporation = Evap Rate x 93 acres.
[4]MinE and MaxE values based on an estimated 5% error.

7. Riparian Evapotranspiration (ETr)

Where groundwater elevations are close to the ground surface, some plants, such as willow, cottonwood, and riparian grasses, can directly remove groundwater from the saturated zone. The plants use the water for growth, and so transpire it into the atmosphere.

LANDFIRE data (USGS, 2016) were used to determine the area of riparian plant coverage. These included 1,013 acres of woody riparian areas, 1,416 acres of riparian grasses, and 180 acres of mesic forest. Reported maximum transpiration rates are about 22 in/yr for woody riparian plants and 3 in/yr for riparian grasses (Hackett and others, 1960; Lautz, 2008; Bobst and others, 2016). Groundwater monitoring (wells 237722, 48626, 277282, 28569, 279263, 279262, 277286, and 48378) shows that depth to water in the floodplain averages about 4.9 ft below ground surface. Assuming that the extension depth for riparian plants is about 10 ft below ground surface (Bobst and others, 2016), the actual transpiration rate should be about 11.2 in/yr (0.94 ft/yr) for woody riparian plants, and about 1.5 in/yr (0.13 ft/yr) for riparian grasses. Mesic forest areas were assigned the same rate as riparian grasses. MinE and MaxE values were based on a range of depth to water between 4 and 6 ft. The total BE ETr for the Whitehall area was calculated to be 1,152 acre-ft/yr.

Table A13. Summary of riparian evapotranspiration.

Plant Type	Acres		Max ET Rate (ft/yr)	% of Max	Actual ET Rate (ft/yr)	ET (acre-ft/yr)
Riparian Woody Plants	1,013	BE	1.83	51%	0.94	947
		MinE		40%	0.73	743
		MaxE		60%	1.10	1,114
Riparian Grasses and Mesic Forest	1,596	BE	0.25	51%	0.13	203
		MinE		40%	0.10	160
		MaxE		60%	0.15	239
					TOTAL BE	1,151
					TOTAL MinE	902
					TOTAL MaxE	1,354

The monthly distribution of ET_r was based on a growing season from May to September based on the minimum monthly temperatures being above 0^0C (Twin Bridges NOAA Climate Normal Values https://www.ncdc.noaa.gov/cdo-web/datatools/normals). ET_r rates were proportioned by month, with weighting based on the difference between average monthly temperature and 0^oC.

Table A14. Summary of monthly ET_r rates.

Plant Type	Acres		Jan	Feb	Mar	Apr	May	Jun	Jul	Aug	Sep	Oct	Nov	Dec	Total
Riparian Woody Plants	1,013	BE	0	0	0	0	89	195	281	252	131	0	0	0	947
		MinE	0	0	0	0	70	153	220	197	103	0	0	0	743
		MaxE	0	0	0	0	105	229	331	296	154	0	0	0	1,114
Riparian Grasses and Mesic Forest	1,596	BE	0	0	0	0	19	42	60	54	28	0	0	0	203
		MinE	0	0	0	0	15	33	47	42	22	0	0	0	160
		MaxE	0	0	0	0	23	49	71	64	33	0	0	0	239

8. Well Pumping (WEL)

Well pumping amounts are based on the number and type of well (MBMG-GWIC, 2018) (table A15).

Table A15. Summary of wells listed in GWIC.

Type	Number
Public Water Supply	8
Irrigation	30
Livestock	25
Domestic	312

Note. Includes 4 wells with unknown used (assumed domestic) and 5 PWS wells for individual buildings (treated as domestic).

Public Water Supply Wells

The City of Whitehall has 8 PWS wells listed in GWIC; however, the MDEQ Drinking Water Watch database (http://sdwisdww.mt.gov:8080/DWW/indes.jsp) indicates that only two of these wells are active.

Per capita water use rate by month for Boulder, Montana (Butler and Bobst, 2017; population 1,183; U.S. Census, 2010) were applied to the Whitehall PWS wells (population 1,038). It is assumed that all of this water is consumptively used since the sewer system uses a series of lined ponds and land application.

Table A16. Consumptive use for City of Whitehall PWS wells.

Month	Boulder (pop = 1,183)		Whitehall (pop = 1,038)				
	Total Rate (gpd)[1]	Rate per Person (gpd)	Total Rate (gpd)	Monthly Pumping (gal)	BE (ac-ft)	MinE[2] (ac-ft)	MaxE[2] (ac-ft)
Jan	363,826	308	319,232	9,896,190	30	29	32
Feb	373,380	316	327,615	9,255,121	28	27	30
Mar	393,904	333	345,623	10,714,322	33	31	35
Apr	450,522	381	395,302	11,859,049	36	35	38
May	494,322	418	433,733	13,445,726	41	39	43
Jun	671,346	567	589,059	17,671,779	54	52	57
Jul	1,242,738	1,050	1,090,416	33,802,894	104	99	109
Aug	1,145,226	968	1,004,856	31,150,534	96	91	100
Sep	789,428	667	692,668	20,780,041	64	61	67
Oct	615,890	521	540,401	16,752,416	51	49	54
Nov	420,674	356	369,112	11,073,363	34	32	36
Dec	389,702	329	341,936	10,600,026	33	31	34
Annual Total					605	574	635

[1]From Butler and Bobst, 2017.

[2]MinE and MaxE values based on estimated 5% error.

Irrigation Wells

The consumptive use rate for the 23 irrigation wells was based on water rights information or on acreage irrigated and the crop demand calculated using the DNRC's Water Use Standards (ARM 36.12.115; 2.5 ft/yr for hay). Each well was matched with irrigated areas, and, when possible, to DNRC water rights information and NAIP imagery. Seven of these wells were dropped because they served no apparent irrigated acreage (unused). The monthly distribution of water pumping was based on the NRCS's IWR programs calculated monthly gross irrigation water requirement (Butler and Bobst, 2017). Any excess water infiltrating to groundwater has already been accounted for as irrigation recharge, so for this calculation the gross application rate is treated as consumptive use. This resulted in a BE total consumptive use of 511 acre-ft/yr.

Table A17. Summary of irrigation well consumptive use.

GWIC ID or Water Right	Acres Irrigated	Annual Use (acre-ft)		
		BE	MinE[1]	MaxE[1]
48380	20	50	48	53
48442	3	7	7	8
48447	5	13	12	13
48449	13	34	32	35
48460	3	8	7	8
48464	5	13	12	13
48591	0.2	1	1	1
49170	20	50	48	53
120013	1	2	2	2
155759	1	3	3	4
167922	1	1	1	1
178392	0.0	2	2	2
184498	0.3	1	1	1
192302	4	7	7	8
195781	0.3	1	1	1
201466	1	1	1	1
228864	1	2	2	2
230496	80	152	144	160
240430	3	8	7	8
249524	1	3	3	3
265192	9	24	22	25
271890	0.4	1	1	1
41-783-00	52	130	124	137
TOTAL	224	511	502	520

[1]MinE and MaxE values based on estimated 5% error.
[2]Total MinE and MaxE based on root sum of squares error propagation.

Pumping of water for irrigation by month was based on crop demand calculated from IWR.

Table A18. Monthly distribution of irrigation well pumping (acre-ft).

	Jan	Feb	Mar	Apr	May	Jun	Jul	Aug	Sep	Oct	Nov	Dec	TOTAL
	0.0%	0.0%	0.0%	0.3%	8.1%	22.0%	31.2%	27.1%	10.5%	0.8%	0.0%	0.0%	100.0%
BE	0	0	0	1	41	112	160	139	54	4	0	0	511
MinE	0	0	0	1	41	110	157	136	53	4	0	0	502
MaxE	0	0	0	1	42	114	162	141	55	4	0	0	520

Livestock Wells

Water used by livestock is assumed to be 100% consumed. The use rate per well was set at an average annual rate of 693 gallons per day, assuming that usage would be similar to that calculated for the Boulder Valley (Butler and Bobst, 2017). Since there are 25 livestock wells, this results in a calculated consumptive use of 20 acre-ft/yr. The distribution of livestock water use was split among months using a time-weighted distribution.

Table A19. Estimated livestock water use (acre-ft).

	Jan	Feb	Mar	Apr	May	Jun	Jul	Aug	Sep	Oct	Nov	Dec	Total[2]
Days	31	28.25	31	30	31	30	31	31	30	31	30	31	365.25
BE	1.65	1.50	1.65	1.60	1.65	1.60	1.65	1.65	1.60	1.65	1.60	1.65	19.4
MinE[1]	1.57	1.43	1.57	1.52	1.57	1.52	1.57	1.57	1.52	1.57	1.52	1.57	19.1
MaxE[1]	1.73	1.58	1.73	1.67	1.73	1.67	1.73	1.73	1.67	1.73	1.67	1.73	19.7

[1]MinE and MaxE values for each month were based on an estimated 5% error.
[2]The total MinE and MaxE values were based on root sum of squares error propagation.

Domestic Wells

GWIC reports that there are 303 domestic wells in the Whitehall area. To this we added the 4 wells that have an unknown use, and the 5 PWS wells that serve individual buildings, for a total of 312 wells. The consumptive use for domestic wells is assumed to be similar to the consumptive use in the North Hills near Helena, MT, where a previous GWIP study (Waren and others, 2013) estimated domestic well rates from subdivision water-use records over a 15-yr period, and the annual average result was 435 gpd. This rate is within the range of domestic consumptive use estimated by the DNRC Water Resources Division (MT-DNRC, 2011). The monthly distribution of water use was also based on estimates from the North Hills study (Waren and others, 2013).

Table A20. Consumptive use for 312 domestic wells.

Month	% Use[1]	Rate Per Well (gpd)[1]	Total Rate (gpd)	Gallons	BE (acre-ft)	MinE[2]	MaxE[2]
Jan	0.3%	15	4,792	148,567	0.5	0.4	0.5
Feb	0.3%	17	5,259	148,567	0.5	0.4	0.5
Mar	0.4%	20	6,390	198,089	0.6	0.6	0.6
Apr	0.7%	37	11,555	346,655	1.1	1.0	1.1
May	10.2%	522	162,944	5,051,265	15.5	14.7	16.3
Jun	18.2%	963	300,435	9,013,042	27.7	26.3	29.0
Jul	26.2%	1,341	418,543	12,974,818	39.8	37.8	41.8
Aug	26.4%	1,352	421,738	13,073,863	40.1	38.1	42.1
Sep	14.2%	751	234,405	7,032,154	21.6	20.5	22.7
Oct	2.5%	128	39,937	1,238,055	3.8	3.6	4.0
Nov	0.5%	26	8,254	247,611	0.8	0.7	0.8
Dec	0.2%	10	3,195	99,044	0.3	0.3	0.3
Annual Total[3]					152	149	156

[1]From Waren and others, 2013.
[2]MinE and MaxE based on estimated 5% error.
[3]The total MinE and MaxE values were based on root sum of squares error propagation.

These different well types were combined for the budget.

Table A21. Summary of well pumping best estimates (BE, acre-ft).

	Jan	Feb	Mar	Apr	May	Jun	Jul	Aug	Sep	Oct	Nov	Dec	Total
PWS	30	28	33	36	41	54	104	96	64	51	34	33	605
Irrigation	0	0	0	1	41	112	160	139	54	4	0	0	511
Livestock	2	2	2	2	2	2	2	2	2	2	2	2	19
Domestic	0	0	1	1	16	28	40	40	22	4	1	0	152
TOTAL	32	30	35	40	100	196	305	276	141	61	36	34	1,288

9. Net Surface-Water Outflow from Groundwater (SWnet)

The net discharge from groundwater to surface waters (primarily the Jefferson River and Jefferson Slough) was based on the difference between the calculated inflows and outflows (table A22).

Calculated BE inflows totaled 12,141 acre-ft/yr, and calculated BE outflows other than surface water (i.e., groundwater outflow, pond evaporation, riparian evapotranspiration, and well pumping), totaled 3,156 acre-ft/yr. Therefore, it is estimated that the average net groundwater discharge to surface waters is about 8,986 acre-ft/yr (~12 cfs), which is consistent with measured flows in the Jefferson River. This annual volume of water was split between the months based on observed flows in groundwater-fed streams near Waterloo; however, it should be recognized that this distribution is rather tentative, and understanding the timing and location of surface-water/groundwater interactions was a primary driver for developing a numerical groundwater model. It should also be noted that since this is a net value, the absolute values for fluxes to and from surface waters will be higher.

10. Overall Budget

Table A22. Overall preliminary water budget.

	Jan	Feb	Mar	Apr	May	Jun	Jul	Aug	Sep	Oct	Nov	Dec	Annual		
													BE	MinE	MaxE
Inflows															
$GW_{in\text{-}al}$	101	92	101	98	101	98	101	101	98	101	98	101	1,188	782	2,752
$GW_{in\text{-}lat}$	18	17	18	18	18	18	18	18	18	18	18	18	215	25	1,075
CL	0	0	0	482	996	964	996	996	964	498	0	0	5,898	5,339	6,457
IR	0	0	0	267	1,152	1,134	773	505	474	535	0	0	4,840	4,346	5,334
Total inflow	119	109	119	864	2,268	2,214	1,889	1,621	1,554	1,152	115	119	12,141	10,799	13,484
Outflows															
$GW_{out\text{-}al}$	35	32	35	34	35	34	35	35	34	35	34	35	410	308	1,026
PE	0	0	0	41	50	54	69	52	40	0	0	0	306	291	321
ET_r	0	0	0	0	108	237	342	306	159	0	0	0	1,152	962	1,340
WEL	32	30	35	40	100	196	305	276	141	61	36	34	1,288	1,255	1,320
SW_{net}	716	591	582	564	720	757	844	1,016	857	793	762	783	8,986	7,583	10,388
Total outflow	783	653	652	679	1,014	1,277	1,595	1,685	1,231	889	833	852	12,141	10,681	13,602
ΔS	-664	-545	-533	186	1,254	936	294	-65	323	264	-717	-733	0	0	0

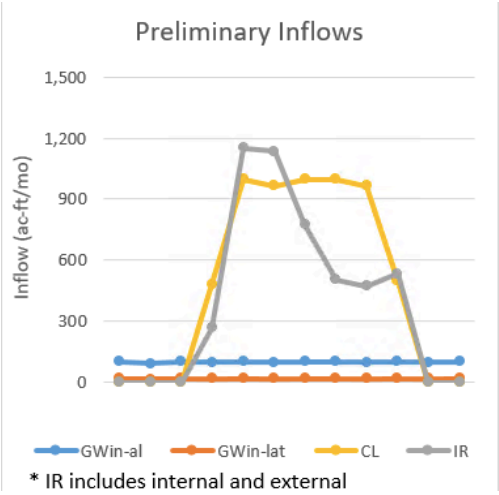

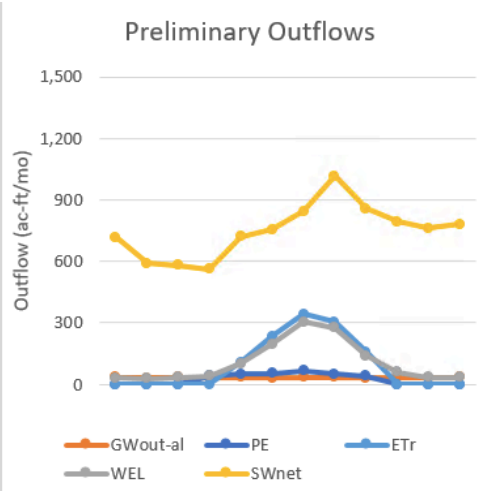

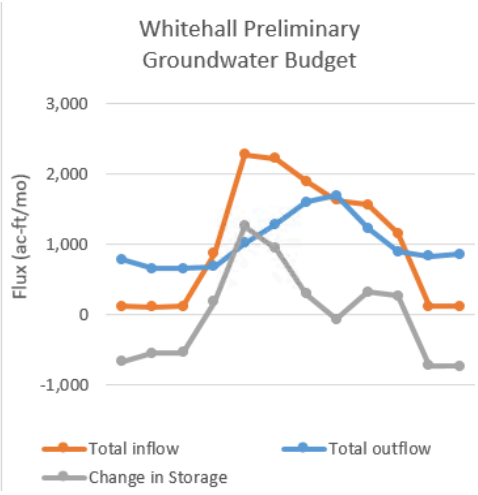

APPENDIX B:

RIVER STAGE—AVERAGE MONTHLY OFFSETS

Month	Fish Creek @ Parrot Castle	JeffRiver_ nrTwin_U SGS	JeffSlough_ WillowGrove	JR @Parrot Castle	JR @ Kountz Bridge	JR @ Mayflower	Pipestone @ Capp Ln Cumulative	Pipestone Mouth
	278400		287489	278863	277193	274566	274885	287491
Jan-14	-0.136	-0.040	-0.561	-0.110	0.009	-0.332	0.230	0.090
Feb-14	-0.140	-0.062	-0.850	-0.136	-0.017	-0.355	0.230	0.090
Mar-14	-0.025	0.617	-1.139	0.634	0.772	0.354	0.310	0.130
Apr-14	0.191	1.907	-1.184	2.095	2.192	1.960	0.452	0.202
May-14	0.455	3.214	-0.344	3.576	3.738	3.017	0.334	-0.030
Jun-14	0.453	3.302	0.385	3.675	3.932	3.036	0.167	-0.118
Jul-14	-0.078	1.012	0.574	0.325	1.152	0.638	-0.223	-0.428
Aug-14	0.017	0.007	0.760	-0.130	-0.178	-0.925	0.097	-0.037
Sep-14	0.000	0.000	0.000	0.000	0.000	0.000	0.000	0.000
Oct-14	-0.150	0.523	0.050	0.459	0.734	0.335	0.134	0.009
Nov-14	-0.167	0.475	0.017	0.550	0.984	0.515	0.228	0.092
Dec-14	-0.049	0.476	-0.272	0.474	0.608	0.207	0.230	0.090
Average Offset =	0.031	0.953	-0.214	0.951	1.160	0.704	0.182	0.007
Stage-Sept-2016 =	4367.2	no data	no data	4368.4	4338.0	4304.7	4367.8	4329.3
Steady State Stage =	4367.2			4369.4	4339.16	4305.4	4367.9	4329.3

RIVER STAGE—AVERAGE MONTHLY OFFSETS

Data from 16 monitoring stations and 35 surveyed points on Jefferson River (September 2016) were used to estimate steady-state and monthly river stages for the transient model at the start and end of each river reach.

Since September 2016 surveyed stages are expected to be lower than the annual average stages (September is a late summer low flow month); therefore, the average for a particular station in 2016 is estimated as the September 2016 stage plus an average annual offset (offset = deviation from September) for that station.

The year 2014 has the most data for the Jefferson River. Assuming the surface water slope between stations remain relatively constant, the surface water slopes in year 2016 are assumed to be similar to those of 2014; therefore, the average offset from the September stage in 2014 remains relatively the same as in the year 2016. Therefore, the average annual stage for each station in 2016 is the surveyed stage in September 2016 plus the average offset of 2014 for that station. Example: the average annual for Kountz Bridge station in 2016 is 4,338.0 ft (September stage) plus 1.16 ft (average offset for 2014) results in 4,339.16 ft (table below).

Utilizing the most recent and complete data from the September 2016 survey, the model steady-state stage for any station is based on September 2016 data plus the 2014 average offset (table below). In transient simulation, for each month, the average stage for each station is calculated as the September 2016 stage for that station plus its 2014 offset for that month. For example, the April 2016 stage at Kountz Bridge station is the September 2016 stage of 4,338.0 ft) plus the April 2014 offset 2.192 ft (4,340.19 ft). For both steady-state and transient linear interpolation is applied to calculate river stages and riverbed elevations for all river cells in the model.

Slaughterhouse Slough @ Kountz Rd	Slaughterhouse Slough @ Parrot Castle	Whitetail Creek @ Whitehall Cemetery	Whitetail @ Salsbury	Whitetail Mouth_2014	JS_Briggs_ 2014	JS_TebayRanch_ 2014	Jefferson SLough @ Tebay Ln
278354	277189	274574	277322	287492	287493	287495	274564
-0.001	0.006	0.000	-0.017	-0.200	-0.195	0.082	0.354
-0.008	-0.005	0.000	-0.016	-0.200	-0.315	-0.148	-0.105
0.204	0.354	0.050	-0.015	-0.200	-0.451	-0.143	-0.105
0.524	1.037	0.135	-0.014	-0.169	-0.254	-0.066	-0.105
1.010	1.729	0.230	0.061	0.009	0.158	0.092	0.093
1.075	1.775	-0.168	-0.113	-0.144	0.278	0.096	0.173
0.213	0.563	-0.375	-0.138	-0.284	-0.217	-0.080	-0.240
0.060	0.031	-0.115	-0.015	-0.064	0.217	0.026	0.027
0.000	0.000	0.000	0.000	0.000	0.000	0.000	0.000
0.158	0.304	0.009	-0.009	0.000	0.015	0.043	0.302
0.227	0.279	-0.014	-0.019	-0.029	0.055	0.058	0.354
0.160	0.280	0.000	-0.018	-0.110	-0.065	0.070	0.354
0.302	0.529	-0.021	-0.026	-0.116	-0.065	0.003	0.092
4340.8	4372.3	4349.2	no data	4325.3	no data	no data	4297.3
		4349.2		4325.2			4297.4

Example: River Package (RIV) input – Whitetail Creek (reach 59)

Row	Col	Layer	Reach	Stage	Bed	Length	Width	Thickness	K
27	96	1	59	4348.94	4344.47	332.65	150	1	162.5
28	96	1	59	4348.53	4344.12	265.29	150	1	162.5
29	96	1	59	4348.13	4343.78	71.39	150	1	162.5
29	97	1	59	4347.78	4343.48	226.87	150	1	162.5
30	97	1	59	4347.10	4342.89	310.28	150	1	162.5
30	98	1	59	4346.67	4342.52	217.39	150	1	162.5
31	98	1	59	4346.27	4342.18	190.96	150	1	162.5
31	99	1	59	4346.06	4342.00	59.57	150	1	162.5
32	98	1	59	4345.74	4341.73	68.77	150	1	162.5
32	99	1	59	4345.41	4341.44	122.82	150	1	162.5
33	99	1	59	4344.96	4341.05	250.00	150	1	162.5
33	100	1	59	4344.01	4340.24	452.27	150	1	162.5
34	99	1	59	4343.17	4339.52	197.75	150	1	162.5
34	105	1	59	4338.10	4335.15	72.26	150	1	162.5
34	100	1	59	4342.81	4339.20	62.17	150	1	162.5
35	100	1	59	4342.45	4338.90	217.32	150	1	162.5
35	101	1	59	4341.85	4338.38	252.30	150	1	162.5
35	102	1	59	4341.21	4337.83	295.64	150	1	162.5
35	103	1	59	4340.73	4337.42	96.17	150	1	162.5
35	104	1	59	4339.70	4336.53	150.77	150	1	162.5
35	105	1	59	4338.46	4335.46	381.90	150	1	162.5
35	106	1	59	4337.53	4334.67	321.20	150	1	162.5
35	107	1	59	4336.55	4333.82	82.32	150	1	162.5
36	103	1	59	4340.42	4337.15	188.94	150	1	162.5
36	104	1	59	4340.01	4336.80	294.96	150	1	162.5
36	105	1	59	4339.07	4335.99	215.04	150	1	162.5
36	106	1	59	4337.00	4334.21	159.83	150	1	162.5
36	107	1	59	4336.16	4333.49	257.18	150	1	162.5
37	107	1	59	4335.55	4332.96	338.72	150	1	162.5
37	108	1	59	4334.48	4332.04	222.97	150	1	162.5
37	109	1	59	4334.10	4331.72	92.81	150	1	162.5
38	107	1	59	4335.10	4332.58	66.76	150	1	162.5
38	108	1	59	4333.32	4331.04	58.73	150	1	162.5
38	109	1	59	4333.63	4331.32	240.57	150	1	162.5
39	108	1	59	4333.01	4330.78	232.05	150	1	162.5
39	110	1	59	4330.46	4328.59	5.36	150	1	162.5
39	111	1	59	4330.41	4328.55	70.73	150	1	162.5
39	113	1	59	4328.27	4326.71	265.66	150	1	162.5
39	114	1	59	4327.64	4326.16	264.54	150	1	162.5
39	115	1	59	4327.21	4325.80	127.83	150	1	162.5
40	108	1	59	4332.42	4330.27	230.07	150	1	162.5
40	109	1	59	4332.00	4329.91	115.01	150	1	162.5
40	110	1	59	4330.78	4328.86	422.60	150	1	162.5
40	111	1	59	4330.03	4328.21	227.32	150	1	162.5
40	112	1	59	4329.38	4327.66	265.27	150	1	162.5
40	113	1	59	4328.88	4327.23	195.35	150	1	162.5
40	114	1	59	4326.52	4325.20	5.71	150	1	162.5
40	115	1	59	4326.85	4325.48	233.66	150	1	162.5
41	109	1	59	4331.68	4329.64	112.24	150	1	162.5
41	110	1	59	4331.68	4329.64	14.73	150	1	162.5
41	114	1	59	4326.36	4325.06	64.21	150	1	162.5
41	115	1	59	4325.96	4324.72	245.42	150	1	162.5
41	116	1	59	4325.50	4324.32	223.22	150	1	162.5

APPENDIX C:
MODEL LATERAL GROUNDWATER INFLUX—
TRANSIENT MODEL

MODEL LATERAL GROUNDWATER INFLUX—TRANSIENT MODEL

Lateral Groundwater Recharge (GWlat) enters the Jefferson Valley along the lateral edges of the valley. GWlat is a combination of water flowing into the valley sediments through the bedrock, and infiltration of water from mountain streams as they transition from being underlain by low permeability bedrock to the more permeable unconsolidated deposits.

Table C1: Lateral groundwater influx through Eastern and Western boundaries (irrigation canals)

Month	Parrot1 ft^{3}/day	Parrot2 ft^3/day	Parrot3 ft^3/day	Parrot4 ft^3/day	Parrot5 ft^3/day	Parrot6 ft^3/day	Jefferson1 ft^3/day	Jefferson2 ft^3/day
Jan	875	148	163	565	523	1258	1962	0
Feb	875	148	163	565	523	1258	1962	0
Mar	875	148	163	565	523	1258	1962	2403
Apr	875	148	163	565	523	1258	1962	2403
May	875	148	163	565	523	1258	1962	2403
June	875	148	163	565	523	1258	1962	2403
July	875	148	163	565	523	1258	1962	2403
Aug	875	148	163	565	523	1258	1962	2403
Sept	875	148	163	565	523	1258	1962	2403
Oct	875	148	163	565	523	1258	1962	2403
Nov	875	148	163	565	523	1258	1962	0
Dec	875	148	163	565	523	1258	1962	0

Table C2: Lateral groundwater influx through Alluvium and Bedrock boundaries

Month	Alluvium1		Alluvium2	Alluvium3	Alluvium4		Bedrock1	Bedrock2	Bedrock3	Bedrock4
	Multiplier	ft^3/day	ft^3/day	ft^3/day	Multiplier	ft^3/day	ft^3/day	ft^3/day	ft^3/day	ft^3/day
Jan	1	44775	12766	13327	1	-24461	384	2921	451	1174
Feb	1	44775	12766	13327	0.5	-24461	384	2921	451	1174
Mar	1.225	44775	12766	13327	0.5	-24461	384	2921	451	1174
Apr	1.2	44775	12766	13327	0.1	-24461	384	2921	451	1174
May	1.4	44775	12766	13327	0	-24461	384	2921	451	1174
June	1.025	44775	12766	13327	0	-24461	384	2921	451	1174
July	1.085	44775	12766	13327	0	-24461	384	2921	451	1174
Aug	1.07	44775	12766	13327	0	-24461	384	2921	451	1174
Sept	0.78	44775	12766	13327	0	-24461	384	2921	451	1174
Oct	0.82	44775	12766	13327	0.1	-24461	384	2921	451	1174
Nov	0.95	44775	12766	13327	0.5	-24461	384	2921	451	1174
Dec	1	44775	12766	13327	1	-24461	384	2921	451	1174

All monthly multipliers = 1 except those shown in the tables

Note that in table C1, the second segment of Jefferson canal (J2) has seasonal influx rates. The seasonality in the nearby target well 48522 (figs. 12B and 19) required changing the lateral influx in the lower layer to simulate this seasonality, i.e., canal leakage and alluvium seasonal rates alone were not enough to simulate the changes in groundwater levels in well 48522.

Initial estimates of groundwater inflow. These values were modified during calibration, as shown in table I1.

B1:
K = Assume silty sand value of 1 ft/d (Renova Formation)

A
Length of the boundary = 4,268 ft
Assume contributing thickness of 40 ft
A = 170,720 ft^2

dh/dl
~25/5547 based on contours = 0.0045
Q = 1 * 170720 * 0.0045 = 768 ft3/d (0.01 cfs)
6.4 acre-ft/yr

B2 (East of Whitetail to bedrock):
K = Assume silty sand value of 1 ft/d (Renova Formation)

A
Total length = 8,078 ft
Assume contributing thickness of 40 ft
A = 323,120 ft^2

dh/dl
(4332-4400)/3761 based on 247793 and contours = 0.018
Q = 1 * 323,120 * 0.018 = 5842 ft3/d (0.07 cfs)
49 acre-ft/yr

B3 (bedrock East of Whitetail):
K = 0.1 for fractured bedrock
A
Total length of the non-alluvial boundary = 9,576 ft
Assume contributing thickness of 40 ft
A = 383,040 ft^2

dh/dl
~100/4247 based on contours = 0.024
Q = 0.1 * 383,040 * 0.024 = 902 ft3/d (0.01 cfs)
7.6 acre-ft/yr

B4 (NE corner of model):
K = Assume silty sand value of 1 ft/d (Renova Formation)

A
Total length = 2,448 ft
Assume contributing thickness of 40 ft
A = 97,920 ft^2

dh/dl
100/4171 based on contours = 0.024
Q = 1 * 97,920 * 0.024 = 2348 ft3/d (0.03 cfs)
20 acre-ft/yr

J1 (Southern portion of Jefferson Canal):
K = Assume silty sand value of 1 ft/d (Renova Formation)

A
Total length = 11,986 ft
Assume contributing thickness of 40 ft
A = 479,440 ft^2

dh/dl
(4517.08-4368.26)/18188 based on 48667 and 171688 = 0.0082
Q = 1 * 479,440 * 0.0082 = 3923 ft3/d (0.05 cfs)
33 acre-ft/yr

J2 (Northern portion of Jefferson Canal):
K = Assume silty sand value of 1 ft/d (Renova Formation)

A
Total length = 14,309 ft
Assume contributing thickness of 40 ft
A = 572,360 ft^2

dh/dl
(4362.99-4360.16)/337 based on 274314 and 274315 = 0.0084
Q = 1 * 572,360 * 0.0084 = 4,806 ft3/d (0.06 cfs)
40 acre-ft/yr

P1 (Upstream segment of Parrot Canal):
K = Assume silty sand value of 1 ft/d (Renova Formation)

A
Total length = 12,384 ft
Assume contributing thickness of 40 ft

dh/dl
based on triangulation using 219670, 280978, and 48577 = 0.00353
Q = 1 * 495,360 * 0.00353 = 1749 ft3/d (0.02 cfs)
15 acre-ft/yr

P2 (Next downstream segment of Parrot Canal):
K = Assume silty sand value of 1 ft/d (Renova Formation)

A
Total length = 2,097 ft
Assume contributing thickness of 40 ft
A = 83,880 ft^2

dh/dl
based on triangulation using 219670, 280978, and 48577 = 0.00353
Q = 1 * 83,880 * 0.00353 = 296 ft3/d (0.003 cfs)
2.5 acre-ft/yr

P3 (Next downstream segment of Parrot Canal):
K = Assume silty sand value of 1 ft/d (Renova Formation)

A
Total length = 2,302 ft
Assume contributing thickness of 40 ft
A = 92,080 ft^2

dh/dl
based on triangulation using 219670, 280978, and 48577 = 0.00353
Q = 1 * 92,080 * 0.00353 = 325 ft3/d (0.004 cfs)
2.7 acre-ft/yr

P4 (Next downstream segment of Parrot Canal):
K = Assume silty sand value of 1 ft/d (Renova Formation)

A
Total length = 7,994 ft
Assume contributing thickness of 40 ft
A = 319,760 ft^2

dh/dl
based on triangulation using 219670, 280978, and 48577 = 0.00353

Q = 1 * 319,760 * 0.00353 = 1129 ft3/d (0.01 cfs)
9.5 acre-ft/yr

P5 (Next downstream segment of Parrot Canal):
K = Assume silty sand value of 1 ft/d (Renova Formation)

A
Total length = 5,021 ft
Assume contributing thickness of 40 ft
A = 200,840 ft^2

dh/dl
based on triangulation using 276427, 280978, and 48577 = 0.00521
Q = 1 * 200,840 * 0.00521 = 1046 ft3/d (0.01 cfs)
8.8 acre-ft/yr

P6 (Most downstream segment of Parrot Canal):
K = Assume silty sand value of 1 ft/d (Renova Formation)

A
Total length = 9,168 ft
Assume contributing thickness of 40 ft
A = 366,720 ft^2

dh/dl
based on mean of:
triangulation using 280978, 276427, and 224219 = 0.00989; AND
line from 250384 to 277286 = 0.00382
MEAN = 0.00686
Q = 1 * 366,720 * 0.00686 = 2516 ft3/d (0.03 cfs)
21.1 acre-ft/yr

APPENDIX D:
NASH SUTCLIFFE EFFICIENCY COEFFICIENT (NS) CALCULATIONS

NASH SUTCLIFFE EFFICIENCY COEFFICIENT (NS) CALCULATIONS (NASH AND SUTCLIFFE, 1970)

It is a method for calculating a statistics (NS) to measure the fit between the modeled (calculated) and measured values. The efficiency coefficient NS is the sum of deviation of the measured values from a linear regression line with a 1:1 slope. The NS coefficient is computed as follows:

$$NS = 1 - [\sum_{i=1}^{n}(\mathrm{Hm} - \mathrm{Hs})^2 / \sum_{i=1}^{n}(\mathrm{Hm} - \mathrm{Hmavg})^2,$$

where NS is the coefficient of efficiency (Nash Sutcliffe coefficient); Hm is the measured head; Hs is the simulated head; Hmavg is arithmetic average of measured values; i is time steps.

Example of NS calculations (well 156080)

156080 - L2				
Date	Obs head (ft)	Sim head (ft)	F = (obs-sim)^2	F_o = [obs-(avg. obs)]^2
7/1/2013	4402.15	4398.536	13.06	12.53
8/1/2013	4401.42	4399.482	3.76	7.90
9/1/2013	4400.8	4400.070	0.53	4.80
10/1/2013	4399.84	4400.349	0.26	1.51
11/1/2013	4398.23	4399.764	2.35	0.14
12/1/2013	4397.28	4398.759	2.19	1.77
1/1/2014	4396.4	4397.622	1.49	4.88
2/1/2014	4395.65	4396.573	0.85	8.76
3/1/2014	4395.72			8.35
5/1/2014	4400.48			3.50
6/1/2014	4400.47			3.46
7/1/2014	4399.81			1.44
8/1/2014	4400.69			4.33
9/1/2014	4401.17			6.55
10/1/2014	4399.44			0.69
11/1/2014	4398.23			0.14
12/1/2014	4397.54			1.14
1/1/2015	4396.7			3.65
2/1/2015	4396.24	4396.414	0.03	5.62
3/1/2015	4395.85	4395.584	0.07	7.62
4/1/2015	4395.36	4394.820	0.29	10.56
5/1/2015	4399.95	4394.660	27.98	1.80
Average =	4398.6		52.87	101.14
NS =1-(F/F_o) =	0.48			

APPENDIX E:
UNCERTAINTY ANALYSIS—FUTURE SCENARIOS PREDICTION ERROR

UNCERTAINTY ANALYSIS—FUTURE SCENARIOS PREDICTION ERROR

Example: How to quantify the model's prediction error (uncertainty) to simulate future stream depletion under the conditions of a future scenario. Assume the uncertainty parameter is the horizontal hydraulic conductivity (Kh) changed by 10% multiplier (90% reduction in conductivity).

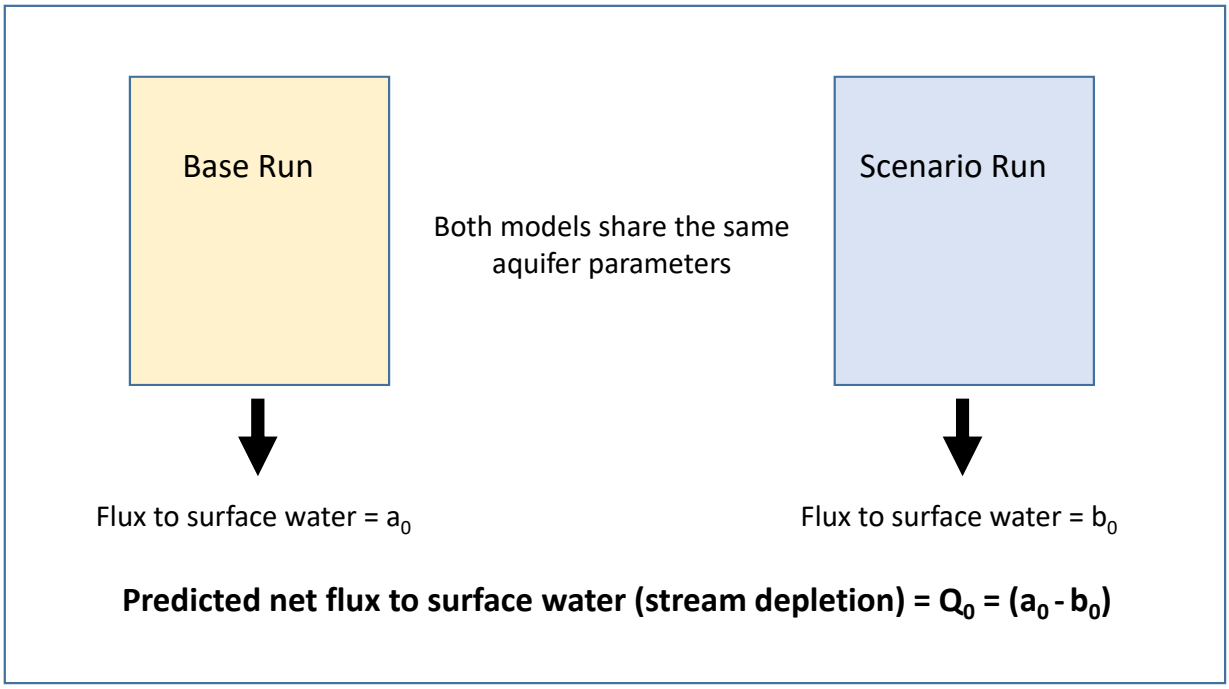

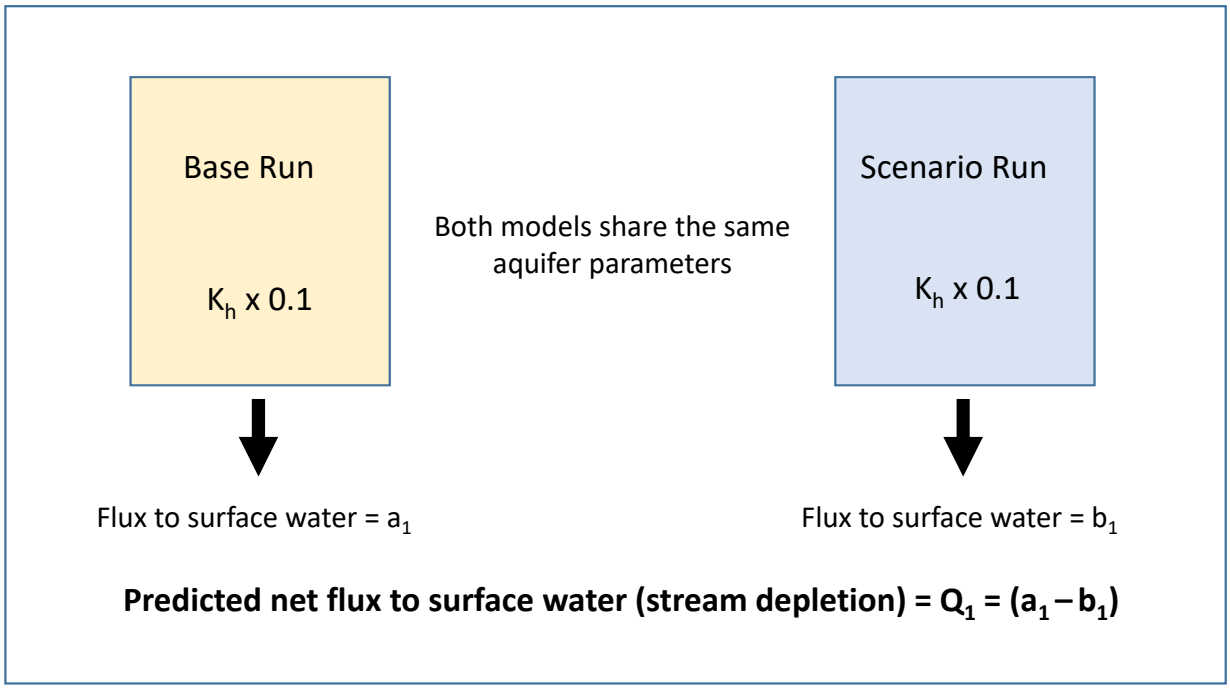

$$\%\text{Error in Prediction} = |(Q_0 - Q_1)| / Q_0$$